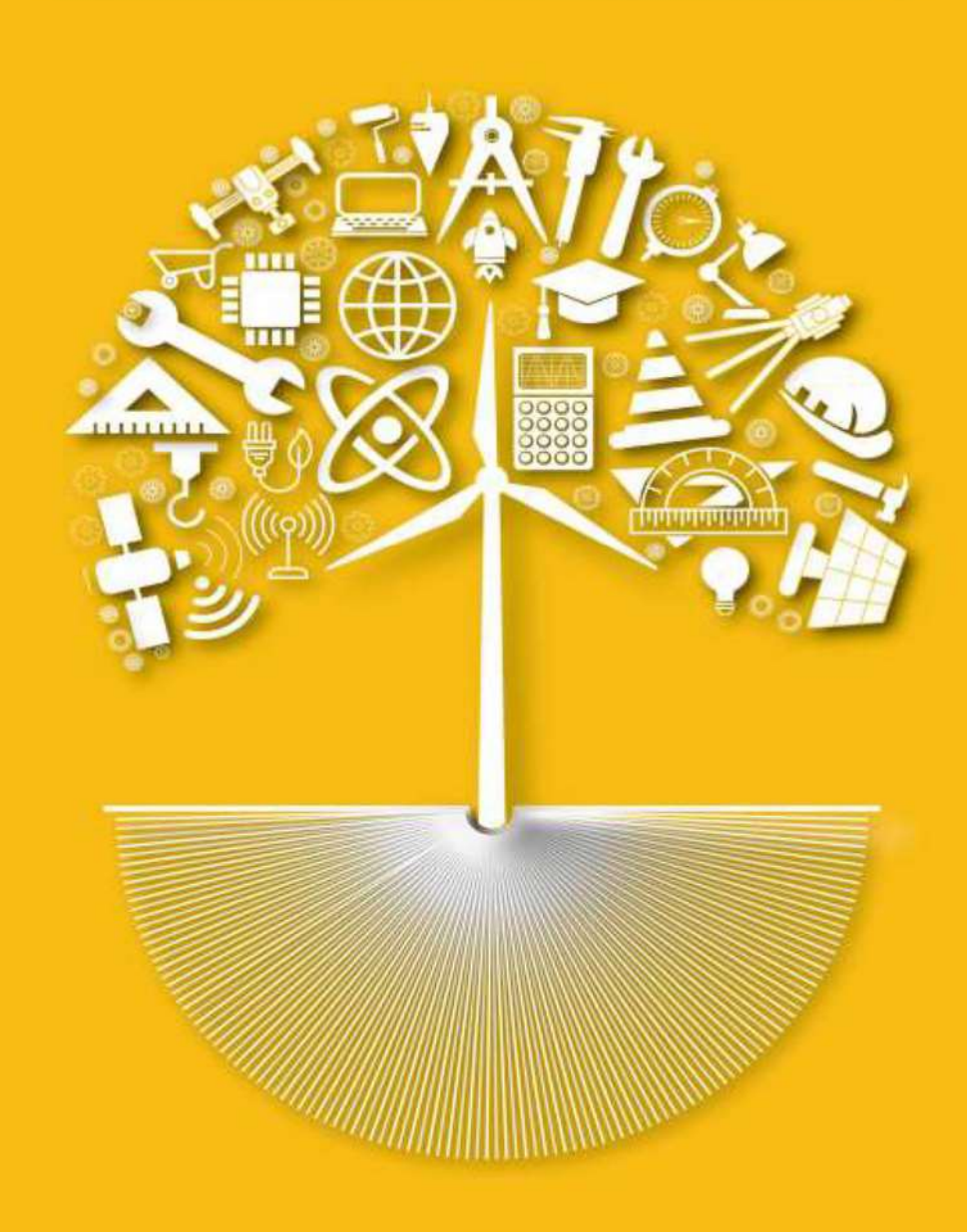


ETHIOPIAN INTERNATIONAL JOURNAL OF ENGINEERING AND TECHNOLOGY

"exploration of novel knowledge" —



ISSN (E): 2959-3921, ISSN (P): 2959-393X

www.amu.edu.et

eijet@amu.edu.et



Volume - 1

ISSUE - 2

December - 2023



ETHIOPIAN INTERNATIONAL JOURNAL OF ENGINEERING AND TECHNOLOGY (EIJET)

ISSN (E): 2959-3921, ISSN (P): 2959-393X VOLUME-1, ISSUE-2

> DECEMBER, 2023 ARBA MINCH, ETHIOPIA

Editorial Team

Editor in Chief

Durga Prasad Sharma, Ph.D, (Professor), Cloud Computing, Intelligent Autonomic Systems, Software Engineering, and Distributed Green Computing. **Email:** sharma.dp@amu.edu.et, Arba Minch University, Ethiopia.

ORCID ID: https://orcid.org/0000-0002-1654-901X

Google Scholar: https://scholar.google.com/citations?user=jFrf5VsAAAAJ&hl=en

Co-Editor in Chief

Samuel Kefale (Asst. Prof), Electrical Power System Engineering, Renewable Energy, Electrical Machines, AI in Power Systems. **Email:** samuel.kefale@amu.edu.et, Arba Minch University, Ethiopia.

ORCID iD: https://orcid.org/0000-0003-1105-1084

Google Scholar:

https://scholar.google.co.uk/citations?hl=en&user=FY6t2FsAAAAJ&view_op=list_works

Editorial Manager

Addisu Mulugeta, (Asst. Prof), Machine Learning, Data Science, Big Data Analytics, Data Mining, Data Warehousing. Email: addisu.mulugeta@amu.edu.et, Arba Minch University, Ethiopia.

ORCID iD: <u>https://orcid.org/0000-0002-6548-9359</u>

Google Scholar: https://scholar.google.com/citations?user=YOti-8wAAAA]&hl=en

Language Editor

Endalkachew Hailu Guluma, Ph.D., (Asst. Professor), English Language and Literature, Literary and Cultural Studies, Environmental Humanities, Indigenous Knowledge Studies, Folkloristics. Email: endalkachew.hailu@amu.edu.et, Arba Minch University, Ethiopia.

ORCID ID: <u>https://orcid.org/0000-0002-6772-4391</u>

Google Scholar: https://scholar.google.com/citations?user=6nsRrO0AAAA]&hl=en

Layout Editor

Chirotaw Kentib, Computer Science,

Email: chirotaw.kentib@amu.edu.et, Arba Minch University, Ethiopia.

Associate Editors

Muluneh Lemma Woldesemayat, PhD in Electrical Engineering, Specialization: Power Electronics & Drives, Research Interest: Electric Vehicles, Renewable Energy, Power Systems, Arba Minch University, Email: muluneh2006@yahoo.com, Arba Minch, **Ethiopia**

Anchit Bijalwan, PhD in Computer Science & Engineering, Specialization: Network Security & Forensics, Research Interest: Botnet Analysis, AI in Healthcare, Cybersecurity, British University Vietnam, Email: anchit.b@buv.edu.vn, Hanoi, **Vietnam**

Mohammed Abebe, PhD in Computer Engineering, Specialization: Machine Learning, Research Interest: AI in Healthcare, Phishing Detection, Speech Recognition, Arba Minch University, Email: moshethio@gmail.com, Arba Minch, **Ethiopia**

Bisrat Gissila, PhD in Geotechnical Engineering, Specialization: Ground Improvement, Research Interest: Landslide Mitigation, Soil Stabilization, Slope Stability, Arba Minch University, Email: Bisratgissila@gmail.com, Arba Minch, **Ethiopia**

Jitendra Kumar Verma, PhD in Computer Science & Technology, Specialization: Cloud Computing, Research Interest: Energy-Efficient Cloud Systems, IoT, AI, Indian Institute of Foreign Trade, Email: jkverma@iift.edu, Kakinada, **India**

Nisha Sharma, PhD in IT Security, Specialization: Cybersecurity, Research Interest: Wormhole Attacks in MANETs, Network Security, Splunk, State of Missouri (ITSD), Email: Nisha.SharmaJC@gmail.com, Jefferson City, USA

Rajesh Ravi, PhD in Mechanical Engineering (Automotive), Specialization: Waste Heat Recovery, Research Interest: Biofuels, Emission Control, Heat Exchangers, Université Internationale De Rabat, Email: rajesh4mech@gmail.com, Rabat, Morocco

Mesay Samuel Gondere, PhD in Computing & IT, Specialization: Artificial Intelligence, Research Interest: NLP, Amharic OCR, Deep Learning, Arba Minch University, Email: mesay.samuel@amu.edu.et, Arba Minch, Ethiopia

Mario Alessandro Bochicchio, PhD in Computer Science, Specialization: eHealth & Data Management, Research Interest: Digital Health, AAL, Big Data, University of Bari, Email: mario.bochicchio@uniba.it, Bari, Italy

S. Balakumar, PhD in Electrical Engineering, Specialization: Renewable Energy, Research Interest: Solar & Wind Energy, Power Electronics, Power System Optimization, Arba Minch University, Email: balakumar25dec@gmail.com, Arba Minch, **Ethiopia**

Worku Jimma, PhD in Health Information Management, Specialization: Health Informatics, Research Interest: Health Information Systems, Knowledge Management, Infodemic Management, Jimma University, Email: worku.jimma@gmail.com, Jimma, **Ethiopia**

Hiwot Tsegaye, PhD in Civil Engineering, Specialization: Infrastructure Materials, Research Interest: Sustainable Construction Materials, Crushed Brick Reuse, High-Performance Concrete, Arba Minch University, Email: hiwitsegsh@gmail.com, Arba Minch, **Ethiopia**

J. Isaac JoshuaRamesh Lalvani, PhD in Mechanical Engineering, Specialization: Automotive Engineering, Research Interest: Alternate Fuels, Biofuels, Hybrid Vehicles, Arba Minch University, Email: isaac.jrl@amu.edu.et, Arba Minch, **Ethiopia**

Vasudeva Rao, PhD in Civil Engineering, Specialization: Geotechnical Engineering, Soil Remediation, Expansive Soils, Arba Minch University, Email: vasudevarao_9@yahoo.com, Visakhapatnam, **Ethiopia**

Vandna Rani Verma, PhD in Computer Science & Engineering, Specialization: Complexity Reduction of Software, Energy Efficient Wireless Networks, Galgotias College of Engineering & Technology, Email: profvandna@gmail.com, Greater Noida, India

Nuredin Edris, PhD in Architecture, Specialization: Healing Architecture, User Perception in Hospital Design, Wollega University, Email: nuredinidris51@gmail.com, Wollega, **Ethiopia**

Zeleke Lulayehu Tadesse, PhD in Civil Engineering, Specialization: Seismic Response & Soil-Structure Interaction of Buildings, Arba Minch University Institute of Technology, Email: zeleke.lulayehu@amu.edu.et, Arba Minch, **Ethiopia**

Efrem Girma, PhD in Construction Engineering & Management, Specialization: Construction Project Management, Project Performance, BIM, Arba Minch University, Email: ephremg41@gmail.com, Arba Minch, **Ethiopia**

Fescha Sahile, PhD in Construction Engineering, Specialization: Geotechnical Engineering, Construction Materials, Concrete Technology, Arba Minch University, Email: sahile21@gmail.com, Arba Minch, **Ethiopia**

Kibreab Adane, PhD in Computing & IT, Specialization: Artificial Intelligence, Cybersecurity, AI in Cybersecurity, Machine Learning, Arba Minch University, Email: kibreab.adane@amu.edu.et, Arba Minch, **Ethiopia**

Solomon Neway, PhD in Automotive Engineering, Specialization: Vehicle Emissions, Sustainable Transportation, EV Technology, Arba Minch University, Email: solomonnewayjida@gmail.com, Arba Minch, **Ethiopia**

Yalisho Girma, PhD in Electrical Power Engineering, Specialization: Power Electronics, Renewable Energy, Power Distribution, Arba Minch University, Email: yalisho.girma@amu.edu.et, Arba Minch, Ethiopia

Negussie Tadege Demeke, PhD in Material Science, Arba Minch University, Email: kibreab.adane@amu.edu.et, Arba Minch, Ethiopia

Advisory Board

Alemayehu Chufamo, PhD in Chemical Engineering, Specialization: Process Engineering, Micro/Milli Channels, Phase Transfer Catalysis, Arba Minch University, Email: alemayehuc@gmail.com, Arba Minch, Ethiopia

Sumit Gautam, PhD in Computer Science, Specialization: Mobility Management & AI, Research Interest: Heterogeneous Networks, AI, Product Innovation, LG Soft India, Email: sumit.gautam@ieee.org, Bengaluru, **India**

Rakesh Kumar Sharma, PhD in Computer Science, Specialization: Cybersecurity, Data Mining, Spatial Decision Support Systems, University of Maryland Eastern Shore, Email: rsharma@umes.edu, Fruitland, United States

Mesfin Abebe, PhD in Software Engineering, Specialization: Artificial Intelligence, Machine Learning, Deep Learning, Autonomous Systems, Adama Science and Technology University, Email: mesfin.abebe@astu.edu.et, Adama, Ethiopia

Beakal Gizachew, PhD in Computer Science and Engineering, Specialization: Artificial Intelligence, Energy Efficiency in SDN, Machine Learning, Addis Ababa University, Email: beakal.gizachew@aait.edu.et, Addis Ababa, **Ethiopia**

Girma Neshir, PhD in Information Retrieval, Specialization: Adaptive Systems, Sentiment Analysis, Transfer Learning, Addis Ababa Science and Technology University, Email: girma.neshir@aastu.edu.et, Addis Ababa, **Ethiopia**

Prathap Mani, PhD in Computing, Specialization: Computer Networks, Cybersecurity, Blockchain, IoT, American University of Kurdistan, Email: prathap.mani@auk.edu.krd, Duhok, **Iraq**

Lissanework Sileshi Alemu, PhD in Urban & Regional Planning, Specialization: Urban Management & Planning, Residential Satisfaction, Urban Renewal, Ethiopian Civil Service University, Email: lisaethfirst@yahoo.com, Addis Ababa, **Ethiopia**

Padmanabhan, PhD in Mechanical Engineering, Specialization: Gearbox Design Optimization, Energy, Design, Optimization, Vel Tech Rangarajan Sagunthala R&D Institute of Science and Technology, Email: padmanabhan.ks@gmail.com, Chennai, **India**

P. Mangaiyarkarasi, PhD in Electrical Engineering, Specialization: Power Systems, Voltage Security Assessment, Hybrid Optimization, University College of Engineering, Panruti, Email: mangaisowneya@gmail.com, Panruti, **India**

About the EIJET

The Ethiopian International Journal of Engineering and Technology (EIJET) is a non-profit peer-reviewed open-access academic research Journal of Arba Minch Institute of Technology under Arba Minch University, Ethiopia. The Journal is indexed in the Asian Science Citation Index (ASCI). The scope of the Journal covers multidisciplinary and cross-disciplinary areas of study in engineering and technology. The peer-reviewed International Journal publishes all types of quality research papers, case studies, review papers, experimental and empirical papers, and shortened thesises/ dissertations in the broad area of engineering and technology.

The Journal is specifically dedicated to publish novel research contributions and innovative research outcomes in the following fields of engineering and technology: -

- Intelligent Computing and Information Technology,
- Mechanical and Metallurgy Engineering,
- Architectural Design and Town Planning,
- Civil and Transport Engineering Systems,
- Electrical Engineering and Power Electronics,
- Emerging areas of Renewable Energy
- Papers related to allied disciplines, emerging technologies, and future-generation engineering will be given priority for publication.

The Journal publishes papers from worldwide sources, especially for covering the emerging issues of engineering and technology from developing and developed countries. The Papers from African continent countries having localized problem-solving research will be given priority.

Table of Contents

About EIJETVII
Modelling for Multiport Converter-Based Hybrid Power Supply using Renewable Energy
Source Applications1
Yalisho Girma ^{1*} , Dr. Ing. Getachew Biru ² , CS. Reddy ¹
Biomimetic Architecture: An Innovative Approach to Attain Sustainability in a Built
Environment36
Zeeshan Haider Khan ^{1*} , Mohammad Salman ² , Alemea Girma ³
Pulmonary Disease Identification and Classification using a Deep Learning Approach 46
Minalu Chalie ^{1*} and Zewdie Mossie ¹
Numerical Investigation of Reinforced Concrete Beam Containing Iron Ore Tailings as Partial Replacement of Sand
Mahmud Abubakar ^{1*} , Muhammad Idris Haruna ² , Hassan Shuiabu Abdulrahman ¹ Bala Alhaj Abbas ¹
Designing an Exploratory Indigenous Knowledge Management Framework for Soil Conservation Mechanism in the Konso Community71
Amin Tuni Gure ¹ *, Addisu Mulugeta Hailu ² , Eyasu Tafere Amenu ² 71

ISSN (E): 2959-3921

(P): 2959-393X

DOI: https://doi.org/10.59122/144CFC13



Copyright and License Grant: CC By 4.0



Volume 1, Issue 2, 2023

Modelling for Multiport Converter-Based Hybrid Power Supply using **Renewable Energy Source Applications**

Yalisho Girma^{1*}, Dr. Ing. Getachew Biru², CS. Reddy¹ ¹Adama Science & Technology University (ASTU), Ethiopia ²Addis Ababa Institute of Technology (AAiT), AAU, Ethiopia *Corresponding Author's Email: yalishogirma1983@gmail.com

Abstract

This study focuses on the design and modeling of a multiport converter-based hybrid power supply that uses solar PV to meet the needs of a small village. The village has a maximum power demand of 50 kW, serving twenty households. The first converter in the proposed multiport system is a high-frequency isolated DC-DC converter powered by an HVDC link, producing an output of 240 VDC. This converter employs a medium-frequency transformer with converters on both the primary and secondary sides, arranged in an input-series output-parallel (ISOP) configuration. Its output is connected to a solar PV and battery system through a buck-boost converter. The second converter is a three-phase modular inverter powered by the solar PV system, designed to supply an AC line voltage of 0.415 kV. The inverter is driven by a solar PV module with an open-circuit voltage of 85 V and a maximum power output of 415 W. To evaluate the system's performance, scenarios involving changes in load and solar irradiance were analyzed. Performance was measured using indicators such as output voltage THD, current distortion, variations in converter output voltage, current magnitude, and overall efficiency. The system was modeled and simulated using the Simulink/PLECS (Piecewise Linear Electrical Circuit Simulation) platform. The simulation results indicate that the proposed multiport converter system serves as a promising alternative to the traditional low-frequency distribution transformer.

Keywords: DC-DC Converter, Hybrid Power Supply, MMC, Multiport Converter, Solar PV, Distribution Transformer

I. Introduction

The high carbon emission due to the use of fossil fuel-fired power plants, coupled with high environmental concerns in recent times pushed the conventional electric distribution system to integrate more and more renewable energy sources (RES) and modern energy distribution infrastructures. Integrating renewable energy sources (RES) into conventional electrical distribution systems requires the active involvement of power electronic converters. Traditional centralized distribution systems depend on low-frequency

(P): 2959-393X

Volume 1, Issue 2, 2023

DOI: https://doi.org/10.59122/144CFC13

Copyright and License Grant: CC By 4.0



transformers, which are unable to meet the additional demands of modern networks. Today's distribution systems require bidirectional power and data flow, seamless integration of distributed energy resources and energy storage, load compensation, and improved power quality and reliability.

A multiport power electronic converter-based power supply system can be viewed as an alternative option to a low-frequency transformer to supply both DC and AC loads. In the multiport converter-based power supply system, both DC port and AC port are available, with the function of using distributed energy resources (Solar PV, battery energy system, micro-wind, etc.), AC loads, and DC loads. An isolated DC-DC converter contains a pulse-width modulated inverter at the primary side, a high-frequency transformer, and a PWM secondary rectifier. The input to the isolated DC-DC converter can be an HVDC or modular rectifier connected to the AC grid. The presence of HFT greatly reduces the size and volume of the system to be designed. The modular multilevel inverter is another key element in the multiport converter-based power supply. This component takes a DC input voltage at the output of the DC-DC stage or solar PV and converts it into AC.

Since disturbances in the low-voltage (LV) grid often occur due to the frequent switching on and off of heavy loads, an output grid filter—both common-mode and differential-mode—is required. Using readily available power switches with low blocking voltages (1.2 kV, 1.7 kV, and 3.3 kV) is a well-established and widely adopted industrial practice for developing power processing converters at this stage. However, this stage also faces challenges related to high current. To manage the high current demand, interleaved PWM and input-series output-parallel (ISOP) converter topologies can be employed.

The presence of a neutral conductor is another essential requirement at this stage, as low-voltage distribution networks typically follow a Terra-Terra (TT) configuration. Additionally, load imbalance and non-linearity—both of which generate zero-sequence currents—must be effectively addressed in three-phase three-wire or three-phase four-wire systems. The most suitable inverter topologies for this application include the conventional two-level voltage source inverter (VSI), the three-level neutral point clamped (NPC) inverter, and the T-type inverter [1].

However, two-level and three-level converters are associated with high conduction losses, switching losses (both turn-on and turn-off), and significant dV/dt stress due to the need for high-frequency operation. To develop highly efficient and reliable inverters, modular inverter configurations such as Cascaded H-Bridge (CHB) or Modular Multilevel Converter (MMC) topologies with low switching frequency operation can be utilized.

Volume 1, Issue 2, 2023

DOI: https://doi.org/10.59122/144CFC13

(P): 2959-393X



Copyright and License Grant: CC By 4.0



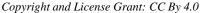
CHB- and MMC-based modular converters offer several advantages, including modularity at both the cell and phase levels, simple voltage and power scalability through the combination of identical cells, and the use of a single capacitor for energy storage in each module. They also enable faulty cells to be easily bypassed during faults, providing fault ride-through capability. Additional benefits include low dV/dt, reduced electromagnetic interference (EMI), cost-effectiveness, good transient response, and the use of commonly available low-voltage power switches. However, these advantages come at the expense of requiring a larger number of passive and active components compared to non-modular systems [2]–[4].

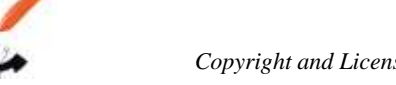
The CHB-based modular inverter requires separate cell voltage, and this may cause complexity in system size and control design. A modular inverter based on MMC topology doesn't need a separate module DC voltage and hence is the focus of this research. A literature survey shows that different PWM techniques have been discussed to operate a modular inverter [2]-[4]. Sub-module capacitor voltage unbalancing is a common problem in MMC and studies conducted [6] have justified the causes of capacitor voltage balancing problems and the strategy to reduce the problem. The input source to the MMC MMC-based modular inverter can be a solar PV battery bank in this research as the location of the project site (Arba Minch) has good solar energy potential as compared with other RES such as wind. The design and modeling of a multiport converter-based hybrid power supply for the small village (Ayssa Residence) in Arba Minch City is the focus of this study.

The remaining sections of this paper are organized as follows: Section Two presents a description of the study area and the layout diagram of the proposed system. Section three includes research methodology, a review of the converter configurations, the basic working principles, a mathematical approach to analyzing MMC, multicarrier PWM techniques, solar PV sizing, and the design of a buck-boost DC-DC converter. Simulation results and a discussion of the proposed system for different scenarios are covered in Section 4. The last section of the paper is the conclusion.

II. Description of Study Area Site

The design research is done for Aysa's common residents, located in Arba Minch city and depicted in Fig. 1. The residence is located 7km from the main distribution substation and contains twenty (20) households having a connected load demand of 10kW per household, giving a total of 200kW. Each household has a maximum demand of 4kW and a system maximum demand of 50kW is obtained by considering a diversity factor of 1.6.







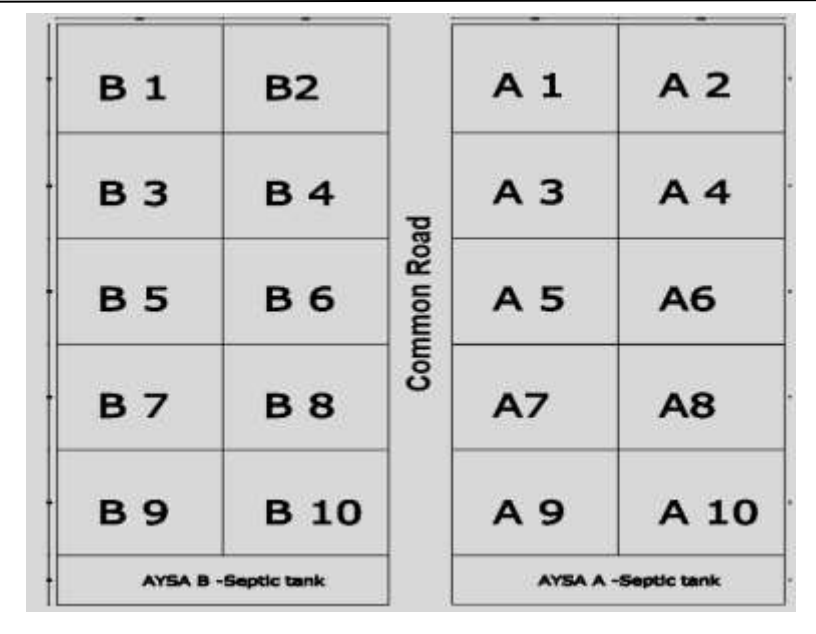


Fig. 1.: Description of Study Area (codes represent household buildings)

The proposed DC-AC hybrid power supply based on a multiport converter for the village is shown in Fig. 2.

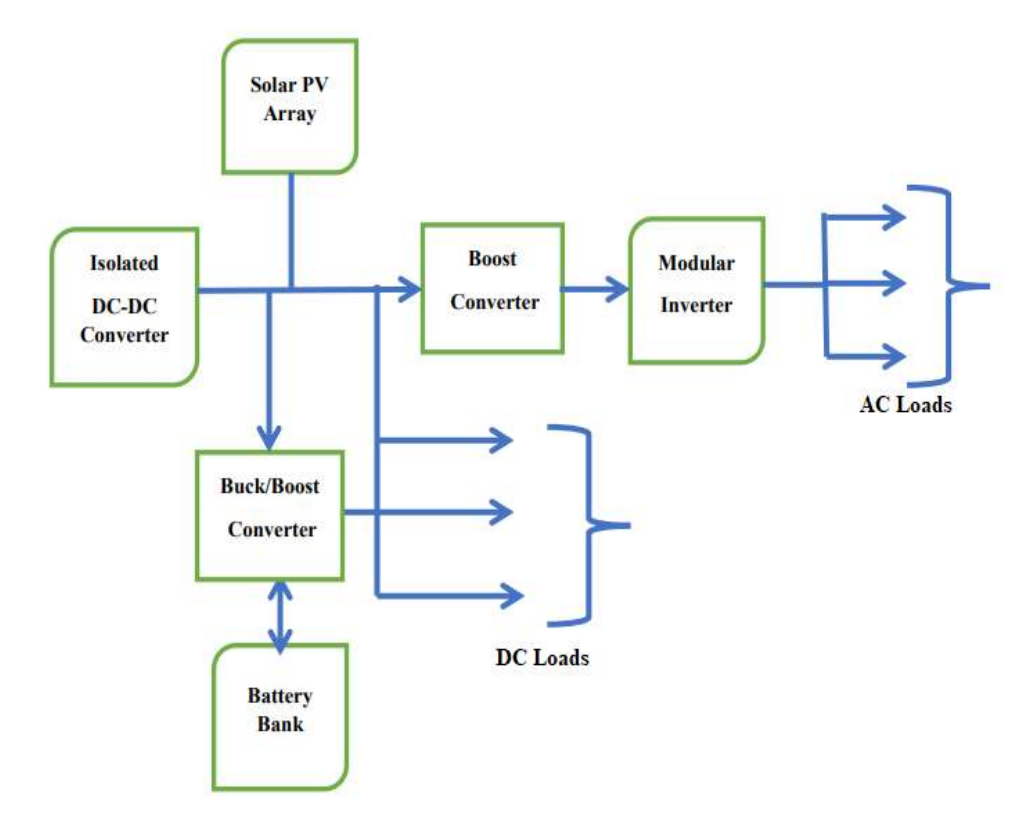


Fig. 2.: Layout of Proposed Multiport Converter-Based Hybrid Power Supply System







Volume 1, Issue 2, 2023

III. **Research Methodology**

This research used modeling and simulation to assess the performance of different converters. The power and modulation circuits of the system were modeled using the Simulink/PLECS simulation package, and their performance was tested under various conditions, including changes in load demand and solar irradiance. Key performance indicators, including output voltage distortion, current THD, and efficiency (losses), were analyzed. The study focuses on supplying a 50 kW load but can be scaled up for higher loads by adjusting the number of submodules per phase, as well as the number of PV modules and batteries.

A. Configuration of Isolated DC-DC Converter

The primary converter in the DC-DC stage receives 24.5 kV from the HVDC transmission network. Several converter topologies, such as standard DAB and MAB in both symmetrical and asymmetrical configurations, can be used. A three-phase DAB can also be applied at this stage, which helps reduce the size of the low-voltage capacitor. In this study, a symmetrical DAB in an ISOP configuration (Fig. 2) is selected for the DC-DC stage, and its performance is evaluated for comparison. The low-voltage DC output from this stage, which is supplied to the modular inverter, is 750 V. The efficiency of this stage depends on factors such as the type of transformer (three-phase or single-phase), its design, core material, and winding configuration. This stage operates at a high frequency, which helps reduce the size of passive components and space requirements. However, since high-voltage isolation limits the operating frequency, a maximum switching frequency of 20 kHz is recommended [19].

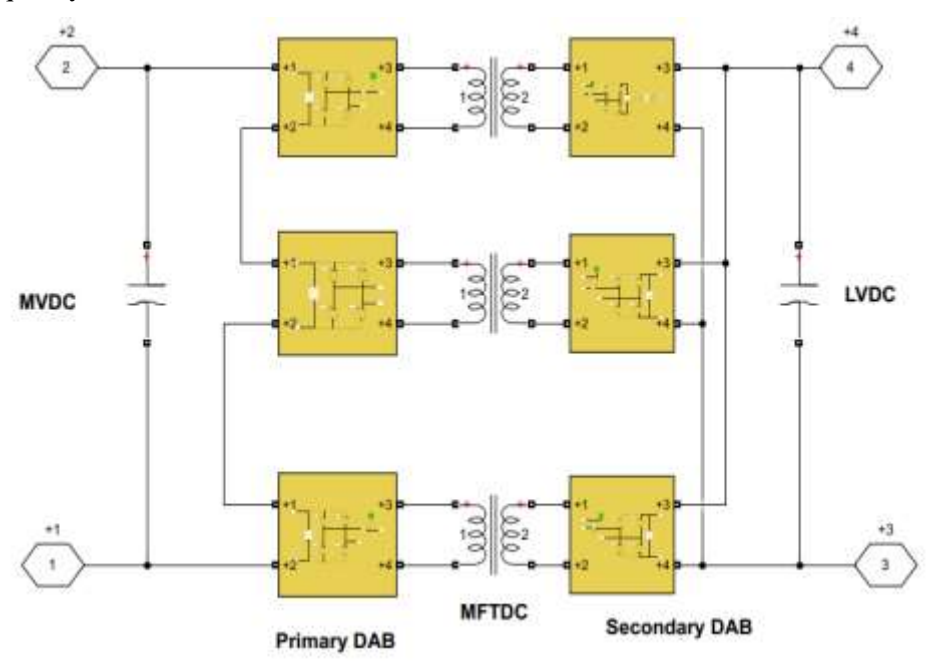


Fig. 2.: Isolated DC-DC Converter in ISOP Configuration

ISSN (E): 2959-3921

DOI: https://doi.org/10.59122/144CFC13

Copyright and License Grant: CC By 4.0



Volume 1, Issue 2, 2023

B. Primary and Secondary Side Converter Parameters for Proposed Topologies

As shown in the basic specification Table I of the DC-DC stage, the input to the PWM inverter or primary DAB is 24.5kV. For the DAB ISOP configuration shown in Fig. 2, the DC link voltage is shared equally in three primary DAB circuits. The peak rectangular AC voltage to each primary DAB should be slightly lower than the DC input to avoid over-modulation. Therefore, a value of 24.5 kV/3 = 8.2 kV is chosen as the peak AC rectangular voltage for each primary converter. The RMS value of primary DAB is calculated as:

$$V_{RMS(P)} = \frac{8.2kV}{\sqrt{2}} = 5.8kV \approx 6kV$$
 (1)

Assuming that total power(S) is shared equally among the three primary DABs, the RMS primary currents for the three proposed configurations can be obtained as:

$$I_{RMS(P)} = \frac{S/3}{V_{RMS(P)}} = 2.77A \approx 3A$$
 (2)

The LVDC requirement as given in the basic specification Table I, is 240V because at this stage, renewable energy resources such as PV can be interfaced. The MFT output (Secondary side) AC RMS voltage should be slightly less than the output LVDC voltage to avoid over-modulation. If we select a value of 230V, the MFT secondary peak voltage is $230V * \sqrt{2} = 325V$.

The MFT turns ratio is given by $\frac{V_P}{V_C} = 36:1$

In DAB ISOP configurations, the value of the secondary side current is shared among the parallelconnected secondary DABs as a result of power sharing among the three secondary side converters

$$I_{RMS(S)} = \frac{S/3}{V_{RMS(S)}} = 72.5A$$
 (3)

Based on the above analysis, the semiconductor switch ratings of the primary side and secondary side converters with sufficient consideration of safety factors are summarized in the Table I below.

Table I: Switching Device Parameter for DC-DC Stage

Primary side Voltage = 10Kv					
Device PN and	I(A)	Ron $(m\Omega)$	Eon/E-off	VG(V)	Configuration
Company			(mJ)		
CPM3-10000-	20	300	6/1		DAB_ISOP,
0270 (CREE)					
Secondary side Voltage = 900V					



Copyright and	License	Grant:	CC By 4.
---------------	---------	--------	----------



Device PN and	I(A)	Ron (mΩ)	Eon/Eoff(mJ)	Vf (V)	Configuration
Company					
SD11740	100	8.6	3.5/0.7		DAB_ISOP
(Solitron)					

C. Configuration of Modular Inverter

Two-level and three-level VSIs face issues such as high dV/dt and di/dt, as well as limited intelligent operation for activating or deactivating modules during partial loading of the distribution grid. A suitable solution to these problems is to use multilevel inverters that operate with low-voltage switches and low switching frequencies, as discussed in [7]. Several topologies can serve as basic building blocks, but the half-bridge submodule shown in Fig. 3 is chosen because it requires fewer switches and therefore results in lower switching and conduction losses.

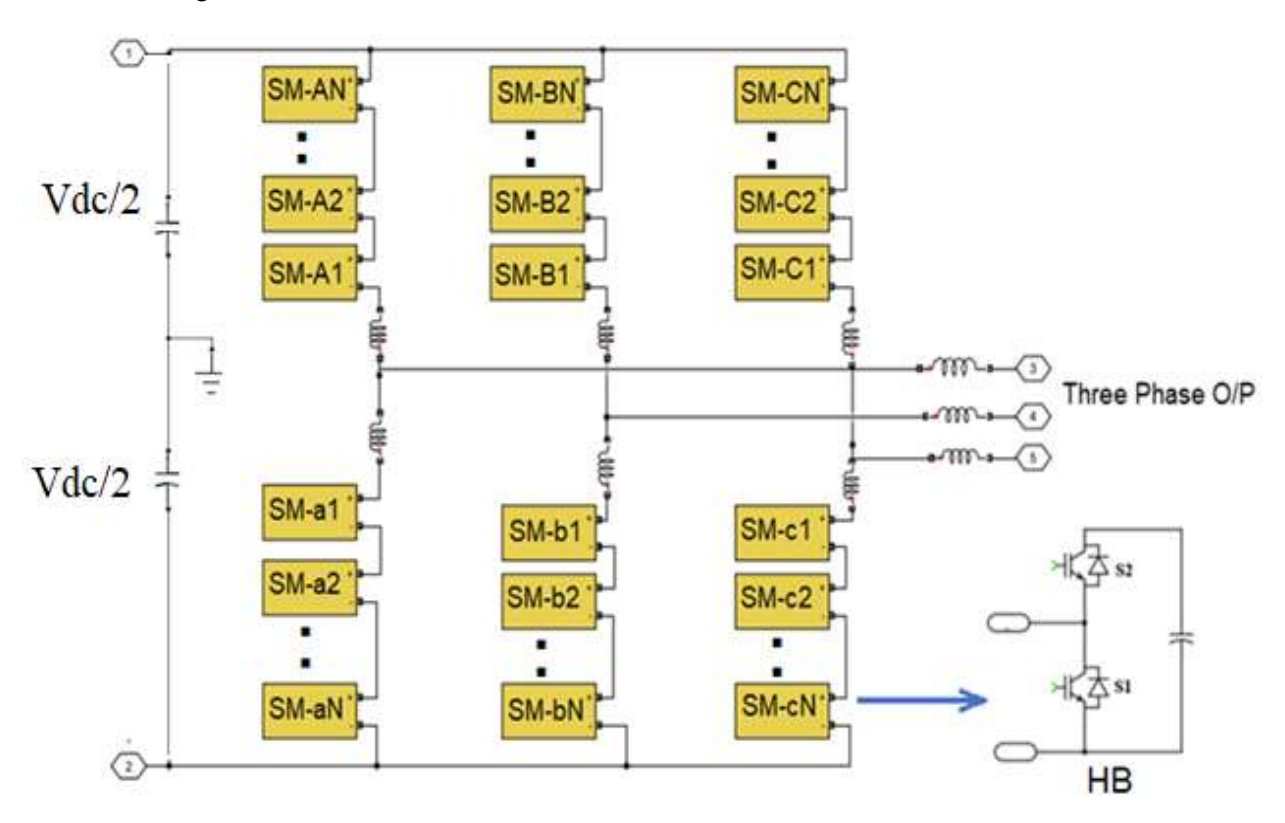


Fig. 3.: Modular Inverter

The half-bridge sub-module (HBSM) which is used as a basic building block can have four operation states based on the direction of current flow. When current flows into the capacitor or out of the capacitor, the sub-module is said to be in insertion mode, in which case current flows through the upper switch or upper diode. On the other hand, when current flows in the lower switch or lower diode, the sub-module is said to be in bypass mode, in which case the sub-module output voltage is zero.



Copyright and License Grant: CC By 4.0



1) Sizing of several sub-modules and passive components: - As shown in Fig.3, the MMC-based inverter is made of an N number of series connected sub-modules per phase leg. The phase legs contain arm inductance which limits the circulating current. The number of sub-modules per phase leg arm (N) is given by the equation below [8]: -

$$N \ge \frac{V_{DC}}{\eta V_{CFS}} \tag{4}$$

Where, V_{CES} is the semiconductor blocking voltage η is the de-rating factor and V_{DC} is the DC link voltage.

If the DC link voltage at the inverter input terminal is 750V, a MOSFET with a blocking voltage of 200V and a device de-rating factor of 0.909 is used in the above equation, the number of sub-modules per phase leg arm becomes four (4).

Submodule capacitance (C_{SM}) as a function of apparent power, power factor, average capacitor voltage, acceptable ripple, switching frequency, and modulation index and number of sub-module is given as follows [8]: -

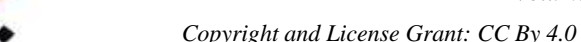
$$C_{SM} \ge \frac{S}{3NmV_C^2 \varepsilon \omega} \left[1 - \left(\frac{mCos\varphi}{2} \right)^2 \right]^{\frac{2}{3}}$$
 (5)

The phase-leg arm inductance helps filter out circulating currents and limits the arm current during a fault. Based on the maximum ripples in the circulating current, the arm inductance can be given by the following expression as discussed in [8]: -

$$L_{arm} \ge 0.25 \frac{U_{C,MAX}}{Nf_C \Delta i_{LMax}} \tag{6}$$

where $U_{C,Max}$ is the maximum voltage of an SM capacitor; $\Delta i_{L,Max}$ is the product of the maximum current ripple and the circulating current, N is the number of sub-modules and f_C is the switching frequency of each SM. It is a good practice to use the maximum current ripple of 15% as mentioned in [9].

The power electronic building block for the back-end converter is chosen based on the application type and the system's maximum-load current and voltage requirements. According to the power distribution specifications, the maximum load current is 70 A, and the line-to-line AC voltage is 415 V with a lagging power factor between 0.95 and 1. Therefore, MOSFETs with a blocking voltage of at least 200 V and a current rating of 130 A or higher are selected from manufacturers such as International Rectifier, Infineon, and others. A nine-level (9-level) back-end converter MMC topology is adopted for this project.





After reviewing the semiconductor device manufacturer's datasheet, the following power switch as depicted in Table II, was selected for simulation purposes:

Table II: Chosen Power Semiconductor Switches for the System

Device part number	Voltage rating (V)	Current rating(A) @25°C	Manufacturer
Power MOSFET	200	130	IR
(IRFP4668PbF)			

2) Converter power and semiconductor loss: - The input DC power to the converter and output AC power supplied by the converter can be related by:

$$P_{dc} = V_{dc}I_{dC} = P_{ac} + losses = 0.5m \frac{Vdc}{2}I_{pp}cos\alpha + Losses$$
 (7)

Power electronic system losses primarily originate from their components, including power devices and resistive elements (stray resistance). Due to the non-ideal nature of these components, three main types of losses occur: conduction losses, switching losses, and blocking losses. Among these, blocking losses—caused by minor leakage currents—are generally negligible and are often omitted in most analyses.

For power electronic devices that include a diode, such as MOSFETs with fast recovery diodes (FRD), losses must be calculated separately for the switch and the diode. Conduction losses occur when the MOSFET or FRD is on and carrying current. The conduction power loss is found by multiplying the onstate voltage by the on-state current. In applications using pulse-width modulation (PWM), this total conduction loss is further multiplied by the duty factor. The total conduction loss for a MOSFET with an integrated FRD can be expressed by the following equation.

$$Pcond(tot) = Pcond(IGBT) + Pcond(Diode)$$
 (8)

Pcond(MOSFET) =
$$\frac{1}{T} \int_{0}^{T} [V_{CE}(t) * I_{C}(t)] dt$$
 (9)

The average conduction loss of IGBT can be computed by the following equation:

$$Pav(cond) = V_{CE(S)} * I_C * \delta$$
 (10)

Where δ refers to the device duty cycle

The transitions of the MOSFET and FRD between on and off states do not happen instantly, which causes switching losses. During these transitions, both the current through the device and the voltage across it remain above zero, resulting in high instantaneous power losses.

(P): 2959-393X



Copyright and License Grant: CC By 4.0



Equations to determine the switching power losses for an IGBT and FRD are given below: -

$$Psw(MOSFET) = E_{ON} + E_{OFF} * f_{SW}$$
 (11)

$$Psw(FRD) = E_{rec} * f_{SW}$$
 (12)

The turn-on energy $(E_{\rm on})$, turn-off energy $(E_{\rm off})$ of the IGBT, and the reverse recovery energy $(E_{\rm rec})$ of the FRD depend on factors such as collector current, collector voltage, gate resistance, and junction temperature.

It is important to normalize the switching losses for any application using the nominal values and conditions provided in the device datasheet.

$$Psw(MOSFET) = \left(\frac{E_{ON} + E_{OFF}}{\pi}\right) * f_{SW} * \frac{I_{pk}}{I_{nom}} * \frac{V_{DC-link}}{V_{nom}}$$
(13)

$$Psw(FRD) = (E_{rec}/\pi) * f_{SW} * I_{pk}/I_{nom} * V_{(DC-link)}/V_{nom}$$
 (14)

By calculating the switching and conduction losses of the IGBT and FRD, the total loss can be determined, which helps in evaluating the system's efficiency and estimating the junction temperature of the devices.

$$P(tot) = P_{cond}(MOSFET) + P_{SW}(MOSFET) + P_{cond}(FRD) + P_{SW}(FRD)$$
 (15)

A piecewise linear electronics circuit system (PLECS) uses a lookup table, formula, or a combination of the lookup table and formula approach to determine conduction and switching losses [10]. The lookup approach estimates device loss values using interpolation and extrapolation methods based on data points from the datasheet. The novelty of this research lies in integrating device thermal models with converter efficiency calculation models. The thermal model for a single MOSFET with an integrated FRD is shown in Fig. 4. For power electronic systems with multiple switches, the same method can be applied using a common heat sink shared by all semiconductor switch packages. To calculate system efficiency, the periodic average of conduction losses and the periodic impulse average of switching losses obtained from probe outputs are combined, as illustrated in Fig. 5 [10].





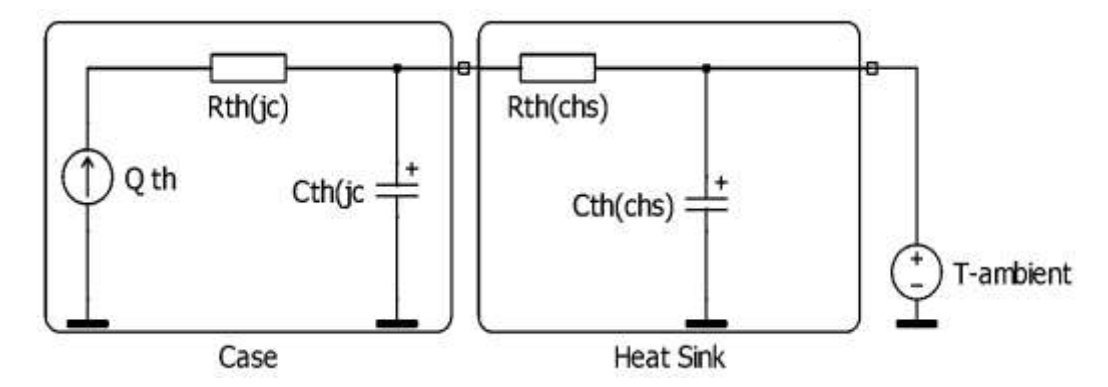


Fig. 4.: Thermal Model of a Single Semiconductor Device

Using the thermal data provided by the device manufacturer, switching and conduction losses are calculated through a combination of look-up tables and formula-based computations.

The converter efficiency calculation diagram shown in Fig. 5 uses thermal loss values to determine the system's efficiency. The efficiency analysis is performed using the thermal model of selected silicon carbide power MOSFETs. For the MMC converter, this is done by combining lookup tables and formulas for a maximum load current and a case temperature of 100°C. All thermal parameters are taken from the device manufacturers' datasheets [8], [11], [14]. Using the efficiency calculation model in Fig. 5, the switching loss, conduction loss, and total semiconductor loss of the converter for the selected submodules are calculated.

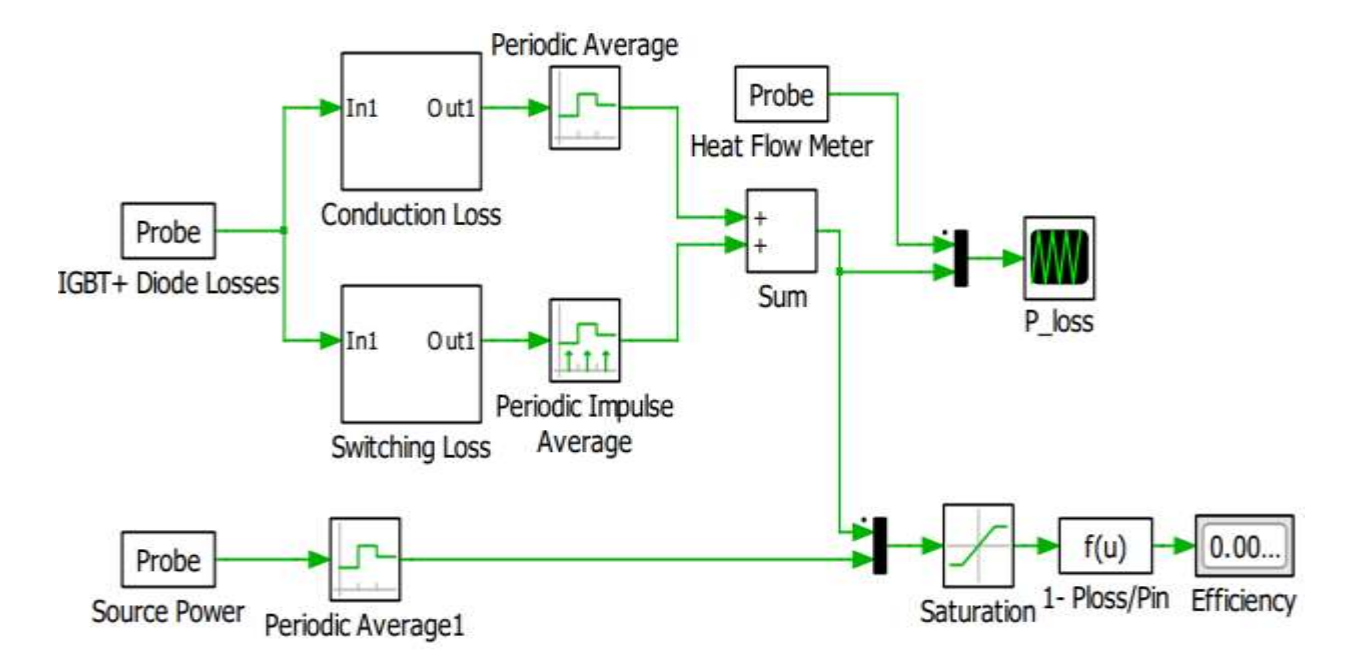


Fig. 5.: Efficiency Calculation Diagram

(P): 2959-393X

DOI: https://doi.org/10.59122/144CFC13



Copyright and License Grant: CC By 4.0



The efficiency of the converter system, as depicted in the model, is calculated as follows: -

$$\eta = \frac{P_{out}}{P_{in}} \tag{16}$$

Expressing P_{out} as a difference of P_{in} and power loss, the above expression is written as

$$\eta = \frac{P_{in} - P_{loss}}{P_{in}} \tag{17}$$

D. Modulation Method

Many modulation methods such as PSPWM, triangular PWM, and trapezoidal PWM are proposed for isolated-stage DC-DC converters, of which PSPWM is the most widely used one [12]. Among many modulation techniques for MMCs proposed by many researchers, multi-carrier pulse width modulation methods such as level-shifted PWM(LSPWM) and phase-shifted pulse width modulation (PSPWM) are frequently employed for MMC-based modular converters made of low-voltage modules.

In level shift, the PWM distribution of the switching signal is uneven and hence creates uneven switching losses and unbalance of sub-module capacitor voltage. It needs a capacitor balancing algorithm which adds complexity to the modulation circuit as the number of voltage levels increases.

In the case of PS-PWM, the SM capacitor voltage is balanced with a PI controller, and the need to use a sorting algorithm can be avoided. Moreover, the switching signals are evenly distributed in the entire submodules, resulting in an equal distribution of switching losses in the converter. The advantage of PS-PWM over LS-PWM is highly observed if the required output voltage level number is large [12]-[14].

To generate the switching signals for a multilevel converter having "N" sub-modules per leg arm, the "N" number of carrier signals is required. The phase difference between consecutive carriers can be found using the equation below:

$$\theta = 360/N \tag{18}$$

However, to produce an output voltage having 2N+1, the signals between upper arm and lower arm submodules have a phase difference given by

$$\theta = \frac{180}{N} \tag{19}$$

Phase-shifted PWM signals are generated by comparing the reference voltage (modulating signal) with a triangular waveform (carrier signal) within a comparator block. This comparison determines the converter's switching sequence: the comparator outputs a high signal (1 = switch ON) when the triangular wave exceeds

Copyright and License Grant: CC By 4.0



the reference voltage, and a low signal (0 = switch OFF) when it is lower. The switches in each leg of the HBSM and FBSM operate in a complementary manner to prevent short circuits. To avoid switching overlap between the upper switch and lower switch in the sub-module, a small dead time (delay time) is added to the PWM signal after the comparator block. The PS-PWM signal generation technique inside the comparator block for two sub-modules (N=2) is demonstrated by the signal diagram in Fig. 6 [14].

Using an MMC-based back-end converter allows the number of output voltage levels to be doubled within the same structure. This is achieved by applying interleaved phase-shift modulation with a π phase angle between the upper and lower arm carriers. This feature of MMC-based BEC gives output voltage with better THD values [15].

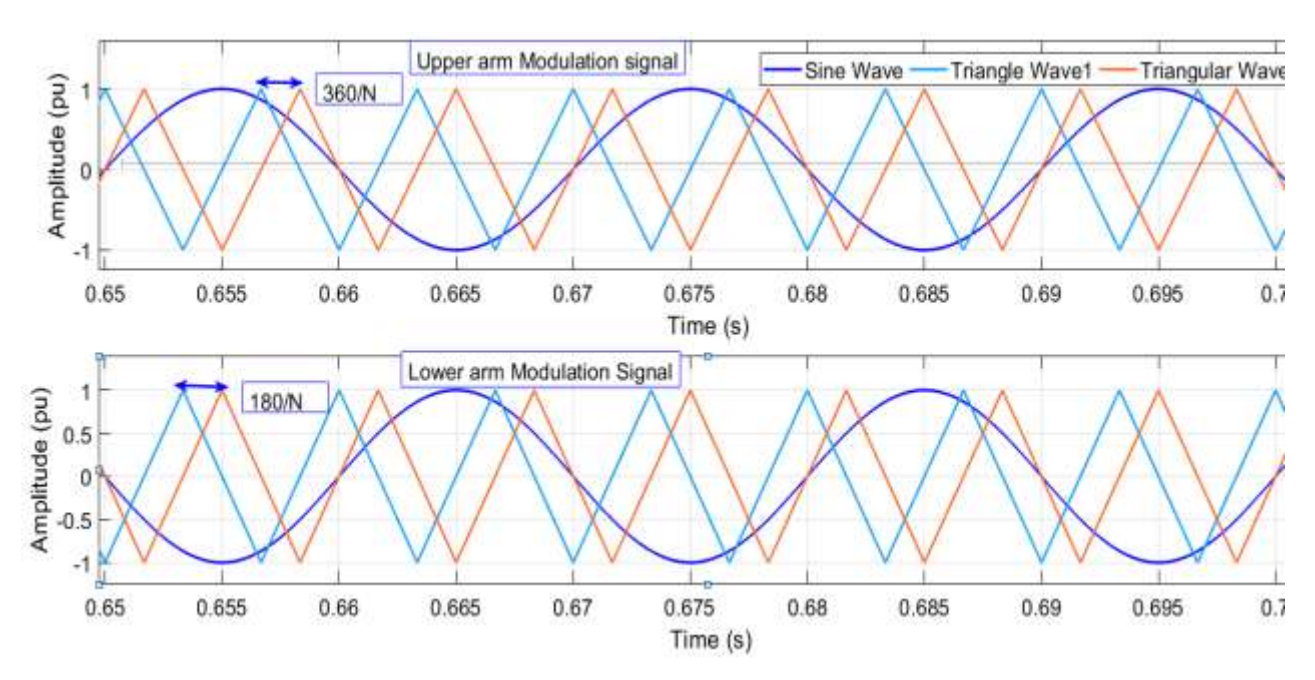


Fig. 6.: Interleaved Phase Shift Modulation

To leverage this advantage, the interleaved phase modulation technique is employed in this project.

E. Solar PV Array Sizing

Solar PV as a renewable energy source is drawing much attention in the day-to-day life of the global power industry. This is because of its free, clean, abundant, green nature, and low running cost characteristics. The maximum irradiance at a 15-degree tilt angle in Arba Minch is 2006W/m². However, the average global irradiance per day varies between 500 to 1000 W/m².

The PV system faces two main challenges. First, its power generation efficiency is low. Second, the amount of electricity produced by solar panels keeps changing due to variations in sunlight caused by clouds, birds,



trees, and other obstacles. The current-voltage (I-V) characteristic of a PV array is nonlinear and changes with both sunlight intensity and temperature. When sunlight changes, it mainly affects the current generated by photons, with little impact on the open-circuit voltage. In contrast, temperature changes have a greater effect on the open-circuit voltage, while the short-circuit current changes only slightly. There is a specific point on the I-V or V-P curve called the maximum power point (MPP), where the PV system, including the array and converter, operate at its highest efficiency and delivers maximum output power. The exact position of the MPP is not constant but can be found using calculation models or search algorithms. However, by using maximum power point tracking (MPPT) algorithms [16], the PV system's efficiency and reliability can be greatly improved, as these algorithms continuously adjust the operating point of the PV panel to stay at the MPP according to changing irradiation and temperature conditions. An incremental conductance algorithm is used in the back-boost converter to handle the problem of MPPT. This algorithm compares the incremental conductance with the instantaneous conductance in the PV system. Based on the comparison, it adjusts the voltage, either increasing or decreasing it, until the maximum power point (MPP) is reached. Fig. 7 shows the power-voltage characteristics of the Sunpower-SPR-415E-WHT-D PV module at 25°C under different irradiance levels.

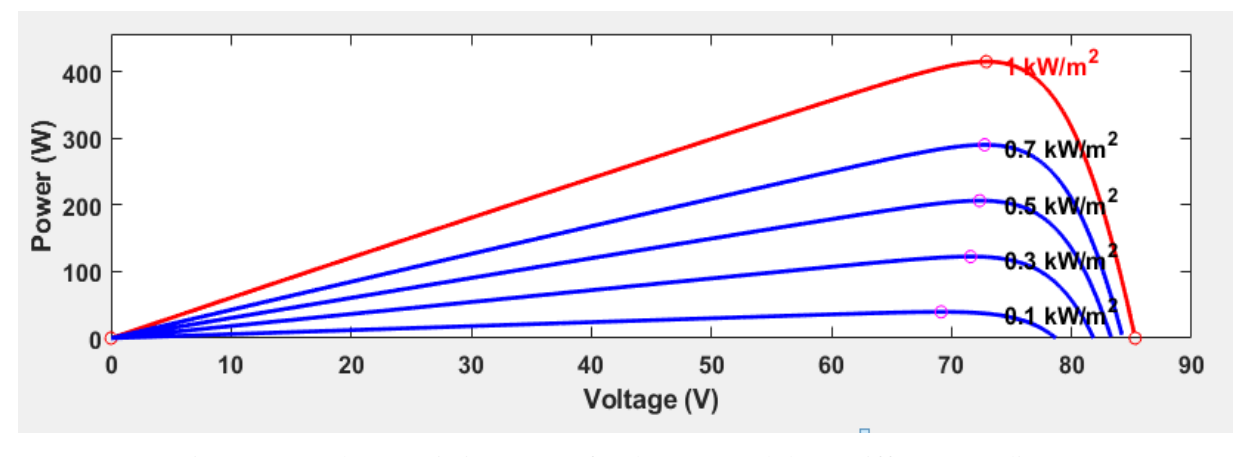


Fig. 7.: P-V Characteristic Curve of Solar PV Module at Different Irradiance

In this research, a solar PV module (Sunpower-SPR-415E-WHT-D) is used. The module has an open circuit voltage of 85.3V; voltage at maximum power is 73V and it has a maximum power of 414W. The designed system should supply a maximum power demand of 50kW, at 230V (PN). For an MMC-based modular inverter made of four modules, the input DC voltage should be 700V obtained from the output of the boost converter connected to the solar panel to get the 230V (PN) AC. The total number of solar PV modules required to supply the load is the ratio of load power demand to solar module maximum power.

No solar modules =
$$\frac{\text{Load demand}}{\text{Maximum power of Solar PV module}*\eta}$$
 (20)

(P): 2959-393X

DOI: https://doi.org/10.59122/144CFC13



Copyright and License Grant: CC By 4.0



If the efficiency of the PV array and that of the buck-boost converter is considered to be 85%, the total number of modules required is 166.

The series connected modules and parallel strings are decided by the total output voltage obtained at the solar PV array i.e., 240V.

No of series-connected modules =
$$\frac{\text{Array output Voltage}}{\text{Module voltage at Maximum power}}$$
 (21)

The total DC voltage requirement at the LV DC link is 240V and substitution of this value in the above equation gives the number of series connected modules to be $3.28 \approx 4$, which gives the number of parallel module strings to be 42.

F. Battery Sizing

The battery acts as an external energy storage unit that absorbs or supplies power depending on the instantaneous load condition. The charging and discharging rates are determined according to the standard specifications provided in the battery handbook. Lead-acid batteries are preferred for standalone applications because they are low-cost and easy to maintain. According to the handbook of the lead acid battery, the charging current of the battery should be less than 0.1CB, where "CB" is the capacity of the battery in ampere-hour (Ah). For a 200 Ah battery the charging current should not exceed 20 A [Battery Charging Current = $0.1 \times 200 = 20$ A]. Also, according to the battery handbook, the discharge current in tens of seconds should not exceed (0.5-0.7) CB and the nominal discharge is 0.1CB. Here (CB/5) is selected as the maximum discharge current. The sizing of the battery is similar to sizing the solar PV as done before in section 3.5. For a given load power to be delivered by the battery through a boost converter, the maximum capacity can be obtained as given below [17]: -

$$C_B = \frac{P_O}{0.1 * \eta_{Conv} * V_{Bat}}$$
 (22)

For a system load power of 50kW, buck-boost converter efficiency of 95%, and battery voltage of 24V, the total capacity of the battery is equal to 21930Ah. If the selected single lead acid battery has a capacity of **200Ah**, a total of **110** batteries are used to supply the system.

G. Buck-Boost Converter

The output voltage from solar photovoltaic (PV) panels is quite low, so it cannot be directly connected to a high-voltage load or the grid. To make this connection possible, a non-isolated DC-DC converter with high voltage gain is needed to interface with the solar PV system. The boost converter is placed between the modular inverter and the solar PV so that the output voltage remains fairly constant with variations in solar irradiance. In the absence of solar power, the system gets power from the battery storage system. During

ISSN (E): 2959-3921

(P): 2959-393X

DOI: https://doi.org/10.59122/144CFC13



Copyright and License Grant: CC By 4.0



normal operation (sufficient solar energy) the battery is charged through the buck-boost converter and stores energy. During night times and cloudy times, the stored battery power supplies the load through the boost converter. Depending on the charging and discharging condition of the battery sensed, the duty cycle of the buck-boost converter is changed. When the battery is in charging mode, the buck-boost converter operates in buck mode and when the battery is discharged, it operates in boost mode. The Duty cycle in charging mode is 0.12 and 0.90 when the battery is in discharging mode.

IV. Simulation Result and Discussion

A. Simulation of Isolated DC-DC stage

The input to this converter is an HVDC transmission network or grid-connected modular rectifier. If the input is obtained from a rectifier connected to the grid having a line voltage of 15kV, a maximum DC voltage of 24.5kV can be obtained, which feeds the isolated DC-DC stage and is depicted in Table III. Primary and Secondary DAB Voltage is depicted in Fig. 8.

Table III: Basic Specification of Isolated DC-DC Converter

Name of Converter	Parameter	Value
	Vin(nominal)	24.5kV DC
	Vout	240V DC
	P_{MAX}	50kW
Isolated DC-DC Converter	Switching frequency	20kHz
	Co	10mF
	Turns ratio	36:1

(P): 2959-393X

Copyright and License Grant: CC By 4.0



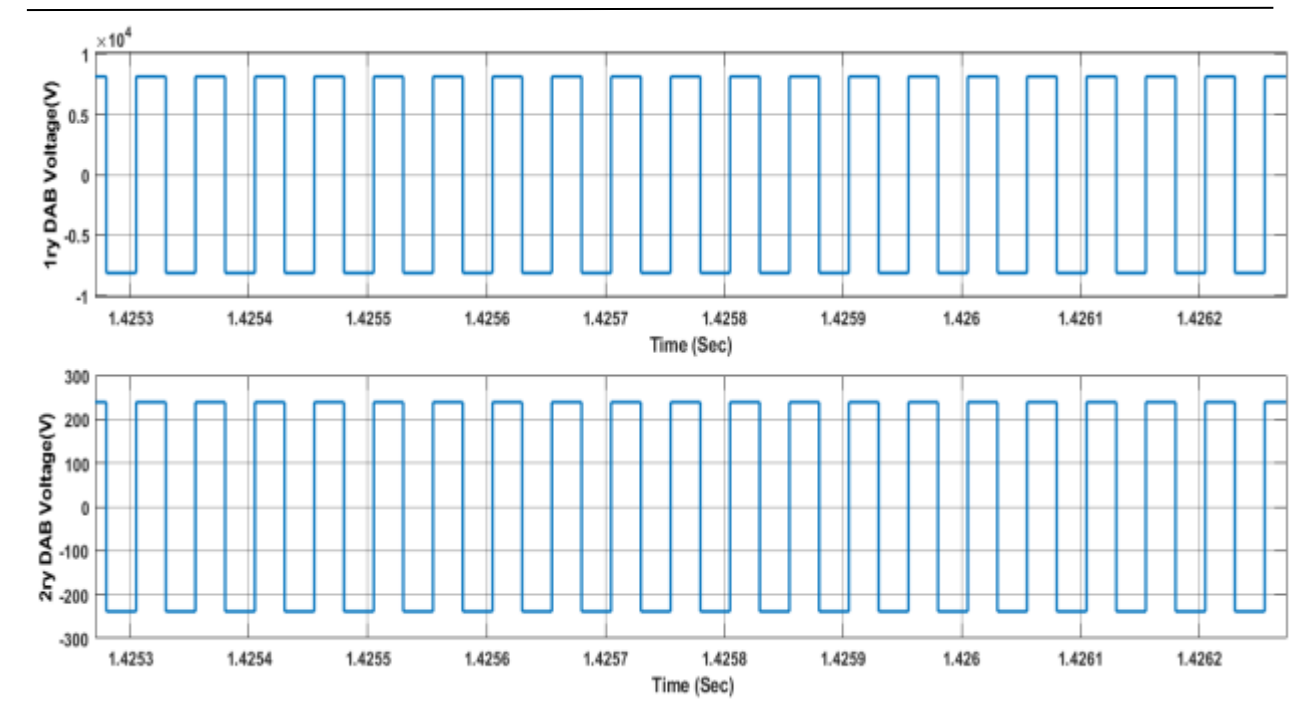


Fig. 8.: Primary and Secondary DAB Voltage

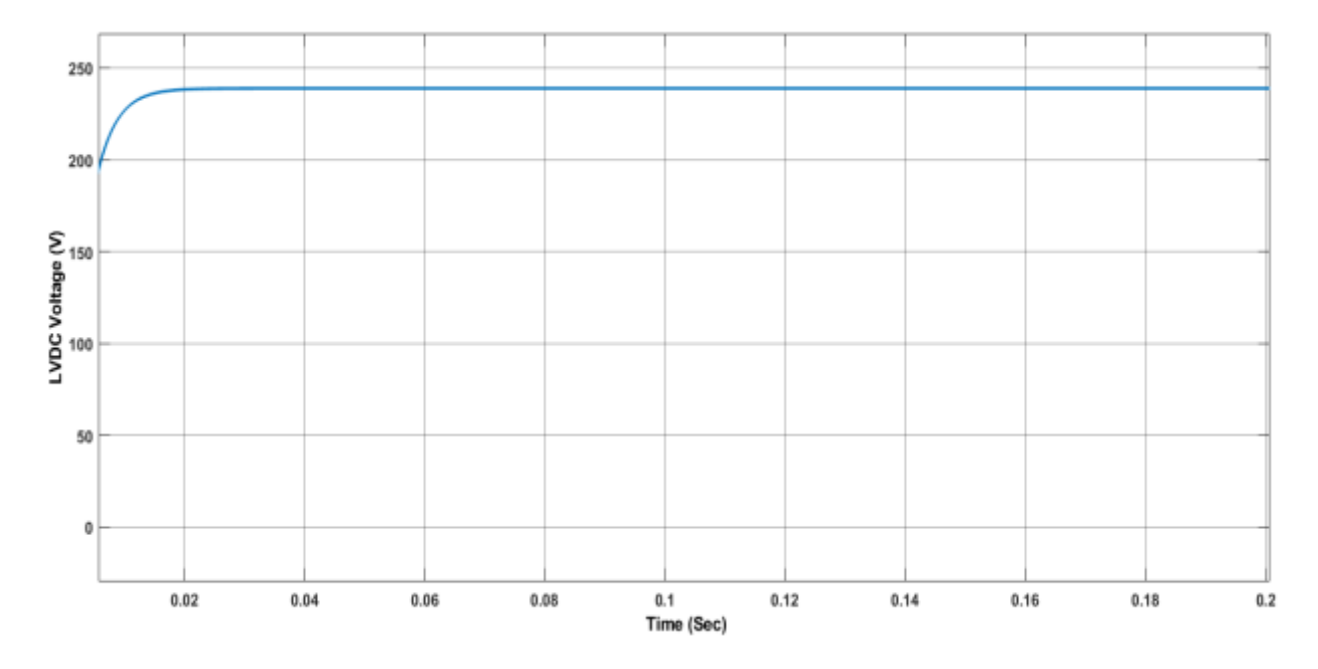


Fig. 9.: LVDC Voltage

Observation: As shown in Fig. 9 and Fig. 10, the primary DAB converters share a total input voltage of 24.5kV. Each DAB converter has a value equal to 8kV. Also, the secondary DAB has a peak voltage of 240V.

Copyright and License Grant: CC By 4.0



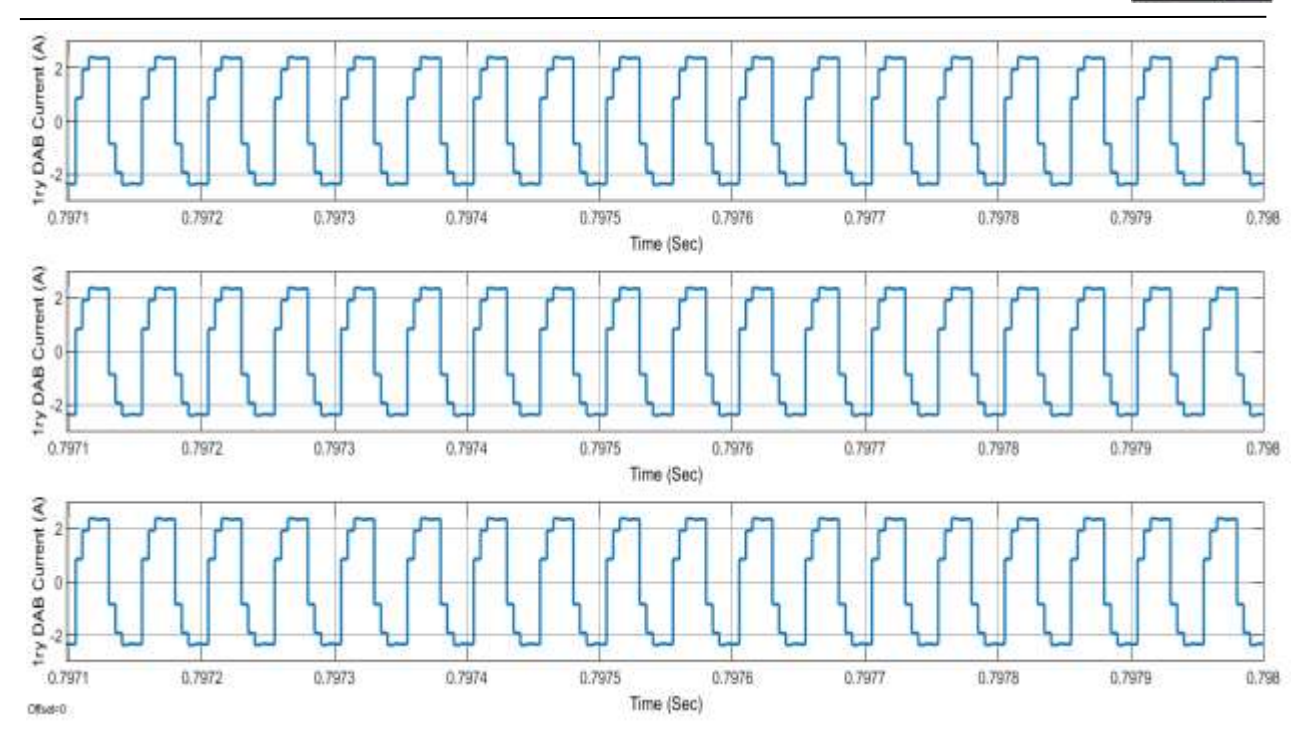


Fig. 10.: Primary DAB Currents

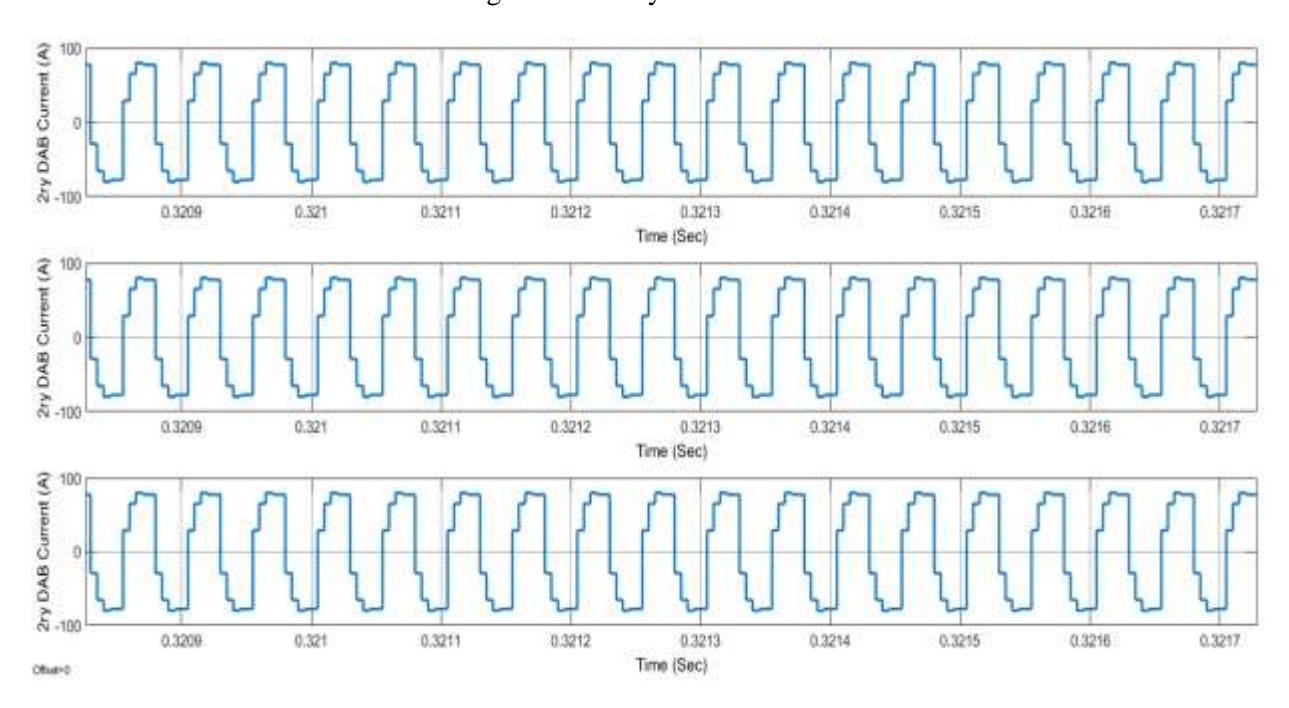


Fig. 11.: Secondary DAB Current

Volume 1, Issue 2, 2023

DOI: https://doi.org/10.59122/144CFC13

Copyright and License Grant: CC By 4.0



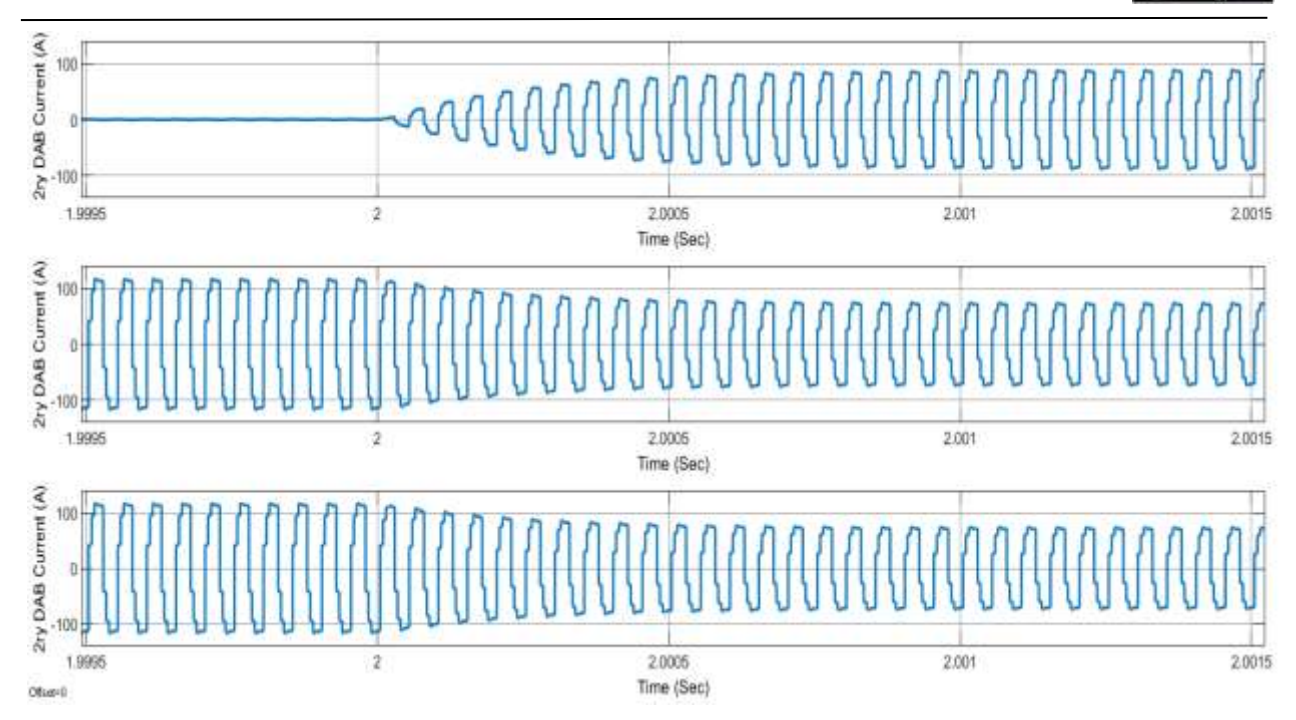


Fig. 12.: Secondary DAB Currents during Fault at DAB_1

Observation: As shown in Fig. 11 and 12, the three primary and secondary DABs share the load current equally when all are active. But, when there is a fault in any one of the DABs (secondary DAB in this case), the load current is shared among the un-faulted DABs as shown in Fig.12. This fault-tolerant feature of the system is very important in increasing the reliability of the overall system and reducing switching loss during light load conditions.

B. Simulation of Modular Inverter Fed with Solar PV

For simulating the models of modular inverters based on MMC topologies, three three-phase star-connected inductive loads (R-L load) having a maximum demand of 50kVA and a power factor of one (1) are used. Also, a maximum solar irradiance of 800W/m2 and a cell temperature of 45°C is used as an input parameter for the Solar PV array. A steady-state system analysis is used to see changes in output voltage and current.

In Tables IV and V, the parameter values of the distribution system, converters, and solar PV module are listed. These absolute values were incorporated into the Simulink /PLECS modeling to create the system.

ISSN (E): 2959-3921

(P): 2959-393X

DOI: https://doi.org/10.59122/144CFC13

Copyright and License Grant: CC By 4.0



Table IV: Technical Specification of Modular Inverter

Parameters	Value
Output AC Line Voltage(Vg)	415V
Load resistance (R _L)	$3.27~\Omega$
Load inductance (L _L)	5.5ηΗ
Maximum Power(S)	50kW
Load Power Factor	0.95 to 1 lagging
Sub-module arm inductance (L_arm)	3mH
Sub-module arm resistance (R_arm)	0.1 Ω
Sub-module arm capacitance $(C_{_SM})$	20mF
Capacitance at DC link (C_DC Link)	10mF
Distribution system frequency(f_g)	50Hz
Carrier frequency (fc)	1000Hz
Modulation index	1
Boost converter duty cycle (D)	0.68
Input DC Voltage to the inverter	240V
No of Sub-module per arm (SM)	4

Table V: Technical Specification of Solar PV Array and Its Accessories

Name of Component	Parameter	Value
	V(open circuit)	85.3V
0.1 DV/0 ODD 415E	V(@Maximum power)	73V
Solar PV(Sunpower-SPR-415E-	P _{Max} /Module	414.8W
WHT-D)	Maximum Irradiation	800kW/cm^2
	Cell temperature	45° C
	Capacity(C _B)	200Ah
Battery	I_{DCH}	$0.1C_B$
	V(open circuit)	26V
Buck-Boost Converter	Duty cycle	0.11/0.90

ISSN (E): 2959-3921

(P): 2959-393X

 Vin/V_{out}

DOI: https://doi.org/10.59122/144CFC13

Switching Frequency

Copyright and License Grant: CC By 4.0

5kHz

240V/24V(buck mode)



Volume 1, Issue 2, 2023

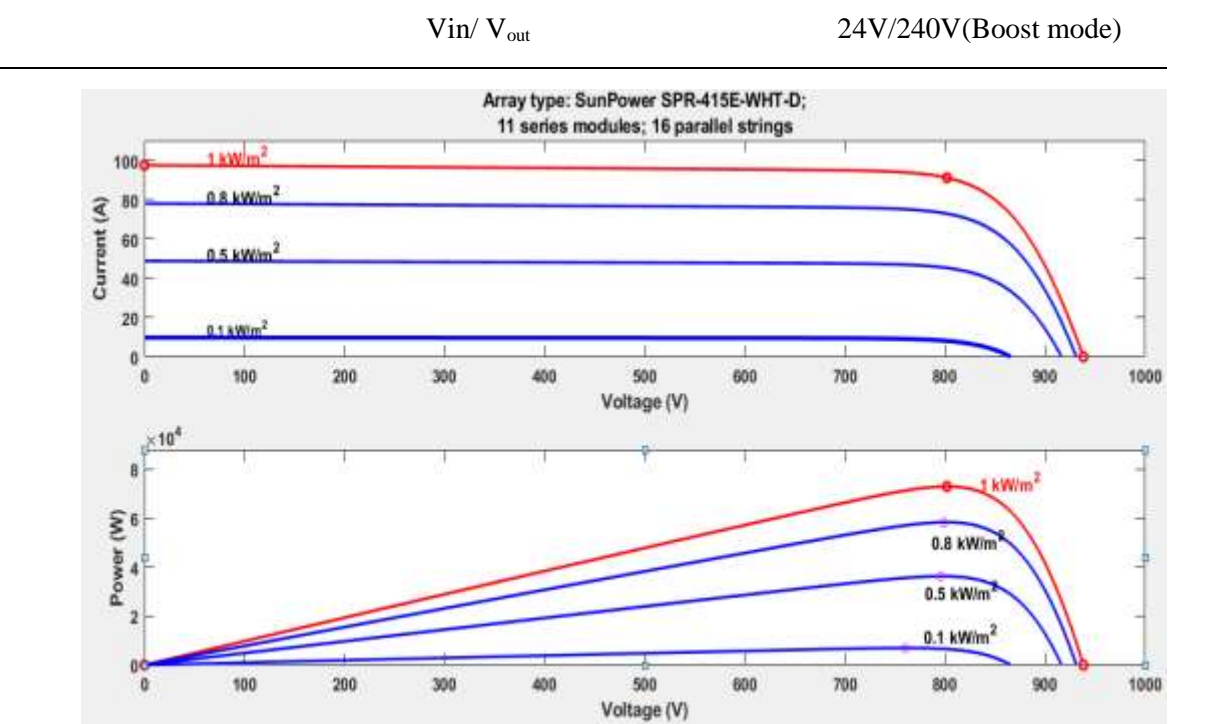


Fig. 13.: Power Versus Voltage and Current Versus Voltage Curve of PV Array

Observation: The PV array supplies the required maximum power demand of 50kW when the solar irradiance is 800w/m²

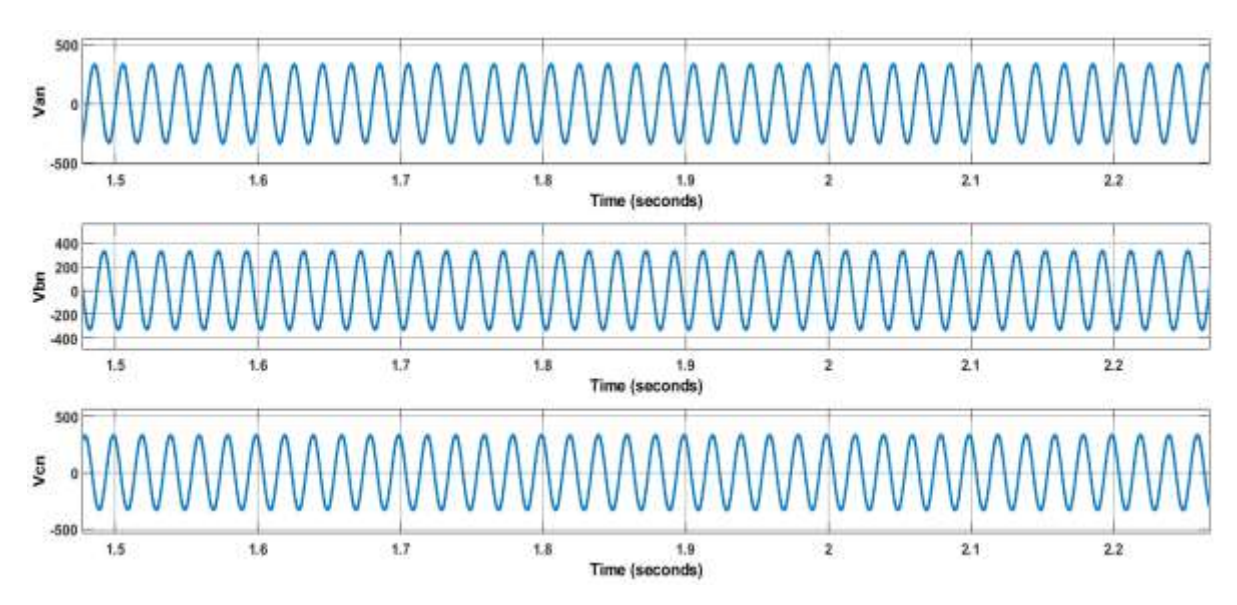


Fig 14. Voltage Wave Shape at Modular Inverter Output



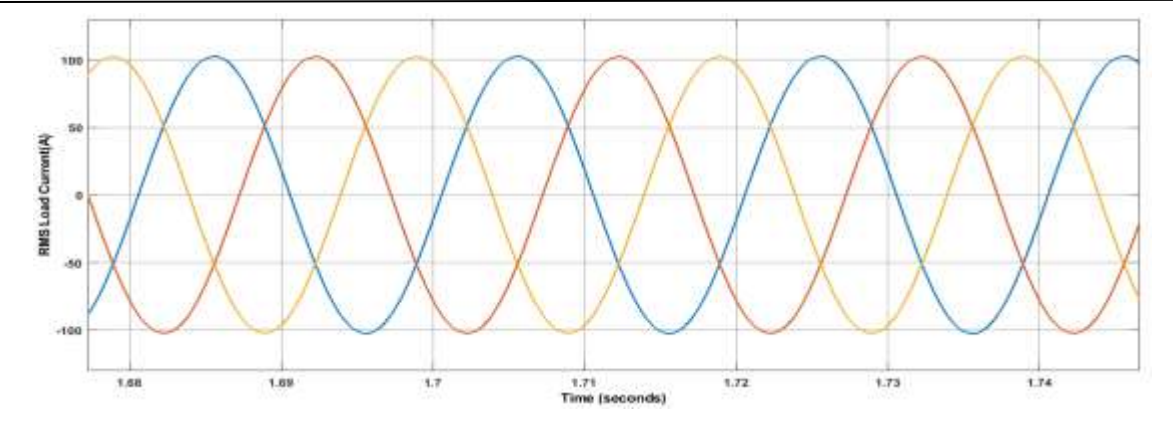


Fig. 15.: Three Phase Load Current Wave Shape of Modular Inverter

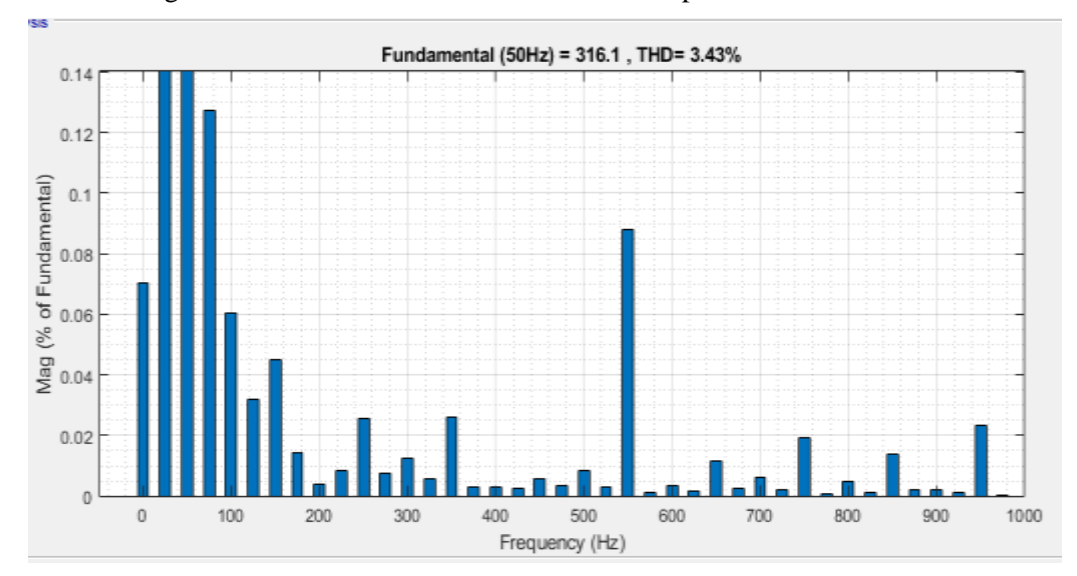


Fig. 16: Voltage THD at Modular Inverter

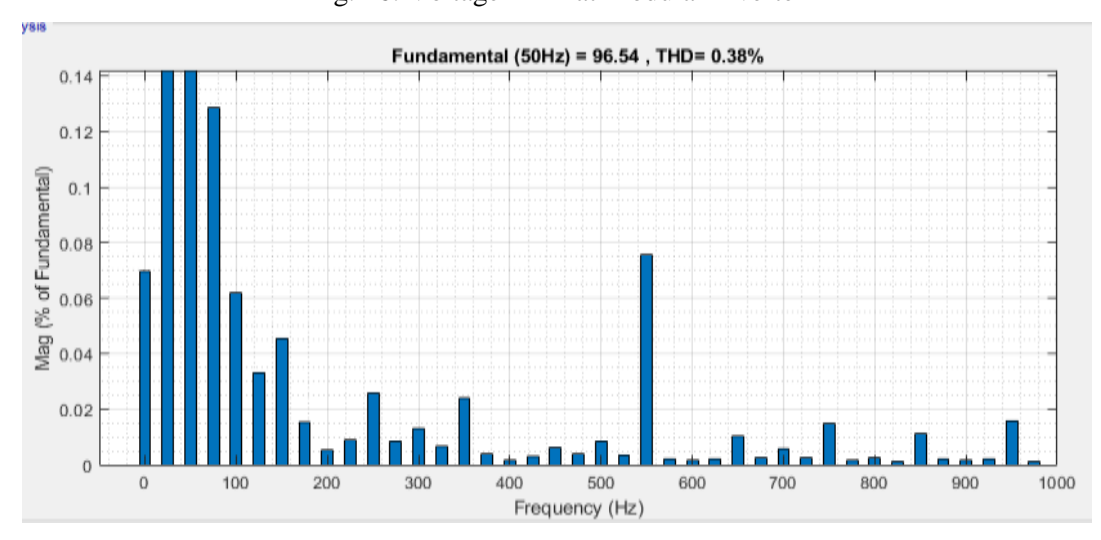


Fig. 17: Current THD at Modular Inverter Output

ISSN (E): 2959-3921

(P): 2959-393X



Copyright and License Grant: CC By 4.0



Volume 1, Issue 2, 2023

Observation: As shown in Fig. 14 to Fig. 17, the modular inverter output voltage is 230V (PN) when delivering a load current of 73A RMS. Also, the voltage and current THD values are 3.43% and 0.38% respectively, both within the IEEE 519-1992 benchmark. The losses happening in the converter and its achieved efficiency are presented in Table VI and Fig. 18 below: -

Table VI: Semiconductor Losses

Device Name	Switching Loss(W)	Conduction Loss (W)	Total Loss (W)	Efficiency (%)
MOSFET	1029.54	818.69	1848.23	96.63

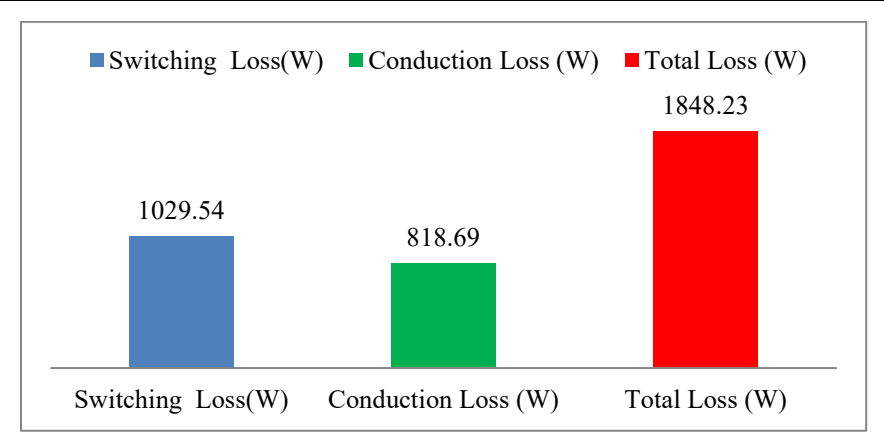


Fig. 18.: Switching and Conduction Losses

Based on the result in Fig. 18 and equation (27), the efficiency of the system is calculated to be 96.63%.

\mathbf{V} . Conclusion

In this research design modeling and technical evaluation of multiport converter-based hybrid power supply for a small village having a maximum demand of 50kW has been done. The multiport converter system contains an isolated DC-DC converter and modular inverter. The isolated DC-DC converter is based on DAB-ISOP configuration whereas the inverter is based on MMC. The DC-DC converter operates at a switching frequency of 20 kHz whereas the modular inverter operates at a switching frequency of 1 kHz. Both converters used a phase-shifted PWM to generate a gating signal. Solar PV array having an output voltage of 240V is used as input to the modular inverter. Also, the system is integrated with battery storage to increase the reliability of the whole system. The battery is charged and discharged through a buck-boost converter having a duty cycle of 0.11(buck mode) and 0.90(boost mode). Simulation results showed that the proposed system is a viable alternative to a low-frequency transformer with many ancillary services such as RES integration and improved availability.

Copyright and License Grant: CC By 4.0



Volume 1, Issue 2, 2023

References

- M. A. Hannan, P.J. Ker, M. S. Hossain L., Z. H. Choi1, M. S. Abd. Rahman, K. M. Muttaqi, and F. Blaabjerg, "State of the art of solid-state transformers: Advanced topologies, implementation issues, recent progress and improvements", *IEEE Access*, vol. 8, pp 19113-19132, Jan. 17, 2020.
- 2. L. Wei, L. Gregoire, J. Bélanger, "Control and performance of a modular multilevel converter system," *CIGRÉ Canada Conf. on Power Systems*, Halifax, Sept. 2011, pp. 1-8.
- 3. A. Lesnicar and R. Marquardt, "An innovative modular multilevel converter topology suitable for a wide power range," *Power Tech Conf. Proceedings, 2003 IEEE Bologna*, Italy, 2003, vol. 3, pp. 1–6.
- 4. L. F. Costa, F. Hoffmann, G. Buticchi, and M. Liserre, "Comparative analysis of mab dc-dc converters configurations in modular smart transformer," *IEEE 8th International Symposium on Power Electronics for Distributed Generation Systems (PEDG)*, April 2017, pp. 1–8. DOI10.1109/PEDG.2017.7972558
- 5. M. Hagiwara, K. Nishimura, and H. Akagi, "A medium-voltage motor drive with a modular multilevel PWM inverter," *IEEE Trans. Power Electron.*, vol. 25, no. 7, pp. 1786–1799, Jul. 2010.
- 6. L. Wei, L. Gregoire, J. Bélanger, "Control and performance of a modular multilevel converter system," *CIGRÉ Canada Conf. on Power Systems*, Halifax, pp. 1-8, Sept. 6-8, 2011.
- 7. Y. Zhang, G. P. Adam, T. C. Lim, S.J. Finney, B.W. Williams, "Analysis of modular multilevel converter capacitor voltage balancing based on phase voltage redundant states", *IET Power Electron.*, vol. 5, no. 6, pp. 726–738, July 2012.
- 8. Ali Shojaei, "Design of modular multilevel converter-based solid state transformers", M.S. Thesis, Dept. of Elect. and Compt. Eng., McGill Univ., Montreal, Canada, November 2014.
- 9. J. Kolb, F. Kammerer, and M. Braun, "Dimensioning and design of a modular multilevel converter for drive applications," *15th International Power Electronics and Motion Control Conf.* (*EPE/PEMC*), 2012, pp. LS1a-1.1-1-LS1a-1.1-8.
- 10. http://www.plexim.com (PLECS User Manual), Jan 14, 2022.
- 11. http://www.irt.com/pachage/ (IRFP4668PbF datasheet), Jan 14, 2022.
- 12. S. Debdnath, J. Qin, B. Bahrani, M. Saeedifard and P. Barbosa, "Operation, Control, and Applications of the Modular Multilevel Converter: A Review", *IEEE Transactions On Power Electronics*, vol. 30, no. 1, pp. 37-53, Jan. 2015.
- 13. S. Rohner, S. Bernet, M. Hiller, and R. Sommer, "Modulation, losses and semiconductor requirements of modular multilevel converters", In *IEEE Transactions on Industrial Electronics*, vol.

Volume 1, Issue 2, 2023

DOI: https://doi.org/10.59122/144CFC13

ISSN (E): 2959-3921 (P): 2959-393X

4

Copyright and License Grant: CC By 4.0



57, no. 8, pp. 2633-2642, 2010.

- 14. Yalisho Girma, Getachew Biru, Chandra Sekhar "A comparative study on modeling and performances of modular converter based three-phase inverters for smart transformer application", *Journal of Science and Inclusive Development*, vol. 5, no. 2, pp. 91-115, 2023. https://doi.org/10.20372/jsid/2023-256.
- T. Kaliannan, J. R. Albert, D. M. Begam and P. Madhumathi, "Power quality improvement in modular multilevel inverter using different multicarrier PWM" *European Journal of Electrical Engineering and Computer Sciences*, vol. 5, no.2, 2023. http://dx.doi.org/10.24018/ejece. 2021.5.2.315
- 16. M. Park and I.-K. Yu, "A novel real-time simulation technique of photovoltaic generation systems using RTDS," *IEEE Transactions on Energy Conversion*, vol. 19, no. 1, pp. 164–169, 2004.
- 17. S. Saravanan, S. Thangavel, "A simple power management scheme with enhanced stability for a solar PV/wind/fuel cell/grid fed hybrid power supply designed for industrial loads", Journal of Electrical and Computer Engineering, vol 2014, Art. ID 319017, 2014. http://dx.doi.org/10.1155/2014/319017

ISSN (E): 2959-3921

(P): 2959-393X

DOI: https://doi.org/10.59122/144CFC14



Copyright and License Grant: CC By 4.0



Cattle Pinkeye Disease Classification Using Machine Learning

Serkalem Mekonnen¹ and Mohammed Abebe^{2*}

¹Department of Computer Science, Wolaita Sodo University, Ethiopia ²Faculty of Computing & Software Engineering, Arba Minch University, Ethiopia *Corresponding Author Email: mohammed.abebe@amu.edu.et

Abstract

Pinkeye (infectious bovine keratoconjunctivitis, or IBK) is a bacterial infection of the cattle eye that causes inflammation and, in severe cases, temporary or permanent blindness. It is a painful, debilitating condition that can severely affect animal productivity. Due to lower weight gain, lower milk production, and higher medical costs, the cattle industry could experience large losses. Previous studies tried to classify livestock diseases using machine learning, but there has been a lack of studies conducted on pinkeye disease classification. The proposed study aims to design a classification model to classify whether the infected cattle have pinkeye or not at an early stage by analyzing a set of attributes. The study collected data from the Wolaita Sodo Kenido Koyisha Wereda Livestock and Fishery Office. The significance of this study is to prevent the expansion of disease among the cattle with early detection for taking precautionary measures. The researchers used the percentage splits 80/20, 70/30, 60/40, and 90/10 to build classification models. Based on the results of the experiments, the researchers chose the 70/30 split due to the better performance obtained. The study trained four different models, including Random Forest, AdaBoost, Artificial Neural Network, and Extreme Gradient Boost algorithms. These models were selected based on an exhaustive study conducted. To assess the algorithm's performance, confusion matrix, accuracy, precision, recall, and f1-score have been utilized. With a 99.15% accuracy, the Artificial Neural Network outperforms the other algorithms by all the metrics except recall.

Keywords: Cattle Pinkeye, IBK, Infectious Bovine Keratoconjunctivitis, Machine Learning, Pinkeye Disease Classification.

I. Introduction

Ethiopia is one of the nations in Africa with the highest number of livestock (over 65 million) [1]. Pinkeye also known as infectious bovine keratoconjunctivitis (IBK), is a frequent cattle disease that produces redness and ulceration in the eye. Pinkeye is a serious eye condition that has an economic influence on animals' performance [2]. It is exceedingly painful and causes huge economic losses due to decreased

(P): 2959-393X

DOI: https://doi.org/10.59122/144CFC14

? Volume 1, Issue 2, 2023

22

Copyright and License Grant: CC By 4.0



weaning weights and livestock value. Pinkeye is caused mostly by the bacteria Moraxella bovis, but it can also be caused by other bacteria and viruses. Environmental variables that increase the risk of pinkeye in cattle include seed heads, dust, pollen, and UV light. These irritants scrape the cornea of the eye allowing the bacteria to attach more easily. These irritants promote an increase in tear production, which attracts face flies, which can spread the bacteria that causes pinkeye [3]. Pinkeye can damage up to 80% of a herd, resulting in weaner calves losing 10% of their total weight. Cattle may die from malnutrition, thirst, or accidents if both eyes are affected with pinkeye. Damage to the eye can sometimes be serious enough to cause lifelong blindness [4]. The degree of inflammation may eventually become severe enough to produce corneal ulceration, which may rupture, potentially ending in blindness.

While not lethal, pinkeye has a significant financial impact on the Ethiopian cattle sector. Pinkeye can have an impact on the prices received for cattle at sale due to price reductions, in addition to the fact that calves weigh 36–40 pounds less at weaning [5]. Furthermore, pinkeye is a costly condition for beef producers. Poor weight gain and appetite reduction in animals affected by visual impairment and ocular pain result in enormous losses [6]. Farms may benefit from identifying cows who are more likely to develop health issues such as clinical mastitis, subclinical ketosis, lameness, and metritis to promptly avoid and treat their harmful impacts [7]. However, allowing serious cases to continue to a severe stage without treatment is poor management and unacceptable from a welfare standpoint. Therefore, this study proposed the development of a machine-learning model for the early detection of cattle pinkeye disease. The proposed model can be able to predict whether the cattle have pinkeye or not at an early stage by analyzing selected attributes from the clinical dataset using machine learning so that appropriate medical decisions can be made to avoid severe damage.

II. Literature Review

Machine learning (ML) is a type of artificial intelligence (AI) that uses historical data as input to forecast new output values. It is a discipline of computer science concerned with the study and interpretation of data patterns and structures to enable learning, reasoning, and decision-making without the involvement of humans. Machine learning allows a user to submit large volumes of data to a computer algorithm, which analyzes the data and produces data-driven recommendations and decisions based only on the data provided. ML plays a critical function in accurately extracting information from the massive amount of data at that point. Various studies have been conducted on the development of assistive tools for cattle diseases. However, only little effort is undertaken in the Ethiopian context. There are various challenges endured by the cattle industry in Ethiopia due to the acute shortage of assistive tools especially in rural areas. The

Volume 1, Issue 2, 2023

DOI: https://doi.org/10.59122/144CFC14



Copyright and License Grant: CC By 4.0



challenges include economic loss due to lower weight gain, decreased milk supply, and so on. It is because of these facts that the researchers believe that AI-enabled tools play a paramount role in alleviating some of the aforementioned challenges. Some of the related works are discussed hereunder.

The study "Application of Artificial Intelligence for Livestock Disease Prediction" used artificial intelligence and Geographic Information System (GIS) to create disease-climate association models to anticipate 13 economically critical livestock disease outbreaks in India. Data on disease outbreaks was gathered from 31 AICRP (All India coordinated research project) centers. The study used two regression models, Generalized Linear Models (GLM) and Generalized Additive Models (GAM). They used six machine-learning algorithms to predict livestock diseases [8]. The study of D. Ashar [9], presented a system to detect the existence of livestock diseases to take precautionary measures and notify the livestock owner if the condition is likely to cause a sudden death. The goal was to raise awareness of an illness that can bring death unexpectedly at any moment in the future. The study developed a machine learning model using support vector machines (SVM). The model classifies diseases based on the information entered by the user. The user can also choose whether to see the website in Hindi or English. The research "Mobile-based Cattle Infectious Disease Prediction System" [10] proposes a novel prediction method for identifying infectious illness in cattle with the help of a mobile-based information system. This research primarily used Naïve Bayes classifiers to categorize the level of risk presented to cattle by evaluating six baseline animal health syndrome patterns.

Another study [11] was conducted to identify the on-farm risk factors associated with pinkeye disease in Australian cattle. Data were gathered from cattle farmers using a custom-designed online questionnaire. Results revealed that farm location, farm grazing area, farmer-reported dust levels, fly levels, rain levels, animal zebu content, and cattle age were significantly associated with pinkeye prevalence. The results confirm that pinkeye disease is multifactorial and is associated with a range of host and environmental factors. The study suggested these findings should be used to assist in the control of the disease and improve pinkeye outcomes in Australian cattle. According to the model and sample preparation technique utilized, a study produced two biomarker models that correctly categorized the M. bovis bacteria according to genotype with an overall accuracy ranging from 85.8 to 100%. These models offer a useful resource for investigations of genetic connections with disease, allowing epidemiological research at the level of subspecies, and can be applied to improve disease prevention methods. In this study, strain classification was the sole use of genetic indicators [12]. Finally, to the best of the researchers' knowledge, an exhaustive

Volume 1, Issue 2, 2023

DOI: https://doi.org/10.59122/144CFC14

Copyright and License Grant: CC By 4.0



literature survey showed that there are no machine-learning models developed for the early detection of pinkeye, hence the originality and significance of the study is justified.

III. Materials and Methods

A. Research Process

Finding a research problem is the first step in any research process. The context of the research problem is then discovered through a literature review. Moreover, to express the research questions and to obtain a deeper comprehension of the subject, a literature survey was conducted to find out the justifiable research gap. Based on the identified research gaps, the problem was formulated. After problem formulation, the research questions, objectives, and hypotheses were articulated. Solving the issue entails putting out and creating a plan for data collection, analysis, and experimentation. The formation of a research study design involves choosing a sample size and gathering data from it. The suggested solutions are put into practice and assessed after the processing and analysis of the gathered data and the determined classification model. The researchers used Open-Source tools for data analysis, model design, and validation. Specifically, the study used Python machine-learning libraries for overall model development and testing. The overall research process followed to undertake this research study is shown in Fig. 1. The goal of this research was to build a pinkeye disease classification model based on data collected from clinical trials. Models were selected based on a detailed experimental comparison, their popularity in various machine learning classification tasks, and their performance in previous research. Artificial Neural Networks (ANN), Random Forest, XGBoost, and Adaboost were used in this work for comparative analysis of supervised machine learning classification for pinkeye disease classification.

B. Data Source and Data Collection

Data collection and preparation techniques aid in the generation of high-quality data and the enhancement of classification outputs. To train the proposed model for accurate classification of cattle pinkeye disease, a large number of eye illness records with complete information is required. In this study, we collected a dataset from Wolaita Sodo Kenido Koysha Wereda Livestock and Fishery office, which contains 5508 eye illness records with 22 distinct features collected between the years 2007 to 2022. The researchers transformed the original data into digital formats to make it suitable for machine learning. The data in this study was gathered in a variety of ways. Primary and secondary data sources were utilized. The main source of the data was secondary data, which was collected from clinical records, the researchers also employed primary sources (interviews) for a better understanding of the research domain. The total size of the dataset

(P): 2959-393X DOI: https://doi.org/10.59122/144CFC14

ISSN (E): 2959-3921



Copyright and License Grant: CC By 4.0



Volume 1, Issue 2, 2023

after preprocessing was 5508 instances with 21 independent attributes and a target class (has pinkeye or not). Out of the total dataset, 3377 records were cattle affected with pinkeye disease and the remaining 2131 are cattle that were not affected by the disease. The dataset had a class imbalance. However, instead of adding synthetic data or removing data, the study opted to use various performance measurement techniques to make sure that the model is not biased towards the class with more observations.

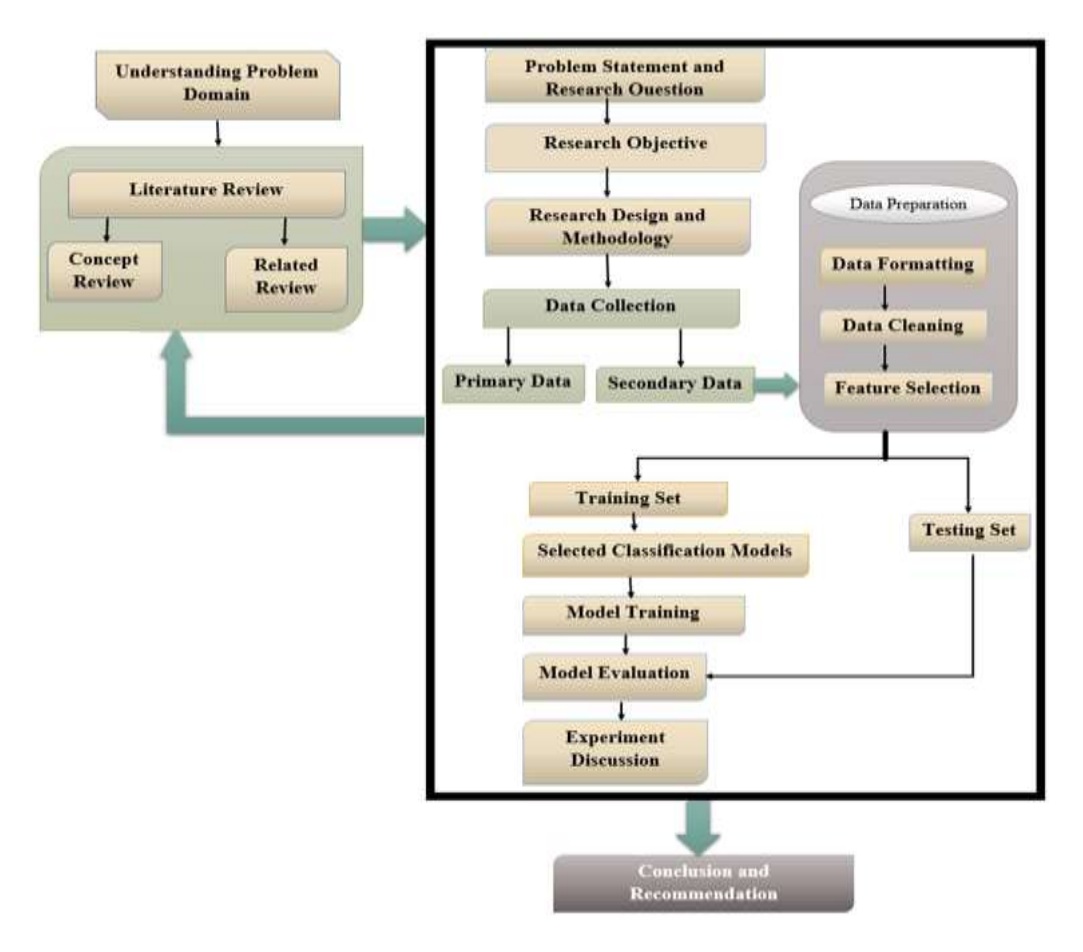


Fig. 1. Overall Research Process

C. Feature Selection

A strategy for selecting, identifying, and eliminating attributes from a dataset to make it suitable for machine learning algorithms is called attribute selection (feature selection). It is a task of selecting a minimal number of features/attributes that are sufficient for correctly classifying the target labels. Feature selection increases the efficacy of the classification model while reducing the computational complexity of the model. Selecting model input variables is an important step in creating an accurate model in machine learning. The study applied feature importance analysis for feature selection.

ISSN (E): 2959-3921

DOI: https://doi.org/10.59122/144CFC14

The feature importance analysis refers to methods for scoring each input feature for a certain model. The scores simply indicate the importance of each feature to the target variable. There are various features and important analysis techniques. Out of those methods, the permutation feature importance method was used in this study. Using the permutation importance technique, we run the model while randomly shuffling the values of a single column to evaluate how the scores change. If the scores were significantly impacted, the feature was found very crucial to the model; otherwise, it does not significantly improve the model's performance. A higher score of 0.7 in the dataset indicated that the particular feature has more impact on the model. The importance scores of other features in the dataset were compared to determine the rank of each feature. Fig. 2 presents feature importance scores of the independent features in descending order. Fig. 2 shows the results of fitting a Random Forest model and accumulating the computed permutation feature significance scores.

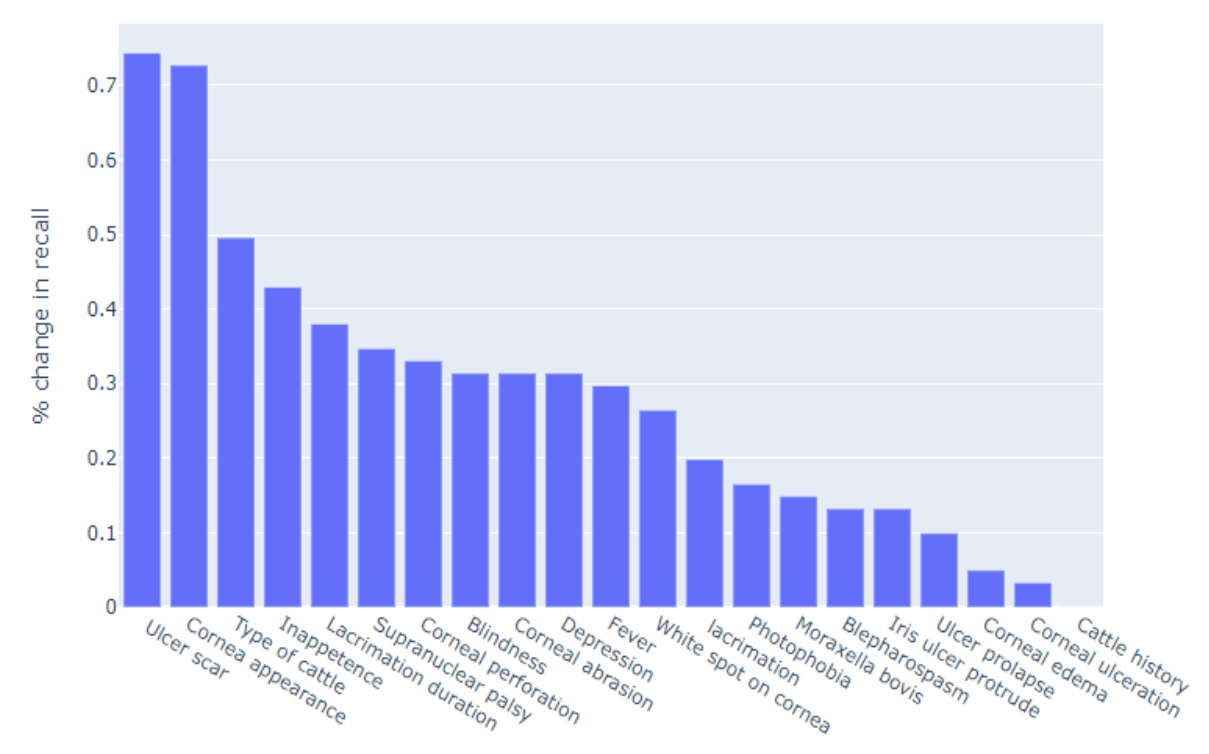


Fig. 2. Permutation Feature Importance Analysis Results

Each feature in the dataset was assigned a score that indicates how useful it is. The most important feature of the model was assumed to be given a higher significance score. The relevance score of each feature was compared to the scores of the other features in the dataset to determine its importance. Based on the findings of the study, ulcer scar, cornea appearance, types of cattle, inappetence, lacrimation duration, supranuclear

Copyright and License Grant: CC By 4.0



perforation, corneal perforation, blindness, corneal abrasion, and depression were the top ten important features in the dataset for identifying pinkeye disease. Whereas, cattle history, corneal ulceration, and corneal edema were the least important features in the dataset. Various experiments were conducted using all attributes, the top 5 and top 10 attributes as depicted in Fig. 2. Due to the insignificant changes in the overall performance of the models, the results presented in this article were based on the full feature dataset.

IV. Results and Discussion

Various experiments were conducted with different train/test split ratios. Depending on the maximum amount of data the researchers found from the source, the study used a trial-and-error method to compare several percentage splits experimentally, including 60/40, 70/30, 80/20, and 90/10. Based on the results obtained from the trial-and-error experiments, a 70/30 split was selected, in which 70% of the pinkeye dataset was used for training and 30% was used for testing (unseen dataset). Additionally, the majority of researchers in machine learning with relatively the same amount of data use the 70/30 percentage split, which is the most popular. Therefore, based on the preliminary experiments and previous research experiences, the 70/30% train/test split ratio was selected. In addition, preliminary experiments and literature surveys have been conducted to select the most appropriate models. Based on this related literature review and previous research experience, the models Random Forest (RF), XGBoost (XGB), AdaBoost (AB), and Artificial Neural Network (ANN) were selected for further experiments. Due to this, further experiments were conducted on four prominent machine learning models RF, XGB, AB, and ANN with a 70/30% train/test split ratio. Furthermore, several performance evaluation methods such as accuracy, recall, precision, and F1-score were used to evaluate and compare the performances of the selected models. Table I shows the results of four machine-learning models using different evaluation metrics. It is also worth mentioning that the researchers employed a grid search method for model hyperparameter tuning. Usually, Grid search is used to find the optimal hyperparameter values for all the selected models for optimal model performance.

Table I: Summary of Evaluation Result

Evaluation Metrics	Algorithms					
Evaluation Metrics	RF	XGB	AB	ANN		
Correctly classified instances	1621	1637	1628	1639		
Incorrectly classified instances	32	16	25	14		
Precision	97.09	99.22	97.85	99.68		

ISSN (E): 2959-3921

(P): 2959-393X



Copyright and License Grant: CC By 4.0

~	(1)
(cc)	•
\sim	BY

Volume 1, Issue 2, 2023

Recall	97.99	98.30	98.30	98.15
F1-Score	97.54	98.76	98.07	98.91
Accuracy (%)	98.06	99.03	98.48	99.15

The test results of the four selected models are presented in Table I. It shows that ANN outperforms the other models with an overall accuracy of 99.15% followed by XGB with an accuracy of 99.03%. Furthermore, ANN outperforms the rest of the models in terms of the other performance measurement methods applied except for recall. Thus, we can assert that the ANN model performs better in all evaluation metrics except for recall than the rest of the classifiers tested. The experiments show that 1639 (99.15%) of the test datasets are correctly classified while 14 (0.84%) of the test datasets are incorrectly classified. Furthermore, one way to visualize the performance of classification models in machine learning is by creating an ROC curve, which stands for the "receiver operating characteristic" curve. Often, we may want to fit several classification models to one dataset and create an ROC curve for each model to visualize which model performs best on the data. Fig. 3 shows the ROC curve plot for the Artificial Neural Network model.

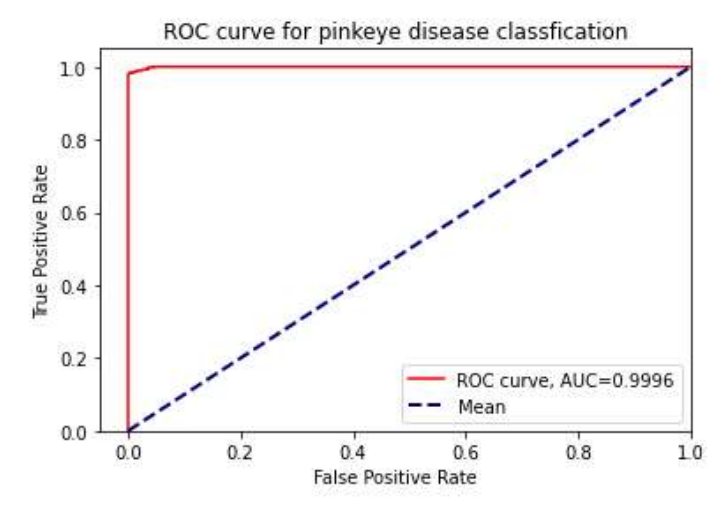


Fig. 3. ROC Curve Plot for ANN Classifier

Finally, based on the results of the feature importance analysis, the top ten determinant features in pinkeye disease classification include ulcer scar, cornea appearance, types of cattle, inappetence, lacrimation duration, supranuclear palsy, corneal perforation, blindness, corneal abrasion, and depression. While the least three important features include corneal edema, corneal ulceration, and cattle history. Further, the ANN model outperforms the other models with an overall accuracy, precision, recall, and f1-score of 99.15%, 99.68%, 98.15%, and 98.91%, respectively. Hence, the researchers attest that the ANN classification model is most suited to classify pinkeye disease.

ISSN (E): 2959-3921

(P): 2959-393X

DOI: https://doi.org/10.59122/144CFC14



Copyright and License Grant: CC By 4.0



Volume 1, Issue 2, 2023

V. Conclusion

The study aimed to build a classification model for cattle pinkeye disease by identifying relevant attributes. The initial data was gathered, converted from a manual to an electronic format, and then preprocessed so that it was suitable for analysis. The dataset contained 5508 records with 21 independent variables and a target class (Pinkeye and Not-Pinkeye). Essential procedures have been applied to realize an optimal pinkeye disease classification model. Based on the findings of the study, ulcer scar, cornea appearance, type of cattle, inappetence, and lacrimation duration are some of the major attributes for identifying the disease. Cattle history, corneal ulceration, and corneal edema do not have a significant effect on the model. Based on the experimental results the ANN classifier is found to be the best classification model with an overall accuracy of 99.15%, which is selected as an appropriate model to classify cattle pinkeye disease.

References

- 1. Feed the Future USAID, "Ethiopia's Livestock Systems: Overview and Areas of Inquiry," Gainesville, FL, USA: Feed the Future Innovation Lab for Livestock Systems (USAID), 2021.
- 2. A. A. Ali, C. J. O'Neill, P. C. Thomson, and H. N. Kadarmideen, "Genetic parameters of infectious bovine keratoconjunctivitis and its relationship with weight and parasite infestations in Australian tropical Bos *taurus* cattle," *Genet. Sel. Evol.*, vol. 44, no. 22, pp. 1 -10, 2012. https://doi.org/10.1186/1297-9686-44-22
- 3. N. Alias, F. N. M. Farid, W. M. Al-Rahmi, N. Yahaya, and Q. Al-Maatouk, "A modeling of animal diseases through using artificial neural network," *Int. J. Eng. Technol.*, vol. 7, no. 4, pp. 3255–3262, 2018.
- 4. A. Seid, "Review on infectious bovine keratoconjunctivitis and its economic impacts in cattle," *J. Dairy Vet. Sci.*, vol. 9, no. 5, pp. 001-008, 2019.
- 5. L. Strickland, "Infectious bovine keratoconjunctivitis cattle pinkeye," UT Ext. Inst. Agric., 2008.
- 6. M. Arnold, "Infectious bovine keratoconjunctivitis (pinkeye) in Cattle," *Vet. Clin. North Am. Food Anim. Pract.*, vol. 31, no. 1, pp. 61–79, 2015.
- 7. X. Zhou, C. Xu, H. Wang, W. Xu, Z. Zhao, M. Chen, B. Jia, and B. Huang, "The early prediction of common disorders in dairy cows monitored by automatic systems with machine learning algorithms," *Animals (Basel)*, vo.12, no.10, pp. 1 14, 2022.
- 8. K. P. Suresh, Dhemadri, R. Kurli, R. Dheeraj, and P. Roy, "Application of artificial intelligence for livestock disease prediction," *ACM SIGSOFT Softw. Eng. Notes*, vol. 13, no. 1, pp. 32–38, 1988.
- 9. D. Ashar, A. Kanojia, R. Parihar, and S. Kudoo, "Livestock disease prediction system," VIVA-Tech

DOI: https://doi.org/10.59122/144CFC14



Copyright and License Grant: CC By 4.0



Volume 1, Issue 2, 2023

Int. J. Res. Innov., vol. 1, no. 4, pp. 1–3, 2021.

- 10. H. P. P. Mon and O. Htwe, "Mobile-based cattle infectious disease prediction system," *Int. J. Sci. Res.*, vol. 7, no. 10, pp. 694–697, 2018.
- 11. M. Kneipp, A. C. Green, M. Govendir, M. Laurence, and N. K. Dhand, "Risk factors associated with pinkeye in Australian cattle," *Prev. Vet. Med.*, vol. 194, no. May, p. 105-432, 2021.
- 12. H. G. Olson, J. D. Loy, M. L. Clawson, E. L. Wynn, and M. M. Hille, "Genotype classification of Moraxella bovis using MALDI-TOF MS profiles," *Front. Microbiol.*, vol. 13, pp. 1–6, Dec. 2022. https://doi.org/10.3389/fmicb.2022.1057621

DOI: https://doi.org/10.59122/144CFC15



Copyright and License Grant: CC By 4.0



Biomimetic Architecture: An Innovative Approach to Attain Sustainability in a Built Environment

Zeeshan Haider Khan^{1*}, Mohammad Salman², Alemea Girma³

¹Department of Architecture, Srinivas Institute of Technology, Mangalore, India

²Faculty of Architecture, Planning & Design, Integral University, Lucknow, India

³Faculty of Architecture & Urban Planning, AMiT, Arba Minch University, Ethiopia

*Corresponding Author Email: ar.zeeshanhaider@gmail@.com

Abstract

Architecture has always inserted itself into and interacted with the natural environment. Biomimetics is an applied science that infers motivation for answering human issues through the investigation of common plans from nature. Biomimetics has been used in design for many years. It is the fastest-growing research in the area of architecture. This is because of the innovative and problem-solving approach to achieving sustainability in design. However, the application of biomimetic design to achieve sustainability requires a proper understanding of the relationship between biology and environmental science. The review of achievements using biomimetic architecture could make understanding the relationship between biomimetic ecosystems and the built environment easier and therefore contribute to environmental sustainability. This paper elaborates on the different approaches to attaining sustainability through different literature studies and case-based analytical studies. Finally, the paper summarizes and concludes that these varied approaches have different outcomes in terms of sustainability.

Keywords: Biomimetic Architecture, Built Environment, Ecosystem, Sustainable Architecture

I. Introduction

Biomimetics is an applied science that acquires inspiration for the solution of built environment problems through the study of Flora and Fauna or the whole ecosystem. This is because of both the way that it is a helpful wellspring of conceivable new advancement and on account of the potential it offers to make an increasingly maintainable assembled condition [1]. Biomimetics or the entire ecosystem are copied as a design base. It is the fastest-developing exploration in the field of architecture. The functional information of biomimetics as a design approach is very cagey. However, the use of these biomimetic approaches in a built environment requires a legitimate comprehension of the elements of an ecological system [2]. To acquire this biomimetic knowledge, one needs a fine understanding of the relation between science and

DOI: https://doi.org/10.59122/144CFC15



Copyright and License Grant: CC By 4.0



ecological science. The review of achievement by the use of biomimetic design could make it easier to understand the relationship between the biomimetic ecosystem and the built environment and therefore contribute to environmental sustainability in building [2]. This paper elaborates on different approaches to different levels of biomimetic design to achieve sustainability. These varied approaches have various results regarding sustainability in general.

II. Research Methodology

The employed research methodology consists of a literature review and numerous case study analyses. The literature review involves an extensive examination of existing research articles, books, journals, and conference papers related to biomimetic architecture and sustainability. The focus is on understanding the relationship between biology, environmental science, and sustainable design. This exhaustive review serves as the theoretical foundation for the study. Multiple case studies are selected to analyze the practical implementation of biomimetic design in achieving sustainability. These case studies encompass a range of building types, allowing for a comprehensive evaluation of biomimetic architecture in different contexts. Data is collected from various sources, including architectural drawings, project reports, photographs, and interviews with architects and designers. The results of the literature review and case study analysis are presented and discussed, highlighting the outcomes achieved through different biomimetic design strategies. These strategies are categorized into organism-level, behavior-level, and ecosystem-level approaches. Finally, the implications and significance of the findings are discussed along with potential applications in future architectural projects.

III. Approaches to Biomimetics Design

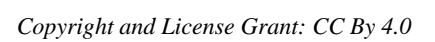
A. Top Down Approach

As depicted in Fig. 1, Top-down Methodology highlights how fashioners seek nature and life forms for arrangements where architects must perceive precisely their structural issues and coordinate their issues with life forms that have tackled comparative issues. This methodology is because of the architect's information on the ecological life and triggers of their structure [3].

DOI: https://doi.org/10.59122/144CFC15

ISSN (E): 2959-3921

(P): 2959-393X





Volume 1, Issue 2, 2023

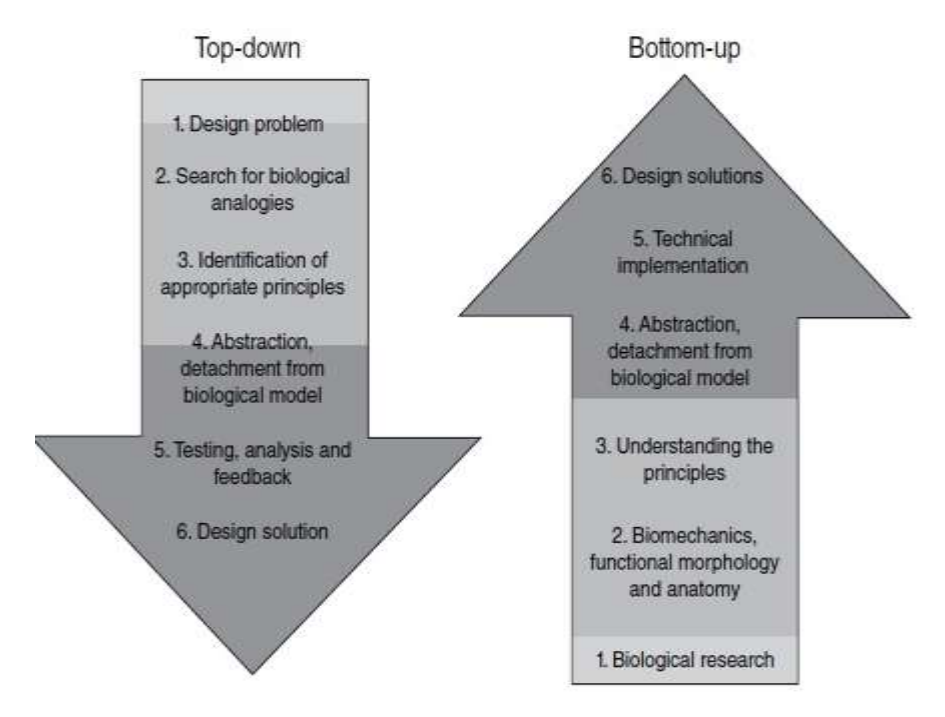


Fig. 1. Biomimetic Approach

B. Bottom Down Approach

As depicted in Fig. 1, the bottom-up approach alludes to a similar significance, where this methodology relies upon the past information on organic examination and arrangements not to look for arrangements in nature, and at that point applying this information on the plan issue[3].

IV. Levels of Biomimetic Designs

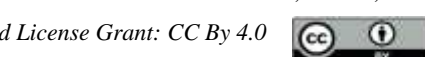
There are three levels of biomimetic Architecture i.e., 1) Organism level, 2) Behavior level, and 3). Ecosystem level. Inside every one of these levels, a further five potential measurements to mimicry exist. The structure might be biomimetic for instance regarding what it resembles (structure), what it is made of (material), how it is made (development), how it works (process), or what it can do (work).

The contrasts between every biomimicry are depicted in Table I and are exemplified by taking a gander at how various parts of levels, or parts of biological systems could be impersonated[3].

Organism Level

This building mimics the Namibia desert bug and steno Cara. The scarab dwells in the desert with irrelevant precipitation. It can catch dampness anyway from the quick-moving haze that moves over the desert by inclining its body into the breeze. Beads structure on the substituting hydrophilic-hydrophobic harsh surface

Copyright and License Grant: CC By 4.0



DOI: https://doi.org/10.59122/144CFC15

of the creepy crawl's back and wings and fold down into its mouth [4]. Motivated by the creepy crawly, a mist catcher structure was proposed for the Hydrological Place at the College of Namibia. The surface of the beetle has been examined and emulated to be utilized for other potential applications such as to clear fog from airport runways equipment[5].

Table I: Organism Level

ISSN (E): 2959-3921

(P): 2959-393X

Levels	Dimension	Remarks
	Structure	The structure appears like a Namibia Desert Scarab
	Material	The Structures are produced using a similar material as a termite, a material that emulates Bug exoskeleton/skin (Mimicry of a Particular life form)
Organism Level	Construction	The Structure is made similarly to a Desert Creepy crawly it experiences different development cycles.
	Process	The structure Works similarly to an individual Beetle.
	Function	It can Catch Dampness from the Quick-moving haze.



Fig. 2. Hydrological Centre for the University of Namibia



Fig. 3. Calla lily flower

B. Behavior Level

This is depicted in Table II. Another Calla lily-formed (Fig. 3) exploration place for Wuhan College is set to sprout in China as one of the most manageable structures in the world. Situated in Wuhan, The Wuhan New Vitality Community (likewise called the Energy Flower) was intended to take after a lily (Fig. 2), with a 140-meter tower on the inside encompassed by lower towers looking like blossoms and shrouded in vegetation. The inside pinnacle extends upwards into a bowl and is covered in an enormous sunlight-based exhibit confronting the sun, absorbing beams simply like a genuine plant. A vertical pivot wind turbine shoots up out of the focal point of the pinnacle like a pistil (Fig. 4). Water is gathered in the bowl and a 120-meter sun-based stack in the pinnacle ousts blistering air from the structure while pulling in cooler air beneath [6]. To limit the requirement for cooling (Fig. 5), the architect Grontmij saw building structures that could amplify the concealing of the southern façade. The Wuhan vitality blossom profits from the enormous overhanging rooftop for another explanation as it expands the zone on which to introduce photovoltaic boards, which the establishment is utilizing to communicate its sustainability[7].

Table II: Behavior Level

Levels	Dimension	Remarks
	Structure	The structure appears as though it is made looking like a calla lily
Behavior Material		The structure is produced using the same material idea as utilized by Calla
Level		Lily.
	Construction	The structure is made similarly to calla Lily Blossom Work.

Received: July 26, 2023; Revised: 16 September 2023; Accepted: 05 October 2023; Published: 31 December 2023.

ISSN (E): 2959-3921

(P): 2959-393X

DOI: https://doi.org/10.59122/144CFC15

Copyright and License Grant: CC By 4.0

1	200
6	(•)
(CC)	00.00

Volume 1, Issue 2, 2023

Levels	Dimension	Remarks				
		The inside pinnacle extends upwards into a bowl and is covered in a huge				
	Process	sun-powered exhibit confronting the sun, absorbing beams simply like a				
	FIOCESS	genuine plant. A vertical pivot wind turbine shoots up out of the focal				
		point of the pinnacle like a pistil.				
	Engation	The functional processes silently at work are inspired by the way calla				
	Function	lily flowers keep themselves cool in hot & humid climates.				



Fig. 4. Wuhan New Energy Center

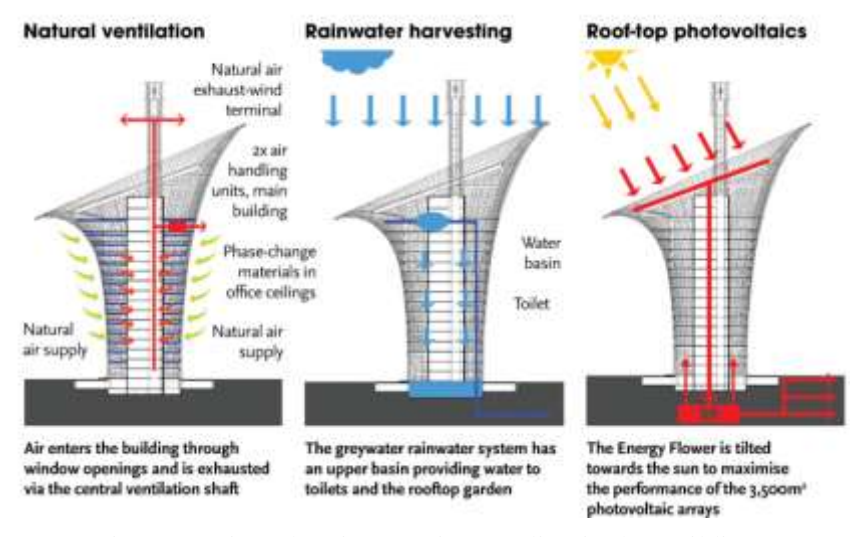


Fig. 5. Section Showing Passive Cooling in the Building

ISSN (E): 2959-3921

(P): 2959-393X

DOI: https://doi.org/10.59122/144CFC15



Copyright and License Grant: CC By 4.0



Volume 1, Issue 2, 2023

C. Ecosystem

The ecosystem level is depicted in Table III. The Sahara Forest Project (Fig. 6) is a facility situated in the core of Qatar's desert intended to use saltwater and CO2 contributions to deliver food, water, and vitality. There is a progression of desalination frameworks, water recovery equipment, and sun panels. The Sahara Forest Project is located on 107,639 sq. ft. The organization guarantees a facility that size can deliver 34,000 tons of vegetables, utilize more than 800 individuals, send out 155 GWh of power, and conceal 8,250 tons of CO2. One of the Goals of the Sahara Forest Project is also to demonstrate the potential for cultivating desert land and making it green. Open-air vertical evaporators will create shielded and sticky conditions for the development of plants [8].

Table III: Ecosystem Level

Levels	Dimension	Remarks
	Structure	The Building resembles an Ecosystem.
Essenten	Material Construction	The structure is produced using a similar sort of materials that the biological system is made of. It utilizes normally happening regular mixes and water as the essential concoction mode for instance The building is gathered similarly as a biological system.
Ecosystem Level	Process	The structure works similarly to a biological system. It catches and changes over vitality from the sun and stores water for instance.
	Function	The building can work similarly to an environment and shape some portion of a mind-boggling framework by using the connections between forms. it can take part in the hydrological carbon nitrogen cycles and so forth like a biological system.



Fig. 6. Sahara Forest Project

DOI: https://doi.org/10.59122/144CFC15



Copyright and License Grant: CC By 4.0



Open-air vertical evaporators will create shielded and humid conditions for the development of plants. The Project will contain outside hydroponic raceways for the development of halophytes – plants lenient toward water system with salty water."[8]. Sahara Forest Project's Algae Test Facility (the first of its kind in Qatar and the larger region) is presented in Fig. 7.



Fig. 7. Sahara Forest Project's Algae Test Facility (the first of its kind in Qatar and the larger region).

V. Conclusion and Recommendations

In conclusion, this research paper explored the application of biomimetic architecture as an innovative approach to attaining sustainability in the built environment. Through a comprehensive literature review and analysis of the case studies, the study has highlighted the potential of biomimetic design principles in addressing sustainability challenges. The findings of the study demonstrate that biomimetic architecture offers promising solutions for achieving sustainability. By drawing inspiration from nature and emulating its design principles, architects and designers can create buildings that are not only aesthetically pleasing but also environmentally friendly and resource-efficient. The three levels of biomimetic design (organism, behavior, and ecosystem) provide a framework for incorporating natural strategies into architectural projects. The case-based analytical studies analyzed in this research paper have showcased various successful applications of biomimetic architecture. These projects have demonstrated improved energy efficiency, reduced carbon emissions, enhanced natural ventilation and lighting, and better integration with the surrounding ecosystem. The outcomes of these research projects serve as evidence of the positive impact that biomimetic design can have on sustainability in the built environment.

DOI: https://doi.org/10.59122/144CFC15

(P): 2959-393X

ISSN (E): 2959-3921



Copyright and License Grant: CC By 4.0



Recommendations

Based on the findings of this research, the following recommendations are proposed for further exploration and advancement of biomimetic architecture in achieving sustainability:

- I. Continued Research: Further research is needed to deepen our understanding of the relationship between biology, environmental science, and architectural design. This will help uncover more biomimetic design principles and strategies that can be applied to enhance sustainability in the built environment.
- II. Collaboration and Interdisciplinary Approaches: Encouraging collaboration between architects, biologists, engineers, and other relevant disciplines can foster innovative solutions. Interdisciplinary research and design teams can work together to develop biomimetic approaches that address complex sustainability challenges effectively.
- III. Knowledge Exchange and Education: Promoting knowledge exchange and educational initiatives among architects, designers, and students can raise awareness and understanding of biomimetic design principles and their potential for sustainability. Integration of biomimicry into architectural curricula can nurture a new generation of architects equipped with the skills and knowledge to create sustainable built environments.
- IV. Policy and Regulation: Governments and regulatory bodies can play a crucial role in promoting biomimetic architecture by incentivizing sustainable design practices and incorporating biomimetic principles into building codes and regulations. This can create a supportive environment for the adoption of biomimetic approaches in architectural projects.

References

- 1. R. Mahmoud and A. El-Zeiny, "Biomimicry as a problem-solving methodology in interior architecture," *Procedia-Social Behav. Sci.*, vol. 50, pp. 502–512, 2012, doi: 10.1016/j.sbspro.2012.08.
- 2. H. Abaeian, R. Madani, and A. Bahramian, "Ecosystem biomimicry: A way to achieve thermal comfort in architecture," *Int. J. Hum. Cap. Urban Manag.*, vol. 1, no. 4, pp. 267–278, 2016, doi: 10.22034/ijhcum.2016.04.004R.
- 3. M. P. Zari, "Biomimetic approaches to architectural design," *Sustainable Building Conference (SB07)*, Auckland, New Zealand, Paper number: 033, 2006.

DOI: https://doi.org/10.59122/144CFC15





Volume 1, Issue 2, 2023

- 4. R. P. Garrod, L. G. Harris, W. C. E. Schofield, J. McGettrick, L. J. Ward, D. O. H. Teare, and J. P. S. Badyal, "Mimicking a stenocara beetle's back for microcondensation using plasmachemical patterned superhydrophobic superhydrophilic surfaces", *Lagmuir*, vol. 23, pp. 689-693, 2007.
- 5. Moheb Sabry Aziz, Amr Y. El Sherif, "Biomimicry as an approach for bio-inspired structure with the aid of computation," *Alexandria Engineering Journal*, Volume 55, Issue 1, 2016, Pages 707-714, ISSN 1110-0168, https://doi.org/10.1016/j.aej.2015.10.015. "LEVELS OF BIOMIMECRY AND ITS IMPORTANCE | Architecture." https://architecturever.com/2019/09/07/levels-of-biomimecry-and-its-importantance-part3/ (accessed Jul. 10, 2020).
- 6. "The Zero Energy Wuhan New Energy Center." https://inhabitat.com/wuhans-lily-shaped-zero-carbon-energy-flower-set-to-bloom-in-china/ (accessed Jul. 12, 2020).
- 7. "Case Study Wuhan Energy Flower" *CIBSE Journal*, January 2015. http://portfolio.cpl.co.uk/CIBSE/201501/case-study-wuhan/ (accessed Jul. 07, 2020).
- 8. "Vertical Farming in the Desert: The Urban Vertical Farming Project." https://urbanverticalfarmingproject.com/2015/03/17/vertical-farming-in-the-desert/ (accessed Jul. 12, 2020)

@ **①**

Copyright and License Grant: CC By 4.0

ISSN (E): 2959-3921 (P): 2959-393X DOI: https://doi.org/10.59122/144CFC16





Pulmonary Disease Identification and Classification using a Deep Learning **Approach**

Minalu Chalie^{1*} and Zewdie Mossie¹

¹Department of Information Technology, Debre Markos University, Ethiopia *Corresponding Author's Email: minaluchal@gmail.com

Abstract

Deep Learning (DL) models have shown strong results in detecting diseases from medical images. In this paper, we explored the challenge of classifying pulmonary diseases (PD) using chest X-rays. The research focuses on three common respiratory conditions: pneumonia, pulmonary tuberculosis, and pleural effusion. We proposed a new framework for detecting and classifying PD from chest X-ray (CXR) images. The process includes noise reduction, image enhancement, data augmentation, segmentation, feature extraction, and classification. To remove noise, we used a Gaussian filter, and for improving image quality, we applied an advanced histogram equalization method. The Region of Interest (ROI) of the lungs was extracted using Otsu's threshold segmentation technique. For feature extraction, we used the Gabor filter to obtain texture details from the images. A Deep Convolutional Neural Network (DCNN) was then used for classification. The system classifies images into four categories: normal, pneumonia, pulmonary tuberculosis, and pleural effusion using a four-way SoftMax classifier. We tested four DCNN models: VGG16, VGG19, ResNet50V2, and DenseNet201. Among these, DenseNet201 performed best, achieving a training accuracy of 97.80% and a testing accuracy of 95.73%. Compared with other advanced models, DenseNet201 showed higher accuracy and better capability in detecting and classifying pulmonary diseases.

Keywords: Feature Learning, Gabor Filter, Pulmonary Disease, Segmentation, X-Ray, Respiratory Conditions

I. Introduction

Pulmonary Diseases (PDs), also known as respiratory diseases, are diseases of the airways and the other structures of the lungs. PD is a disease that has many types under it that prevent the lungs from functioning properly. It can affect lung respiratory function, or the ability to breathe[1]. It is one of the world's most serious public health issues. This disease is a collection of chronic illnesses that damage the lungs' airways and other structures. It mostly affects the lungs and respiratory system [2].

Physicians used a variety of measures to distinguish between healthy and abnormal lung tissue anatomical structures, including intensity, shape, and texture[3]. However, due to the large amount of data collected

Received: July 26, 2023; Revised: 16 September 2023; Accepted: 05 October 2023; Published: 31 December 2023.

ISSN (E): 2959-3921

(P): 2959-393X DOI: https://doi.org/10.59122/144CFC16



Copyright and License Grant: CC By 4.0



by an X-ray image, it is a difficult task. As a result, the development of automatic Computerized Aid Diagnostic (CAD) tools is required to assist physicians in more properly analyzing and evaluating X-ray images.

The World Health Organization (WHO) reveals that pulmonary disease is one of the leading causes of increased mortality in humans [3]. To reduce the risk of high mortality rate to prevent respiratory diseases or illnesses appropriate treatment is required. Clinical examination is one of the methods used to diagnose various pulmonary diseases to save patients with appropriate treatments. The most common technique in clinical diagnosis is to use a CXR image to diagnose lung disease. In a clinical examination, the diagnosis is made by reading lung scan images. A highly skilled medical radiologist is required to read X-ray images of lung diseases or illnesses. However, this approach requires many medical professional workers to read scanned X-ray images.

The proposed method is based on the DCNN algorithm, which uses a group of neurons to convolve and extract significant characteristics from a given image. CNN is a neural network that uses the convolution operation as one of its layers [4]. Multiple convolutions and pooling layers may be present in a CNN, which is then followed by a fully connected network. This enables CNN to create a concept hierarchy in which more complex notions are built on simpler concepts. The notion is that the features are generated by a sequence of convolution and pooling layers, and the final classification function is learned by a normal neural network[5].

II. **Related Works**

Based on various experiments, Betsy Antony and Nizar Banu P. K. [6] investigated the detection of lung tuberculosis using methods such as filtering, segmentation, feature extraction, and classification. The researchers used a total of 662 X-ray images from the National Health Institute, 326 of which were normal and 336 of which were pulmonary tuberculosis. To remove unwanted noise from an image, a Gaussian filter and a median filtering technique were performed. The researchers used K-nearest neighbor, sequential minimal optimization, and simple linear regression models to detect whether pulmonary tuberculosis was represented or not. The classification accuracy in simple linear regression, sequential minimal optimization, and K-nearest neighbor is 79%, 75%, and 80% respectively.

Norval, Wang, and Sun [7] studied the accuracy of two methods for detecting tuberculosis based on CXR images of patients using CNN. Various image preprocessing methods have been developed to find the highest precision. A total of 406 normal images and 394 abnormal images were used in the simulation. They used X-ray equipment from Shenzhen Hospital and X-ray equipment from Montgomery County.

Volume 1, Issue 2, 2023

DOI: https://doi.org/10.59122/144CFC16



Copyright and License Grant: CC By 4.0



Simulations show that the clipping region of interest plus the contrast enhancement produces excellent results. A hybrid method of combining primitive statistical CAD methods and neural networks has been studied. When the hybrid method is used to further enhance the image, better results can be obtained.

The researchers [8] studied the analysis of tuberculosis by DL with segmentation and augmentation of CXR. This study addresses the accuracy of the prediction of tuberculosis for relatively small datasets. The CNN was trained on the pre-processed dataset obtained after lung segmentation. The study [9], proposed based on preliminary results on pulmonary tuberculosis detection in chest X-ray using CNN. This study shows an experiment with a CNN architecture on public CXR databases to apply to diagnose pulmonary tuberculosis in chest X-ray images. As a consequence, depending on the network architecture, the study's AUC ranged from 0.78 to 0.84, sensitivity from 0.76 to 0.86, and specificity from 0.58 to 0.74.

The study [10], tried to simplify the diagnosis of pneumonia for professionals as well as for newcomers. The researchers recommend a novel DL framework for filtering using the concept of transfer learning to detect pneumonia. Another study [11], proposes a CNN model trained from scratch to detect and classify the presence of pneumonia from a collection of chest X-ray images. The researchers developed several data improvement algorithms to improve the image verification and classification accuracy of the CNN model and to enhance impressive verification accuracy.

Researchers [12] proposed a convolutional neural network for the classification of images and early diagnosis of pneumonia. For producing feature maps of the preprocessed X-ray image, they used a convolutional neural network technique. They found out that the accurate experimentation model classified the images with an accuracy of 85.73%. Ayan et al.[13], trained two classic CNN models, XceptionNet and VGG16Net, to use transfer learning and adjustment to classify images containing pneumonia. The accuracy results of the Vgg16 model and the XceptionNet model are 0.87% and 0.82% respectively.

Researchers in the study [6], surveyed state-of-the-art issues, and future directions that are used to provide deep learning of the lung's diagnosis in medical imaging. The paper is intended to provide an extensive survey of PD using deep learning, especially focusing on tuberculosis, pneumonia, and COVID-19. Another study [14], aimed to solve the problem of a lack of medical information regarding the work of diagnosing chest lung disease X-ray images using small data sets. In that study, the researchers combined two relatively small data sets of less than 103 images per class for classification images (detection of pneumonia and tuberculosis) and objectives of segmentation. In the best performance framework, researchers used network segmentation and InceptionV3 deep model classification.

Volume 1, Issue 2, 2023

DOI: https://doi.org/10.59122/144CFC16



Copyright and License Grant: CC By 4.0



Generally, several research works have been carried out in the area of respiratory disease recognition, but there are unexplored areas in binary classification (Pulmonary tuberculosis and pleural effusion) and ternary classification (pneumonia, pulmonary tuberculosis, and pleural effusion). In conclusion, the previous research works do not include the above classifications.

III. Materials and Methods

We discussed a detailed description of the proposed system structure for the detection and classification of PD. It is required to pass through a series of steps starting from the preprocessing of images, segmentation of the ROI, feature extraction, and learning to classify into predefined classes. The proposed research methodology architecture is depicted in Fig. 1.

A. Proposed System Architecture

The proposed system includes five main components: preprocessing, data augmentation, segmentation, feature extraction, and classification.

ISSN (E): 2959-3921

(P): 2959-393X

DOI: https://doi.org/10.59122/144CFC16



Copyright and License Grant: CC By 4.0



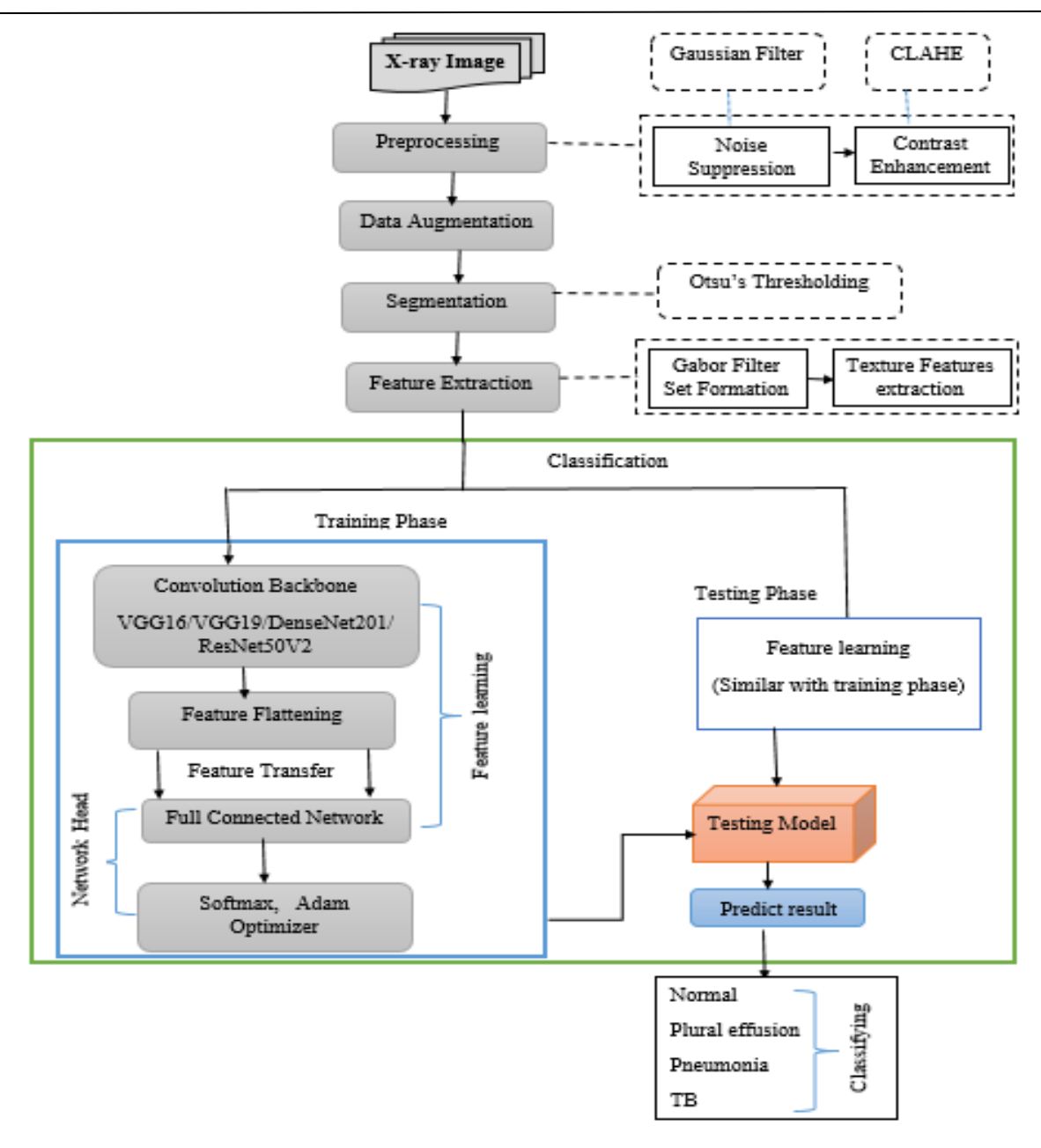


Fig. 1. Architecture of the proposed research methodology

B. Data Collection

Sample X-ray images are required to perform image processing operations on it. The researcher needs a lot of X-ray image samples to carry out this work. We collected chest X-ray images from Debre Markos Referral Hospital. In the image acquisition phase, normal and diseased images were taken. The sample data source contains representatives from each class type such as normal, pneumonia, pleural effusion, and pulmonary tuberculosis. A total of 1,019 X-ray images were collected in DICOM file format.

Volume 1, Issue 2, 2023

Copyright and License Grant: CC By 4.0



DOI: https://doi.org/10.59122/144CFC16

The amount of collected X-ray image data was very small. When the amount of sampled dataset available is limited, some transformation is to be applied to the existing dataset to increase the amount of training sample set. As the size of training samples increased, the proposed system model was significantly improved. Due to the small size of our sample data source, we have increased data collection capacity using data augmentation techniques to improve system performance.

As a result, we increased our total data amount from 1019 to 2460 because this number has achieved the desired result for our system performance model. The training dataset consisted of 80% of the randomly selected images. The remaining 20% were used during testing, and their class distribution was labeled as normal, pneumonia, pleural effusion, and tuberculosis. During the model process, the training dataset was divided into a training set and a validation set using a 0.10 (10%) validation split.

C. Preprocessing

Pre-processing aims to improve the quality of the X-ray image so that the model analyzes it in a better way. In this process, we have smoothed or blurred the X-ray images to improve the quality of the X-ray image by enhancing unnecessary distorted features during image pre-processing.

- 1) Standardize images: In the preprocessing stage, the image size was resized to 224 x 224 pixels. Most advanced models [15] use the same image size as input, making it suitable for comparison. Using the same dimensions ensures consistency when evaluating our network against existing state-of-the-art models.
- 2) Adjust image quality: In this study, image smoothing was used to remove noise from the samples. Reducing noise to restore the original image is often a complex process. To address this, we applied the Gaussian Blur technique to clean the images. The Gaussian filter was implemented using the function cv2.GaussianBlur with a kernel size of 5x5.

The following function is used to calculate the Gaussian kernel [16]:

The two-dimensional image Gaussian filter equation is given by:

$$G(x,y) = \frac{1}{2\pi\sigma^2} e^{-\frac{x^2 + y^2}{2\sigma^2}}$$
 (1)

Where σ is the standard deviation of the distribution containing the x and y coordinates in two-dimensional images.

3) Contrast enhancement: As depicted in Fig. 2, we used histogram equalization in this study to increase image contrast enhancements by enhancing the brightness difference between lung objects and their

(P): 2959-393X

ISSN (E): 2959-3921

DOI: https://doi.org/10.59122/144CFC16



Copyright and License Grant: CC By 4.0



backgrounds. There are two advanced histogram equalization techniques: these are Adaptive Histogram Equalization (AHE) and Contrasted Limited Adaptive Histogram Equalization (CLAHE).

CLAHE has been used to improve the contrast of X-ray medical images. The contrast limitation of CLAHE distinguishes it from typical AHE. The CLAHE technique divides an input original image into non-overlapping contextual parts known as sub-images, tiles, or blocks. There are two parameters in CLAHE: block size and clip limit, which are used to control image quality. The CLAHE method applied histogram equalization to each region of the X-ray image context. The clipped pixels are redistributed over each grey level, and the original histogram is cropped [17]. In the redistributed histogram, the intensity of each pixel is limited to a fixed maximum value, unlike in a standard histogram.

After using the CLAHE method, we obtained improved X-ray images. The enhanced image was obtained by creating a histogram equalization mapping for all pixels. Improving contrast enhancement shows differences in image brightness. During the histogram equalization mapping process, this study used clip Limit 2.0 and tile Grid Size (2, 2). These two parameters are used to improve X-ray image brightness as shown in the image below, Fig.2.

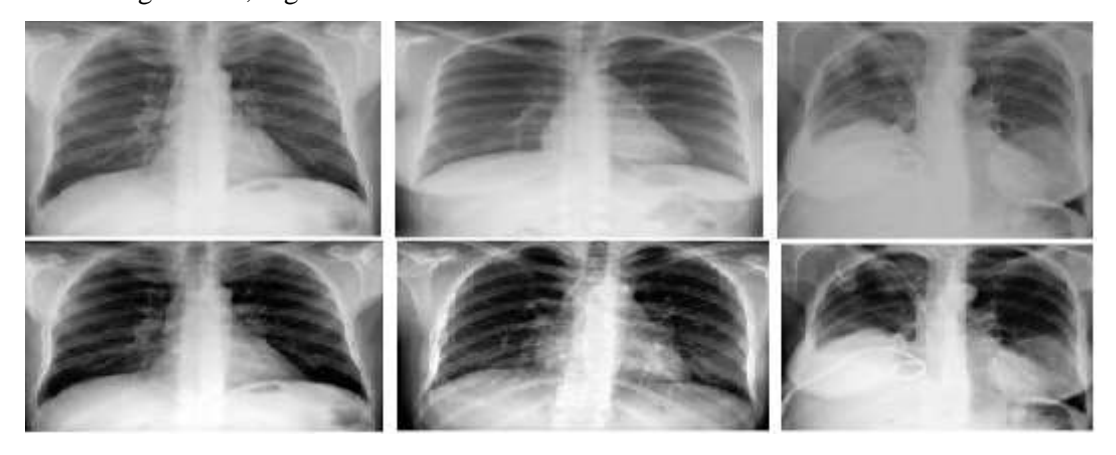


Fig. 2. Effect of CLAHE (below) on the blurred input image

D. Data Augmentation

We used data augmentation techniques on the X-ray image dataset to increase the number of useful images and improve the diversity of the dataset. Data augmentation techniques have different criteria to make different identical content such as rotation range, horizontal shift, vertical shift, shear range, zoom range, and horizontal flip. We have used the above criteria in data augmentation operation to increase the size of our data sets. In our situation, we rotated our input images by 10 degrees at random. The random rotations' degree range is controlled by a 10-degree rotation range. We also used the horizontal transformation of the images by 0.2 percent, and a vertical transformation of the images by 0.2 percent, which is called the width

DOI: https://doi.org/10.59122/144CFC16



Copyright and License Grant: CC By 4.0



and height shift respectively. In addition, the image angles are clipped in a counterclockwise direction by a shear range of 0.2 percent. The shear range controls the angle in an anti-clockwise direction as a radian in which our input image is allowed to be sheared. The image was then flipped horizontally after the zoom range was randomly zoomed to a ratio of 0.2 percent.

E. Segmentation

Image segmentation is well known for allowing the splitting of an image into targeted image objects or segments that appear as distinct categories of pixels, with each category becoming a segment. In this study, we used Otsu's thresholding technique, which has been widely reported to yield interesting findings. It is important to distinguish between ROI and other image regions. This technique allows for automatically computing the optimum threshold value from the input image[18].

So far, we have used a 5x5 Gaussian kernel to eliminate noise from our image samples, followed by Otsu thresholding. As a result, threshold segmentation was used to divide the image into the area of interest and another region. The main work is to separate the image histogram into two clusters by minimizing the weighted variance of these classes denoted by σ_{ω}^2 (t). The total computation equation is described as follows: -

$$\sigma_{\omega}^{2}(t) = \omega 1(t)\sigma_{1}^{2}(t) + \omega 2(t)\sigma_{2}^{2}(t)$$
 (2)

 $\omega 1(t)$, $\omega 2(t)$ are the probabilities of the two classes divided by threshold t, with values ranging from 0 to 255. There are two options for finding thresholding. The first is to minimize the class variance described in the above $\sigma_{\omega}^2(t)$ and the second is to maximize the variance between classes by using the following expression. The variance between classes is defined as[19]:-

$$\alpha_b^2(t) = \omega 1(t)\omega 2(t) (\mu_1(t) - \mu_2(t))^2$$
 (3)

$$\alpha_{\rm T}^2 = \alpha_{\rm b}^2(t) + \sigma_{\rm \omega}^2(t) \tag{4}$$

Where α_T^2 and μ are the total variance of the image and the mean of the class, respectively. As shown in Fig.3, when we applied the Otsu method to the raw image, we obtained the ROI result on the image.



Fig. 3. ROI Segmentation

Copyright and License Grant: CC By 4.0







F. Feature Extraction

ISSN (E): 2959-3921

The structure of a human lung is interesting, and it holds a lot of textural information. It has distinguishing textural features that are used to determine whether a person is infected or not. We have used the Gabor filter technique to extract features of the X-ray images. Gabor filters have long been popular in computer vision, particularly for texture analysis. Textural properties in images can be utilized to detect lung illnesses accurately. The Gabor filter is one of the most widely used techniques for extracting or analyzing texture features [20]. A collection of Gabor filters with varying frequencies is used to extract textural characteristics from the image.

As depicted in Fig.4, when we apply a Gabor filter on raw images, the textures on the image are easily visible and easy to identify and classify for lung disease for the CNN model.





Fig. 4: Left: raw image right: image on the left applied with Gabor filter

G. Classification

Classification is the final task of this work. As we discussed in the literature review, there are different algorithms used for classification purposes. In this study, we selected VGG16, VGG19, ResNet50V2, and DensNet201 classifiers with SoftMax activation functions for classification. The reason we chose these classic learning models is based on popularity as they are now highly rated for feature extraction and classification. Classification is done by using the knowledge from the learning model, which is constructed by using the training and testing phases. In the training phase, the training dataset is used. By using the knowledge from the learning model, we categorize each image (in the testing dataset) into a specific or predefined class (normal, pneumonia, pulmonary tuberculosis, and pleural effusion).

IV. **Experimental Setup and Result Analysis**

A. Experimental setup

We defined several system hyperparameters and selected their values carefully based on experimental results. Designing and developing a high-performing system model is a critical task. The performance of the system depends largely on the choice of network parameters. Since many hyperparameters need to be tested at each stage, we identified the best values for each one in network architecture. In the proposed

Volume 1, Issue 2, 2023

DOI: https://doi.org/10.59122/144CFC16

Copyright and License Grant: CC By 4.0



system, different parameter combinations were tested, and the model with the lowest loss or error rate was chosen.

We have been feeding neural network training data throughout epoch 30. We got a better fit when we fed it a new "unseen" input (test data). After training our model using epoch 30, we got optimal model performance. Our network was trained with Adam Optimizer. Adam is one of the deep neural network training optimizers that uses an adaptive learning rate optimization mechanism. We used the ReLU activation function. For multiclass classification tasks, the SoftMax function is utilized. We have developed a network or model for four-class classification, and the network's output layer has the same number of neurons as the target's number of classes. For this reason, we used the SoftMax activation function for pulmonary disease classification to improve performance and computational time.

B. Models

The models were expanded with feature flattening, a fully connected layer having 512 and 256 neurons, dropout, and a SoftMax classifier. When we chose and used this neuron, we achieved the highest accuracy according to our goals. When measuring network performance, we found a good representation of our test goals using metrics. The deep neural networks had a total of 6,423,812 trainable parameters for VGG16, 25,695,236 for VGG19, 51,382,788 for ResNet50V2, and 48,171,524 DenseNet201. Before feeding the input images into deep neural networks used for feature extraction, all image batches were adjusted to match the same format (batch size, input scale, etc.) as those used in the trained models. During training, our neural network classifiers learned bias and weight parameters by backpropagating errors to minimize categorical cross-entropy using the Adam optimizer.

The models were later validated using different sets of hyper-parameters observed during the training process. The SoftMax classifier produces a vector of probabilities indicating whether or not an input image belongs to one of the classes. The final class is the one that corresponds to the highest value, and its position is then mapped back to a class.

The model is trained on 30 epochs, a batch size of 32 and 64, and a starting or initial learning rate of 0.001 (1e-3). The data is partitioned into a training and testing dataset, which means that the training dataset is used to train the model, and the test dataset is assigned to test the performance of the model.

C. Results

We have used precision, recall, and F1-score to measure the performance of our model. We showed the performance of our model by applying the Gabor filter. The training phase is the sequence of feature



Copyright and License Grant: CC By 4.0



flattening, activation function, and fully connected layers and dropout after the final fully connected layers and before the SoftMax classifier. The training process was then stopped, and the final results were measured as an average of all results obtained at that step. The final step was to demonstrate the performance of selected models on previously unknown data (test set).

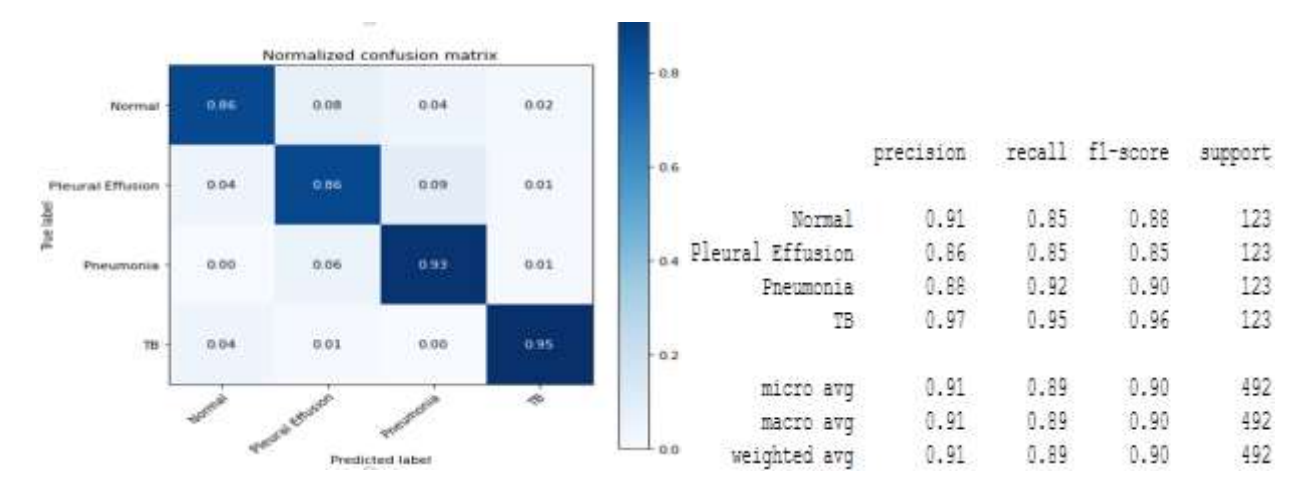


Fig. 5. Confusion matrix and classification accuracy VGG16 model on batch size 64

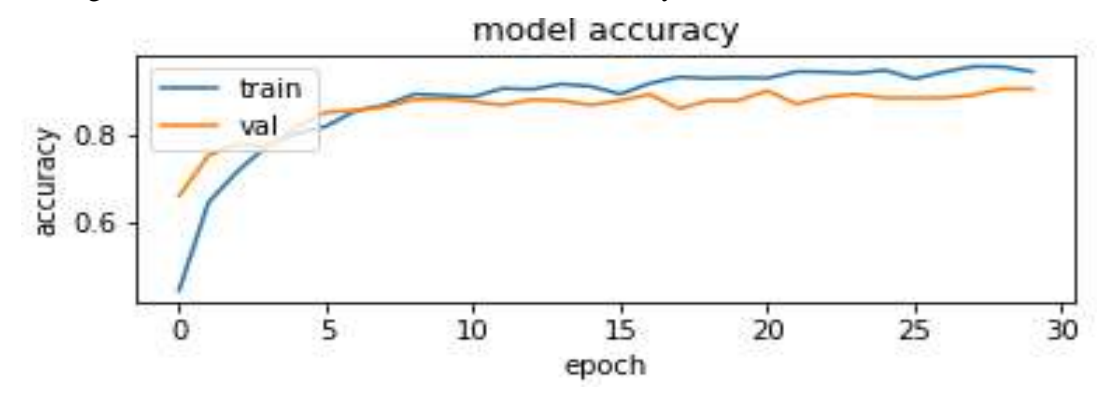


Fig. 6. Training and validation accuracy curve of VGG16 on batch size 64

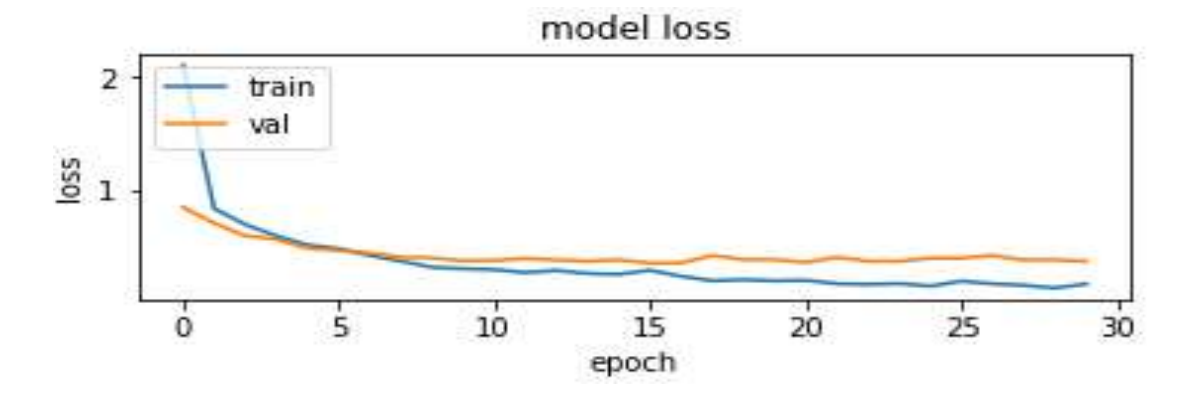
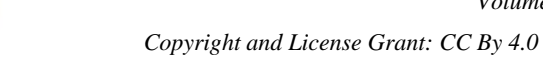


Fig. 7: Training and validation loss curve of VGG16 on batch size 64

DOI: https://doi.org/10.59122/144CFC16





@ **①**

Table I: Experimental Test Result

Madal	Europh	Learning rate	Ontinina	Batch	Training	Test	Loss	Model
Model	Epoch		Optimizer	Size	Accuracy (%)	Accuracy (%)	Accuracy (%)	size (in MB)
VCC16	20	0.001	A dom.	32	92.21	90.04	43.31	4.6
VGG16	VGG16 30 0.001	0.001	Adam	64	94.12	90.24	36.14	4.6
VCC10 20 (0.001	A .1	32	96.65	90.24	37.87	25.69	
VGG19	30	0.001	Adam	64	97.47	92.07	30.26	25.69
ResNet50V2	30	0.001	Adam	32	95.05	94.31	24.93	51.38
Resnetsuv 2 30	30	0.001	Auaiii	64	96.82	94.51	33.08	51.38
D N (201	20	0.001	A 1	32	95.65	95.12	19.01	48.17
Deliserret201	DenseNet201 30 0.001 A	Adam	64	97.80	95.73	16.92	48.17	

V. Discussion

Experimental results of the proposed model for automatic detection and classification of PD are described in detail hereunder. The dataset used and the implementation of the proposed model are described briefly. We have developed four deep CNN models, which are VGG16, VGG19, ResNet50v2, and DensNet201. These models were trained using the same epoch, learning rate, and optimizer. We have defined the experimental result for each model. For each model as depicted in Fig. 5, 6, and 7, we described in detail the confusion matrix, classification report, accuracy, and loss curve.

The models are trained using the same image size. In these trained models, we used standard image sizes (224,224). We have evaluated the performance of our model by comparing its performance with the state-of-the-art models. To begin with, using two different batch sizes, we showed the performance of the models. We trained models using two different batch sizes: 32 and 64. When we changed the size of the batch, our model performances showed a little difference in training accuracy and test accuracy. As shown in Table I above, the trained models in batch size 64 performed better than those in batch size 32. In addition, comparisons of the models are performed based on accuracy, loss, and size of parameters. In terms of size, the training is better to train the model quickly on a small size (small number of parameters). The VGG16 model has a small number of parameters, so it is better to train the model. However, this model has high validation loss and smaller test accuracy compared to the other models. As a result, VGG16 has made the computational resources especially those used in memory more efficient. Based on the accuracy of the model, the DenseNet201 model has achieved a higher accuracy for the detection and classification of diseases. The experiment result of the DenseNet201 model trained in a batch size of 32 achieved 95.65% training accuracy and 95.12% testing accuracy. As well, the experiment result of the DenseNet201 model

DOI: https://doi.org/10.59122/144CFC16

ISSN (E): 2959-3921

(P): 2959-393X

4

Copyright and License Grant: CC By 4.0



trained in batch size 64 achieved 97.80% training accuracy and 95.73% testing accuracy. The DenseNet201 model trained on a batch size of 64 has a low validation loss value (16.92%), making it better for classifying pulmonary disease cases.

Generally, the DenseNet201 model ensured the best result without overfitting or underfitting problems. The result of the DenseNet201 model did not show much difference in terms of training and testing accuracy. The DenseNet201 model has higher classification accuracy than VGG16, VGG19, and ResNet50V2. Therefore, the DenseNet201 model is better for finding new pulmonary disease cases.

VI. Conclusion

In this study, we focused on exploring lung disease classification problems using deep neural networks. A deep CNN model was developed for the detection and classification of PD using images of both normal and infected lungs. We used Gabor filter techniques before the DCNN algorithm to improve our model performance. The Gabor filter technique is used for textural features to determine whether a person is infected or not. The textural features in images are used to detect lung illnesses accurately. As a result, the use of the Gabor filter has made our model's performance better.

The significance of the developed system has changed in the progress of diagnosis in terms of accuracy and efficiency. The CXR images were used in the proposed method to separate four classes into normal, pneumonia, pulmonary tuberculosis, and pleural effusion. We also compared our proposed deep CNN with other neural learning networks (Including VGG16, VGG19, ResNet50V2, and DensNet201). The model results are summarized in Table I, in which we used accuracy to evaluate the performance since the test dataset in the class was equally distributed. In our models, the DenseNet201 proposed model has achieved better results in terms of accuracy and loss. In terms of accuracy, we have 97.80% training accuracy and 95.73% testing accuracy which are far above state-of-the-art models. So, the DenseNet201 model that records higher accuracy is better for detecting and classification of pulmonary diseases. Due to the good performance of the proposed algorithm, it can be used as a smart computer assistant in the field of medicine for rapid diagnosis.

References

- J. L. López-Campos, J. J. Soler-Cataluña, and M. Miravitlles, "Global strategy for the diagnosis, management, and prevention of chronic obstructive lung disease 2019 report: future challenges," *Arch. Bronconeumol.*, vol. 56, no. 2, pp. 65–67, 2020.
- 2. M. Varmaghani, M. Dehghani, E. Heidari, F. Sharifi, S. S. Moghaddam, and F. Farzadfar, "Global prevalence of chronic obstructive pulmonary disease: Systematic review and meta-analysis," *East*.

ISSN (E): 2959-3921 (P): 2959-393X

DOI: https://doi.org/10.59122/144CFC16



Copyright and License Grant: CC By 4.0



- Mediterr. Heal. J., vol. 25, no. 1, pp. 47–57, 2019, doi: 10.26719/emhj.18.014.
- 3. J. Y. Choi et al., "Comparison of clinical characteristics between chronic bronchitis and non-chronic bronchitis in patients with chronic obstructive pulmonary disease," *BMC Pulm. Med.*, vol. 22, no. 1, pp. 1–9, 2022, doi: 10.1186/s12890-022-01854-x.
- 4. M. A. Wani, F. A. Bhat, S. Afzal, and A. I. Khan, "Introduction to Deep Learning," in *Advances in Deep Learning*, M. A. Wani, F. A. Bhat, S. Afzal and A. I. Khan, Eds., Gateway East, Singapore: Springer, 2020, pp. 1–11. doi: 10.1007/978-981-13-6794-6_1.
- 5. J. Wu, *Introduction to Convolutional Neural Networks*, Nanjing University, China: LAMDA Group National Key Lab for Novel Software Technology, May 1, 2017, pp. 1–31.
- 6. S. T. H. Kieu, A. Bade, M. H. A. Hijazi, and H. Kolivand, "A survey of deep learning for lung disease detection on medical images: State-of-the-art, taxonomy, issues, and future directions," *J. Imaging*, vol. 6, no. 12, p. 131, 2020, doi: 10.3390/jimaging6120131.
- 7. M. Norval, Z. Wang, and Y. Sun, "Pulmonary tuberculosis detection using deep learning convolutional neural networks," 3rd *ACM Int. Conf. Proceedings Ser.*, October 2020, pp. 47–51, 2019, doi: 10.1145/3376067.3376068.
- 8. S. Stirenko et al., "Chest X-ray analysis of tuberculosis by deep learning with segmentation and augmentation," *arXiv*, 2018 IEEE 38th International Conference on Electronics and Nanotechnology (ELNANO), Kiev, 2018, pp. 422-428.
- 9. M. E. Colombo Filho et al., "Preliminary results on pulmonary tuberculosis detection in chest x-ray using convolutional neural networks," *Computational Science ICCS 202020th International Conference*, Proceedings, *Part IV* Amsterdam, The Netherlands: PMCID: PMC7303695, June 3–5, 2020, 12140, pp. 563-576
- 10. V. Chouhan et al., "A novel transfer learning based approach for pneumonia detection in chest X-ray images," *Appl. Sci.*, vol. 10, no. 2, 2020, doi: 10.3390/app10020559.
- 11. T. Gao, "Chest X-ray image analysis and classification for COVID-19 pneumonia detection using deep CNN," medRxiv, pp. 1–14, 2020, (Preprint) doi: 10.1101/2020.08.20.20178913.
- 12. H. Magar, S. J. Patil, S. R. Waykole, S. D. Sandikar, and N. D. Parakh, "Pneumonia detection using x-ray images with deep learning," *Inter. J. of Comp. Appl. Tech. and Research* vol. 9, no. 5, pp. 183–185, 2020.
- 13. E. Ayan and H. M. Ünver, "Diagnosis of pneumonia from chest X-ray images using deep learning," *Sci. Meet. Electr. Biomed. Eng. Comput. Sci.* EBBT 2019, pp. 0–4, 2019
- 14. M. Zak and A. Krzyżak, "Classification of lung diseases using deep learning models," Computational

DOI: https://doi.org/10.59122/144CFC16 Copyright and License Grant: CC By 4.0





- Science ICCS 2020, 12139 LNCS, pp. 621–634, 2020.
- 15. M. B. Jerubbaal John Luke, Rajkumar Joseph and Cognitive, "Impact of image size on accuracy and generalisation of convolutional neural networks," *Int. J. Res. Anal. Rev.*, vol. 6, no. 1, 2019.
- 16. A. Padmanabhan and S. Dinesh, "The effect of Gaussian blurring on the extraction of peaks and pits from digital elevation models," *Discrete. Dyn. Nat. Soc.*, vol. 2007, no. 1, 2007.
- 17. J. Ma, X. Fan, S. X. Yang, X. Zhang, and X. Zhu, "Contrast Limited Adaptive Histogram Equalization Based Fusion for Underwater Image Enhancement," no. March, pp. 1–27, Preprints 2017, 2017030086. https://doi.org/10.20944/preprints201703.0086.v1.
- 18. J. Yousefi, "Image Binarization using Otsu Thresholding Algorithm," Guelph, ON, Canada: University of Guelph, April 2011. https://www.researchgate.net/profile/Jamileh-Yousefi 2/publication /277076039

 _Image_Binarization_using_Otsu_Thresholding_Algorithm/links/55609b1408ae8c0cab31ea42/Image-Binarization-using-Otsu-Thresholding-Algorithm.pdf
- 19. A. Kumar and A. Tiwari, "A comparative study of Otsu thresholding and K-means algorithm of image segmentation," *Int. J. Eng. Tech. Res.*, vol. 9, no. 5, pp. 12–14, 2019.
- 20. Y. Wicaksono and V. Suhartono, "Color and texture feature extraction using Gabor filter," *J. Intell. Syst.*, vol. 1, no. 1, pp. 15–21, 2015.

ISSN (E): 2959-3921

(P): 2959-393X

DOI: https://doi.org/10.59122/144CFC18



Copyright and License Grant: CC By 4.0



Numerical Investigation of Reinforced Concrete Beam Containing Iron Ore Tailings as Partial Replacement of Sand

Mahmud Abubakar^{1*}, Muhammad Idris Haruna², Hassan Shuiabu Abdulrahman¹ Bala Alhaji Abbas¹

¹ Federal University of Technology, Minna, Niger, Nigeria

² Jigawa State Polytechnic, Dutse, Jigawa, Nigeria

*Corresponding Authors Email: mahmud1879@futminna.edu.ng

Abstract

The production of industrial and agricultural residual byproducts can generate significant environmental impact. In response, incorporating supplementary materials made from agro-industrial wastes to create more sustainable concrete is being undertaken. However, testing the performance of these waste-based concrete mixtures can be time-consuming and expensive. To resolve this problem, this study utilized three-dimensional non-linear Finite Element simulation using the ABAQUS/Computer Aided Engineering software/ to predict the behavior of a reinforced concrete beam that incorporated 20% IOT as partial sand replacement. The ultimate load obtained from the 20% IOT concrete beam was compared with experimental results, which showed a 19% positive difference in terms of the load-carrying capacity. Hence, the simulated experiments successfully predicted the damage behavior of the 20% IOT concrete, indicating the potential of this modeling approach to accurately predict the performance of waste-based concrete mixtures in various designs.

Keywords: ABAQUS, Computer Aided Engineering, Iron Ore Tailings, Numerical Analysis, Rein-forced Concrete Beam

I. Introduction

Concrete is a popular construction material worldwide [1]. It is made up of a combination of coarse and fine aggregates, cement, water, and sometimes other components. The high demand for aggregates has led to a scarcity of their non-renewable natural sources and the search for more sustainable options [2]. On the other hand, the production of cement results in significant greenhouse gas emissions and air pollution [3]. Research has indicated that the ordinary Portland cement industry is responsible for approximately 7% of the world's CO₂ emissions, with the majority being released during concrete production [4]. It takes 1.6 tons of raw materials and emits 1 ton of CO₂ to produce just 1 ton of ordinary Portland cement [5]. To

Volume 1, Issue 2, 2023

DOI: https://doi.org/10.59122/144CFC18



Copyright and License Grant: CC By 4.0



minimize the negative impact on the environment, there is a need to find alternatives to cement with a lower carbon footprint.

Iron ore tailings are a common waste product of the mining industry that is generated during the extraction and processing of iron ore. These tailings are typically composed of a mixture of crushed rock, water, and chemicals used in the beneficiation process, and they can be disposed of in a variety of ways, including in tailings storage facilities or backfilling into mining pits.

The disposal and management of iron ore tailings can pose significant environmental challenges. These tailings can release harmful chemicals and heavy metals into the environment, leading to soil and water contamination and potentially harmful effects on human health and ecosystems [6], [7]. In addition, the construction and maintenance of tailings storage facilities can be expensive and resource-intensive [8].

However, iron ore tailings also present opportunities for resource recovery and reuse. They can be used as a source of valuable metals and minerals, as well as for the production of construction materials such as concrete, bricks, and ceramics [9], [10]. The utilization of iron ore tailings as a substitute for natural aggregates in concrete has shown great potential in recent years, providing a sustainable solution to reduce the demand for virgin aggregates and waste accumulation [10], [11].

In related works, the contribution of the iron ore tailings material to the flexural behavior of the reinforced concrete beam elements is described in terms of load-concrete strain, load-steel strain, load-deflection relationships, cracking behavior, and the ultimate load at failure [12]. [13] investigate the replacement of natural quartz sand with an iron-rich mine tailing in PVA-reinforced AAM. [14] study geopolymer bricks using iron ore tailings, slag sand, ground granular blast furnace slag, and fly ash. Development of geopolymer binder-based bricks using fly ash and ground granulated blast furnace slag has been carried out. [15] aim to identify the influence of the incorporation of iron ore tailings (IOT) obtained from the Germano dam in Brazil in the substitution of sand fractions in concrete. 15%, 30%, 50%, and 70% iron tailings were used to replace the natural sand in concrete, and 1.5% steel fiber and 0-0.75% PVA fibers were added to the iron tailings concrete [16]. Other influential work includes [17]. However, while the usage of alternative materials in concrete mixes, such as IOT, has been considered a solution to the environmental and economic impacts of natural sand depletion, there is a lack of comprehensive understanding of the structural behavior of concrete containing these materials under long-term loading and environmental exposure.

DOI: https://doi.org/10.59122/144CFC18



Copyright and License Grant: CC By 4.0



This paper presents a numerical investigation of reinforced concrete beams containing iron ore tailings as a partial replacement for sand. The research aims to evaluate the mechanical and structural performance of reinforced concrete beams with 20 percent iron ore tailings replacement. The investigation focused on the flexural strength, crack pattern, and failure modes of the beams. The findings of this research will provide valuable insights into the potential of iron ore tailings as a sustainable and cost-effective alternative to natural sand in concrete production.

II. Finite Element Model

The study of the performance of concrete has been made possible by advances in finite elements and highend computers. One of the computer software used to solve complex engineering problems and applicable across industrial disciplines such as mechanical engineering and civil engineering is ABAQUS. According to failure behavior criteria, a geometry model can be constructed [18]. The ABAQUS explicit dynamics finite element program is a mathematical technique used for integrating equations of motion through time. Previous research [19] and [20] have shown that predicted load defection curves, the linear law, even though slightly neglected the initial stiffness, and the test peak curve for plain concrete (though steep for triangular mesh) were in good agreement with the corresponding standard experimental values.

A. Description of the FE Model

To model reinforcement in ABAQUS, a truss element called T3D2, which is a 3D element with 2 nodes, is used. For simulating the behavior of concrete, a 3D general-purpose linear brick element, C3D8I, with 8 nodes and 1 integration point is employed. An elastic-perfectly plastic model is utilized to simulate the material behavior of the longitudinal and transverse reinforcement in ABAQUS. This model ensures that the reinforcement is embedded in the same degree of freedom as the concrete, ensuring perfect bonding between the two materials. Tables I and II present the concrete properties and the concrete damage parameters used for modeling the concrete in ABAQUS.

Table I: Materials Properties Parameter for Concrete Containing 20 % Iot

Dilation	Eccentricity	Initial biaxial/uniaxial	K	Density	Young's Modulus	Poisson
Angle	(mm)	ratio		(kg/m^3)	$(x10^{-6} MPa)$	ratio
400	1.0	1.16	0.667	2430	26,530	0.26



Copyright and License Grant: CC By 4.0



Table II: Concrete Damage Plasticity Parameters

Compression Behavior			Tension Behavior			
Yield Stress	Inelastic	Damage	Yield Stress	Cracking	Damage	
(Mpa)	Strain	Parameter	(Mpa)	Strain	Parameter	
12.87000	0.00000	2.41370	0.00000	0.00000	0.00000	
13.01573	0.00000	2.33619	0.54410	0.00420	0.03211	
15.44780	0.00001	1.78654	0.61722	0.00496	0.25983	
17.77072	0.00002	1.37712	0.67193	0.00569	0.42946	
19.96187	0.00003	1.11500	0.71392	0.00641	0.53805	
22.00059	0.00006	0.93943	0.74694	0.00712	0.61079	
23.86922	0.00008	0.81500	0.77346	0.00782	0.66234	
25.55379	0.00012	0.72249	0.79516	0.00851	0.70067	
27.04457	0.00016	0.65104	0.81320	0.00920	0.73027	
28.33630	0.00021	0.59415	0.82841	0.00989	0.75384	
29.42813	0.00027	0.54773	0.84140	0.01057	0.77308	
30.32330	0.00034	0.50907	0.85261	0.01125	0.78909	
31.02866	0.00041	0.47634	0.86237	0.01193	0.80265	
31.55409	0.00049	0.44823	0.87094	0.01261	0.81430	
31.91175	0.00057	0.42381	0.87853	0.01328	0.82441	
32.11546	0.00067	0.40237	0.88529	0.01396	0.83330	
32.18000	0.00076	0.38337	0.89134	0.01463	0.84117	
32.06651	0.00087	0.36641	0.89680	0.01531	0.84820	
27.79177	0.00170	0.35116	0.90175	0.01598	0.85452	
22.27407	0.00258	0.33736	0.90624	0.01665	0.86023	
17.88359	0.00341	0.32481	0.91035	0.01732	0.86543	
14.67073	0.00420	0.31335	0.91412	0.01799	0.87018	
12.31800	0.00496	0.30282	0.91758	0.01866	0.87454	
10.55733	0.00569	0.29311	0.92078	0.01934	0.87856	
9.20590	0.00641	0.28413	0.92374	0.02001	0.88229	
8.14341	0.00712	0.27579	0.92649	0.02068	0.88574	
7.29007	0.00782	0.26802	0.92906	0.02135	0.88896	

III. Experimental Set-Up

Previous research has shown that the ultimate replacement level for IOT in concrete is 20 %. Thus, on this basis, concrete grade 25 was designed using the DoE method and incorporating OPC. The quantities obtained are presented in Table III. Testing of the beam specimen was conducted after 28-day curing in water to determine the flexural behavior of the beam in terms of cracking pattern, failure mode, and load vs deflection.



Copyright and License Grant: CC By 4.0



Table III: Constituent Materials for A Cubic Meter of Concrete

	Constituent Materials (Kg/m³)					
Concrete	Water	Cement	Fine	Iron Ore	Coarse	
Samples		Cement	Aggregate	Tailings	Aggregate	
0% IOT	210	362.06	668.88	0.0	1189.12	
20% IOT	210	362.06	535.10	133.78	1189.12	

For this study, six beam specimens were cast and tested: three for the control group and three with a 20% IOT sand replacement level. The length of each beam was 1500mm with a cross-sectional area of 200mm depth and 100mm width. The beams were double reinforced using 2Y8 high tensile bars and R4 mild steel round bar stirrups. Testing was conducted following BS EN12390-5:2009, using a four-point load to measure the ultimate failure load after 28 days of curing. Fig. 1 illustrates the experimental setup of the beam.



Fig. 1: Experimental set-up

A. Flexural Strength of the Beam

The flexural strength test result is presented in Table IV. It is observed that the flexural strength gains of the concrete containing IOT was superior to control specimens. It is observed that the flexural strength of concrete containing 20% IOT for M25 at the age of 28 days was found to develop a higher flexural strength of 19.4% above that of the control concrete beam. In general, concrete containing IOT showed higher rates of flexural strength development throughout the curing period.

Table IV: Flexural Strength of 20% IOTs Concrete Beam

Type of Concrete Mix	Age (days)	Flexural Strength (MPa)	% difference	
Control mix	28	7.2		
20% IOT mix	28	8.6	19.4	

Received: June, 2023; Revised: 16 September 2023; Accepted: 05 October 2023; Published: 31 December 2023.



B. Cracking Pattern in the Beam

From Fig. 2, both control (0% IOT) and 20% IOT concrete beams can be observed to have primary cracking patterns at the middle region which propagates diagonally towards flexural failure. However, minimal failure concentration in the FE model is shown in Fig. 3 while in the experimental beam, multiple cracks were visible. However, it can be said in general terms that cracking patterns in both the experimental beam and ABAQUS model have a good agreement and compare well.



Fig. 2(a). Experimental Cracking Pattern in Control Beam



Fig. 2(b). Experimental Cracking pattern in 20%

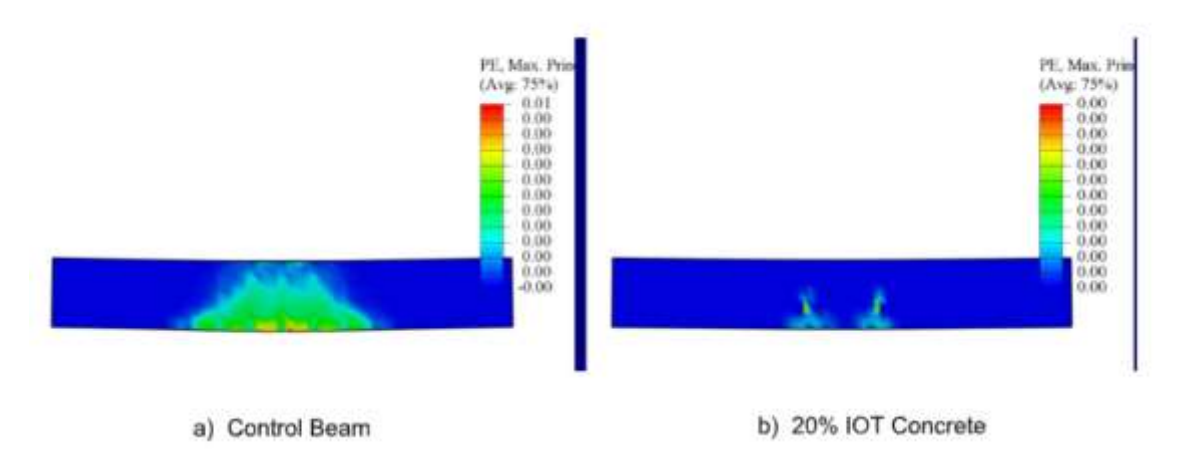


Fig. 3. FE Model Cracking Pattern

C.Axial Load Vs Displacement

During the ABAQUS analysis, the history output request was utilized to examine the vertical load versus displacement for a beam model in FEA. Fig. 4 and 5 show the load against the corresponding displacement

ISSN (E): 2959-3921

Copyright and License Grant: CC By 4.0



of the beam model for both control and 20% IOT concrete respectively. The results reveal that the 20% IOT concrete has a greater load-bearing capacity in both the experimental and FE models. The load increment trends against displacement were also similar between the experimental beam specimen and the simulation model, indicating that the FE model can accurately predict the behavior of the IOT concrete beam.

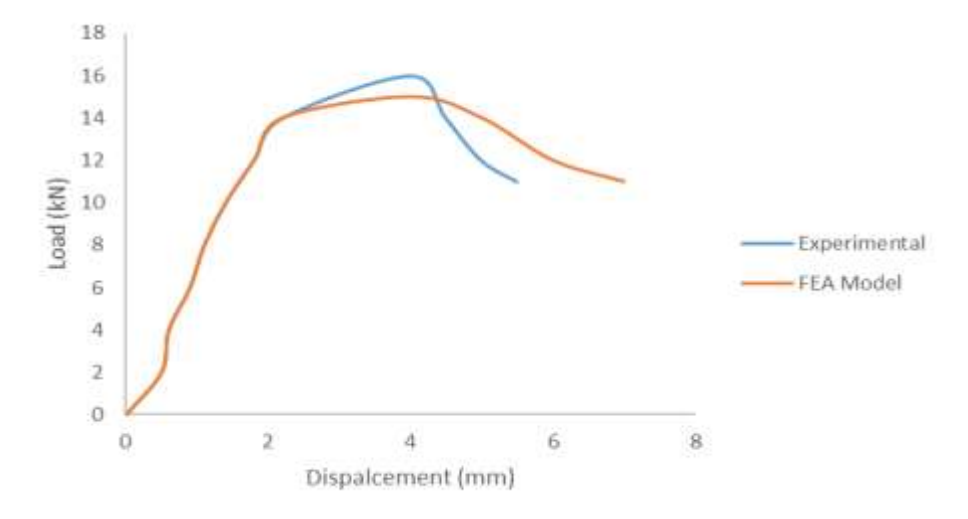


Fig. 4. Load vs Displacement for FE Model and Experimental Beam Control

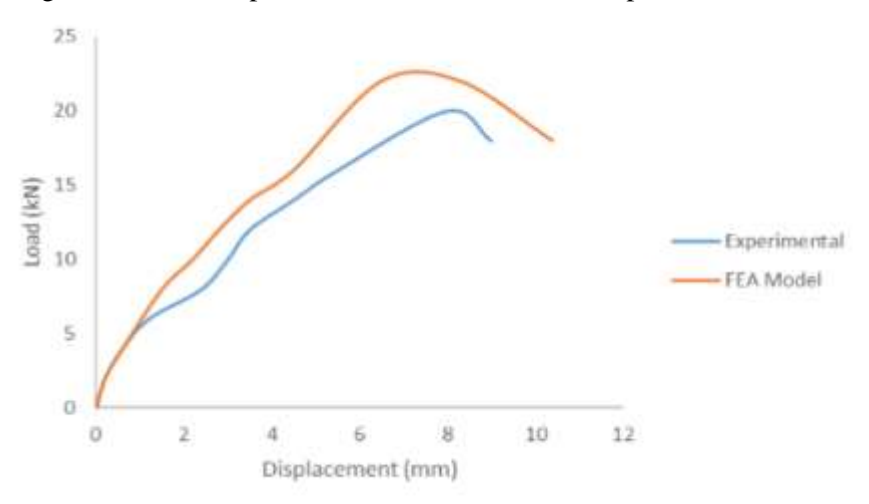


Fig 5. Load vs Displacement for FE Model and Experimental 20% IOT

D. Parametric Study

A study was conducted to analyze the failure mode of a beam model by varying its geometric parameters. This parametric study aimed to investigate the failure criterion across different cross-sectional dimensions and lengths that were not covered in previous experimental works.

ISSN (E): 2959-3921

(P): 2959-393X

Copyright and License Grant: CC By 4.0



Volume 1, Issue 2, 2023

In Fig. 6(a) and 6(b), the beam failure mode for a 450mm x 230mm beam with a 3m length, 10mm links, and 2Y16 and 3Y16 as top and bottom reinforcements, is shown. The stress pattern cracking mode for both the control and 20% IOT concrete beams showed similar behavior at 3m length. The red color indicates the locations of the concrete with large plastic strains, which correspond to the points with significant shear cracks. Meanwhile, the blue color represents points with low strain values.

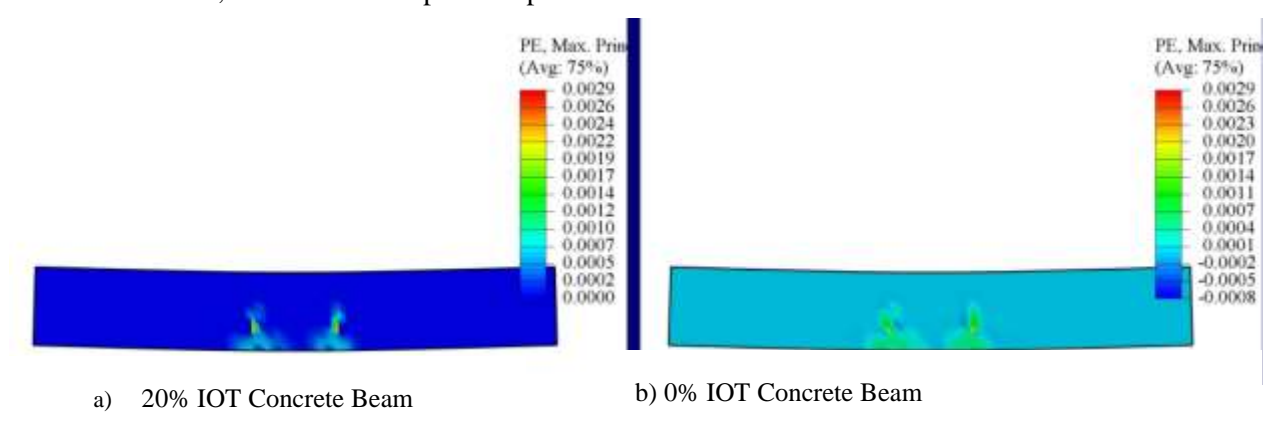


Fig. 6 (a&b). FE Model Cracking Pattern for a 3m Beam

IV. **Conclusion and Recommendations**

In conclusion, the study suggests that incorporating Iron Ore Tailings (IOT) as partial cement replacement has the potential to reduce the environmental damage caused by the waste. The focus was on analyzing the flexural strength and displacement of a 20% IOT concrete beam model, which performed better than the beam from a traditional concrete mixture. The ultimate load obtained from the 20% IOT concrete beam was compared with experimental results, which showed a 19% positive difference in terms of the loadcarrying capacity. Additionally, a parametric study was conducted by varying the length, which showed a steady increase in the ultimate load capacity. However, the mode of failure remained the same, with more visible cracks.

It is recommended to incorporate IOT as a partial sand replacement of up to 20% in concrete to reduce the environmental damage caused by the waste. Further studies with different boundary conditions, beam model dimensions, and various material properties are suggested to overcome financial and time constraints. The concrete damage plasticity model can be used to effectively predict the failure behavior of the concrete. The use of IOT in concrete production can contribute to sustainable development efforts.

Overall, the study is a step toward sustainable development, and the hope is that the findings will be beneficial to researchers and practitioners in the field.



Copyright and License Grant: CC By 4.0

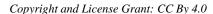


References

- 1. C. R. Gagg, "Cement and concrete as an engineering material: An historic appraisal and case study analysis," *Eng. Fail. Anal.* vol. 40, pp. 114–140, 2014. [Online]. Available: https://doi.org/10.1016/j.engfailanal.2014.02.004
- 2. S. Gupta, B. N. Mohapatra, and M. A. Bansal, "A review on the development of Portland limestone cement: A step towards low carbon economy for Indian cement industry," *Current Research in Green and Sustainable Chemistry*, vol. 3, 2020. [Online]. Available: https://doi.org/10.1016/j.crgsc.2020.100019
- 3. A. C. Ganesh, N. Deepak, V. Deepak, S. Ajay, A. Pandian, "Utilization of PET bottles and plastic granules in geopolymer concrete," *Materials Today: Proceedings*, vol. 42, pp. 444–449 2021. [Online] Available: https://doi.org/10.1016/j.matpr.2020.10.170
- 4. F. C. Lo, M. G. Lee, S. L. Lo, "Effect of coal ash and rice husk ash partial replacement in ordinary Portland cement on pervious concrete," *Construction and Building Materials*, vol.286, no.11, 2021. [Online] Available: https://doi.org/10.1016/j.conbuildmat.2021.122947
- 5. S. S. Rahman, and M. J. Khattak, "Roller compacted geopolymer concrete using recycled concrete aggregate," *Construction and Building Materials*, vol. 283, 2021. [Online] Available: https://doi.org/10.1016/j.conbuildmat.2021.122624
- 6. Z. Chen, Y. Yuan, W. Li, and Z. Li, "Environmental risks of tailings dams in China: A review," *Journal of Cleaner Production*, vol. 226, pp. 959-972,2019.
- 7. M. Zhang, Y. Li, H. Li, X. Li, X. Zhang, and W. Li, "Contamination and potential ecological risk assessment of heavy metals in soils around a large iron tailing pond," *Environmental Science and Pollution Research*, vol. 28, no. 10, pp. 11807-11820 2021.
- 8. H. Wang, Y. Yang, X. Wang, Y. Zhou, and Y. Zhao, "A review of research progress in the field of tailings disposal," *Journal of Cleaner Production*, vol. 261, 2020.
- 9. G. Rana, A. Sharma, and M. K. Yadav, "Evaluation of iron ore tailings as replacement for fine aggregate in concrete," *Journal of Materials in Civil Engineering*, vol. 30, no.6, 2018.
- 10. C. Liu, M. Wang, L. Yu, X. Cao, H. Wang, and X. Ren, "Feasibility study on the utilization of iron ore tailings as aggregate for preparation of concrete," *Journal of Cleaner Production*, vol. 263, 2020.
- 11. S. Zhao, J. Fan, and W. Sun, "Utilization of iron ore tailings as fine aggregate in ultra-high-performance concrete" *Construction and Building Materials*, vol. 50, pp. 540-548., 2014. [Online] Available: https://doi.org/10.1016/j.conbuildmat.2013.10.019

(P): 2959-393X

DOI: https://doi.org/10.59122/144CFC18





- 12. S. F. Oritola, "Flexural Behaviour of Reinforced Iron Ore Tailings Concrete (IOTC) Beams", *Nigerian Journal of Technological Research*, vol. 14, no.2, pp. 1-9, 2019.
- 13. R. P. Batista, J. O. Costa, P. H. R. Borges, F. A. Dos Santos, F. S. Lameiras, "High-performance Alkaliactivated Composites Containing an Iron-ore Mine Tailing as Aggregate", *Matec Web of Conferences*, vol. 274, pp. 1-7 2019. [Online] Available: https://doi.org/10.1051/matecconf/201927402004
- 14. R. Kumar, P. Das, M. Beulah, H. R. Arjun, "Geopolymer bricks using iron ore tailings, slag sand, ground granular blast furnace slag, and fly ash", *IntechOpen*. 2020. [Online] Available: http://doi.org/10.5772/intechopen.81748
- 15. F. N. M. Protasio, R. R. De Avillez, S. Letichevsky, F. D. Silva, "The use of iron ore tailings obtained from the Germano dam in the production of a sustainable concrete", *Journal of Cleaner Production*, vol. 278, 2021. [Online] Available: https://doi.org/10.1016/j.jclepro.2020.123929
- W. Zheng; S. Wang; X. Quan; Y. Qu; Z. Mo; C. Lin, "Carbonation resistance and pore structure of mixed-fiber-reinforced concrete containing fine aggregates of iron ore tailings," Materials vol. 15, no.24, 2022. [Online] Available: https://doi.org/10.3390/ma15248992
- 17. W. Zhang, X. Gu, J. Qiu, J. Liu, Y. Zhao, X. Li, "Effects of iron ore tailings on the compressive strength and permeability of ultra-high-performance concrete," Construction *and Building Materials*, vol. 260, no.4, pp. 1-10, 2020. [Online] Available: https://doi.org/10.1016/j.conbuildmat.2020.119917
- 18. M. H. Thakrele, "Experimental study on foam concrete," *Int. J. Civ. Struct. Environ. Infrastruct. Eng. Res. Dev.*, vol. 4, no.1, pp. 145-158, 2014.
- 19. A. Earij, G. Alfano, K. Cashell, X. Zhou, "Nonlinear three-dimensional finite element modeling of fiber reinforced-concrete beams: Computational challenges and experimental validation," *Engineering Fail. Ana.*, vol. 82, pp. 92-115, 2017.
- 20. J. Georgea, J. S. K. Rama, M. V. N. Siva Kumar, A. Vasan, "The behavior of plain concrete beam subjected to three-point bending using concrete damaged plasticity (CDP) model," International Conference on Recent Trends in Engineering and Material Sciences (ICEMS-2016). *Materials Today: Proceedings*, pp. 9742-9746 2016.

(P): 2959-393X

4

Copyright and License Grant: CC By 4.0



Designing an Exploratory Indigenous Knowledge Management Framework for Soil Conservation Mechanism in the Konso Community

Amin Tuni Gure^{1*}, Addisu Mulugeta Hailu², Eyasu Tafere Amenu²

¹Department of Information Systems, Arsi University, Ethiopia

²Faculty of Computing and Software Engineering, Arba Minch University, Ethiopia

*Corresponding Authors Email: atuni22@gmail.com

Abstract

In Ethiopia, there are diverse Indigenous Knowledge systems across different regions and ethnicities. The Konso people, specifically, possess unique indigenous knowledge used for various purposes, such as weather forecasting, traditional medicine, soil conservation, and environmental protection to enhance productivity. The primary objective of this research study is to explore and design an Indigenous Knowledge Management framework specifically focused on soil conservation mechanisms among the Konso people. Therefore, it is crucial to explore and design an IKM framework and develop a prototype that simplifies the processes involved in knowledge management. The research adopts an exploratory research method and a design science research design to gather knowledge from various sources. Both qualitative and quantitative research approaches were employed, utilizing data collection tools such as interviews (questionnaires), surveys, technical observations (checklists), and analysis of existing documents. The collected data revealed new insights, leading to the design and development of a newly proposed IKM framework for soil conservation, implemented using the SWI Prolog tool. Furthermore, the designed and developed IKM framework for soil conservation was evaluated and validated according to ISO-1826 I standards. The findings of this study indicate its significant importance in terms of knowledge sharing, transfer, utilization, and preservation, particularly in combating soil erosion and land degradation in Ethiopia, specifically among the Konso people. User and expert evaluations were conducted, with the results showing that 70% of respondents acknowledged the knowledge deliverability, 87.5% found the framework attractive, 75% agreed on its accessibility, and 62.5% deemed it suitable for their needs. These results strongly support the notion that the proposed IKM framework and prototype for soil conservation among the Konso people can effectively share, transfer, and preserve indigenous knowledge for future generations.

Keywords: Indigenous Knowledge, KM Framework, Knowledge Management, Knowledge Preservation, Soil conservation

Received: June, 2023; Revised: 10 October 2023; Accepted: 05 Nov 2023; Published: 31 December 2023.

Copyright and License Grant: CC By 4.0



DOI: https://doi.org/10.59122/144CFC17

ISSN (E): 2959-3921

(P): 2959-393X





I. Introduction

Currently, the role of Indigenous knowledge (IK) which is traditional knowledge has different roles for different purposes that exist in the different ethnic groups of one country in this world. Ethiopia has more than 80 ethnic groups that own their indigenous knowledge systems. Among Ethiopian ethnicities, Konso is one very well-known ethnicity that has its different indigenous knowledge used for different purposes like weather forecasting, traditional medicine, soil conservation, etc. Accordingly, among the Konso People, soil conservation is one of the mechanisms used for environmental protection and prevention of land degradation by using their indigenous knowledge. Since the Konso people have their own localized soil conservation mechanisms, IK starting from ancient times is highly needed to be transferred to the next generation. The transfer of this very power to environmental protection that increases productivity and the use of computing technology for knowledge preservation from generation to generation is thus vital. Therefore, exploring and designing the framework for this indigenous knowledge of the Konso people's soil conservation mechanism has a great impact on knowledge sharing and preservation.

Also, this IK provides a very important input to socio-cultural capital that is essential for communities to not only survive but also to go beyond and flourish within the given contexts of that community's geography, environment, culture, and economy.

However, IK has a great role not only in solving problems but also in socio-economic development that faces one community, particularly soil erosion, based on their local norm and serves as a bridge to cultivate and tie community with its surrounding phenomena to communicate with it [1]. Hence, in this research study, the researchers explore and design the IK framework with a functional prototype for the Konso people's soil conservation mechanisms.

A. Statement of the Studied Problem

Nowadays, the soil conservation mechanism IK of Konso people is serving the community in the socioeconomic activities and this knowledge has been playing a great role in the protection of the soil from erosion and the increasing of agricultural productivity. Practicing this IK of the Konso community in all parts of our country Ethiopia is very important. However, there are different gaps in how the IK access, share, and preservation tasks are carried out in the community. This is due to a lack of computing technology that captures, represents, shares, and preserves the IK of the community. To practice this IK, it is necessary for the community to first know and understand the basic principle of the mechanism and correctly apply it, but no KM approach facilitates the utilization and preservation of this knowledge.

The utilization and management of this relevant IK are still extremely poor and still not supported by the KM approach and practiced in a computing way extensively in IK sharing and preservation. Based on a

Received: June, 2023; Revised: 10 October 2023; Accepted: 05 Nov 2023; Published: 31 December 2023.

(P): 2959-393X

Volume 1, Issue 2, 2023

DOI: https://doi.org/10.59122/144CFC17



Copyright and License Grant: CC By 4.0



deep review of the literature, there is a crystal-clear lack of research studies focused on managing IK using knowledge management approaches. Also, the exploration and application of the KM approach for designing the IKM framework are still not fully exploited to support soil conservation for managing and enhancing the usability of the soil conservation IK. The importance of the IK obliges a need to manage the IK for effective leverage of the IK and continued innovation, supported with computing. Here is the gap where the researcher is motivated to propose and introduce appropriate solutions by designing a framework for this IK that facilitates the full management, preservation, and usage of this IK.

Because the KM approach is not applied in this specified area, different problems have occurred like lack of Indigenous knowledge sharing, utilization, preserving, and lack of IK management approach which are the most challenging for the users. Depending on this indigenousness and the importance of this IK in the different socio-economic lives of the people in Ethiopia, the researcher is inspired to introduce suitable KM approaches that can increase the utilization of this IK.

Soil degradation in the structure due to water erosion is one of the most extreme and critical environmental problems of sub-Saharan Africa in general and Ethiopia in particular because of its consequences on subsistence agriculture upon which the livelihood of not less than 75% of the populace depends. In response to that, countless soil and water conservation practices on the grounds have been undertaken. However, the impact of the campaigns failed because the techniques that have been delivered used in soil and water conservation had been of little interest to the local community. They did not consider whether or not the neighborhood could observe and understand the techniques without problems based on their existing practices.

In addition, over the previous decades, Ethiopian government organizations have been attempting to assist higher land use and promote exclusive methods to end soil degradation and enhance peoples' living. Furthermore, the previous development efforts had given much less attention to IK practices and farmers' participation in solving their environmental problems. The past 10 years have witnessed extreme soil degradation in Ethiopia. This was because the indigenous practices have been challenged by present-day land management. Indigenous communities advance and allocate land use structures closely interconnected to their lifestyle and well adapted to their ecosystem [8].

Agricultural practices in Ethiopia have long been accompanied by soil erosion. The estimated annual soil loss in Ethiopia is approximately 1.5 billion tons [8]. Sustainable use and management of soil are thus pivotal to enhance the immense role of agriculture in the present economic development. However, soil conservation through indigenous knowledge practices is frequent in some parts of the world where the communities develop the norm of conservation practices and perpetuate it from generation to generation.

Copyright and License Grant: CC By 4.0



DOI: https://doi.org/10.59122/144CFC17





B. Significance of the Study

(P): 2959-393X

In this study, we explored the IK-designed framework and a developed functional prototype that has great significance for the development of this environmental protection IK and increase of the agricultural productivity in Ethiopia by solving soil degradation and greenhouse effects. So, the Konso people and the Ethiopian government (Agriculture sector) will directly benefit from this proposed research study.

II. Literature Review

Different scholars defined Knowledge Management (KM) differently in different domains. According to [9] and [10] KM is an impression that one company or organization, group or individual collects, transfers, and arranges the knowledge and brings the importance from their understanding. Also, KM can be defined as a sharing of knowledge between enterprises, teams, or individuals that are located in the same or different locations [9].

In addition to this according to [5], IK is part KM that is a non-codified knowledge in the mind of individuals or communities' way of working and lifestyle of one or more communities to support individuals, groups, and organizations. According to some scholars' findings, IK is a knowledge that appears traditionally in one society to teach generations about knowledge of the ecosystem [6] [7].

As per [12], different scholars show in their findings Nonaka knowledge management model that Socialization, Externalization, Combination, and Internalization (SECI) are very important for the discovery, creation, capturing, sharing, utilization, and preservation of knowledge.

According to [11], knowledge representation (KR) is the process of application of logic and ontology to construct a computational model for a specific domain to solve problems like conflict resolution, reconciliation, and compensation. In this study, the researcher tries to represent extracted knowledge using the knowledge representation technique.

III. Research Methodology

A. Research Design and Approach

Different types of research designs can be used by researchers as per the purpose of the study. Furthermore, the design stands to ensure that pertinent information for the research is acquired [14]. Also, it is considered a plan of action to solve the research problem by analyzing data and drawing conclusions [15]. Accordingly, in this research study, design science research design was used and depicted in Fig.1. This research design contains different steps of action like problem identification and motivation, the definition of the objectives for a solution, design and development, demonstration, and evaluation. Fig. 2 depicts the research process design process.



In this research study, both qualitative and quantitative (mixed) research approaches were used. Thus, a mixed research approach was used to collect data from primary and secondary sources to solve specified domain problems.

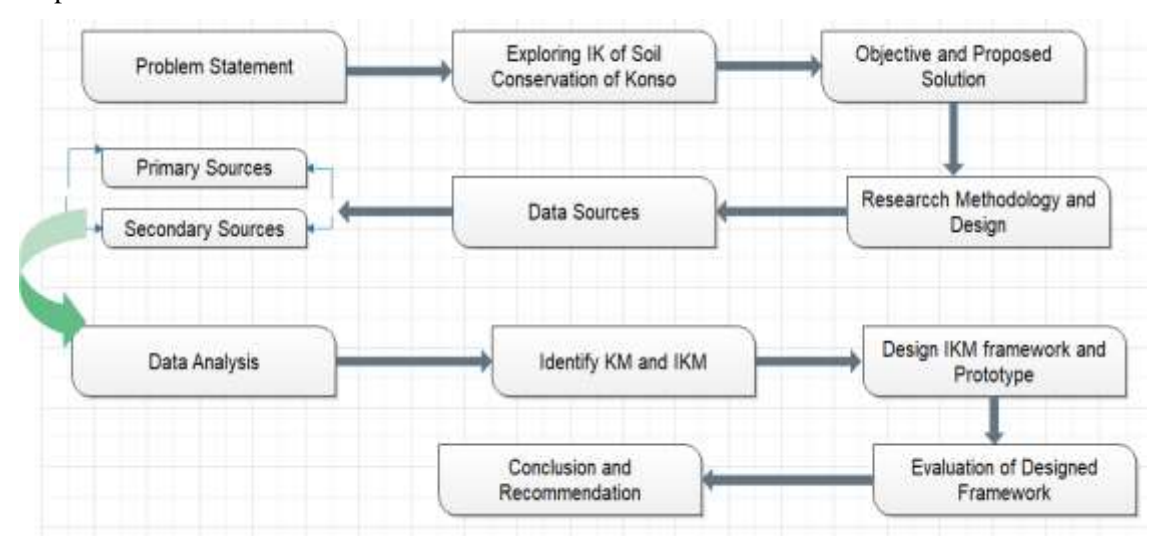


Fig. 1. Design: science research design [16]

B. Data Collection Method

In the research study, data were collected from primary and secondary sources using different data collection tools like surveys (questionnaires), interviews, technical observation (checklist), and focus group discussions. Primary data sources are community leaders, elders, community, communication, the culture and tourism office, and the environmental protection office. Also, secondary data sources used are published books, manual records, articles, magazines, and newspaper feature articles [20] about soil conservation mechanisms.

C. Tool Selections

As depicted in Fig. 2 the tool selection process is carried out to select the tools for designing the framework and develop the proposed functional prototype.



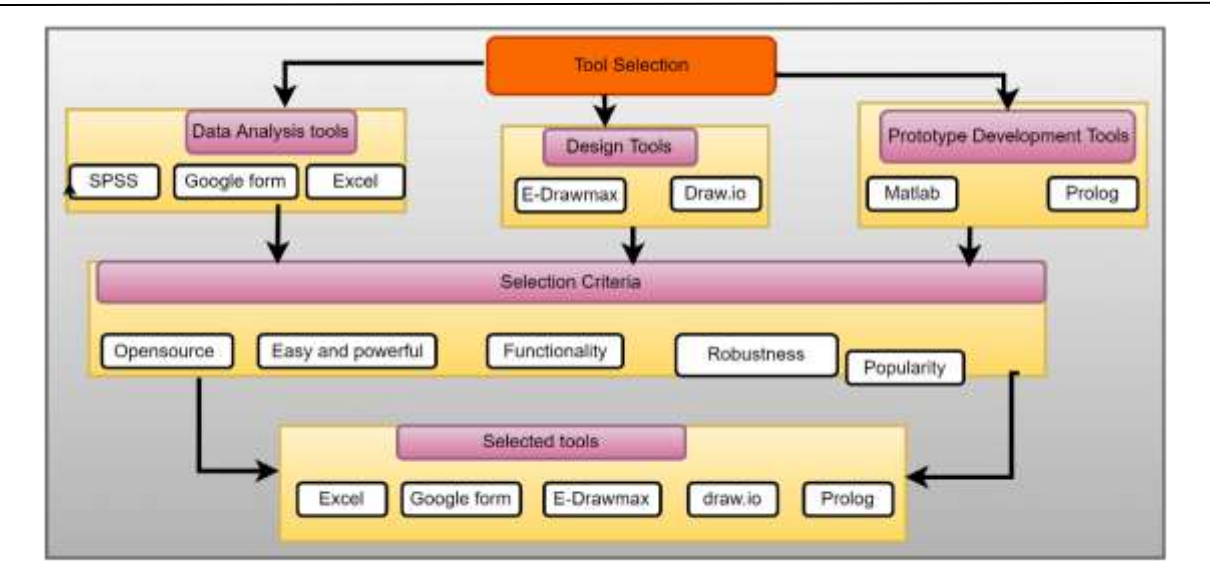


Fig. 2. Tool selection

D. Design of a proposed Indigenous Knowledge Framework

KM framework is a knowledge management application to construct (integrate) knowledge management (KM) components together to enhance the KM process performance for organizational competitiveness [22]. According to [23], the KM framework is used to connect the organization with the main area of the KM process to support the KM approach, awareness, objective, and overall planning of the organization.

In this research study, the proposed IK framework was designed, and the functional prototype was developed by combining some KM components like acquisition, capturing, storing, transferring, sharing, utilizing, and preserving IK in Konso Soil Conservation Mechanisms. Therefore, the newly proposed IK framework for oil conservation was explored, designed, and developed as depicted in Fig. 3.

IV. Result Discussion and Findings

To understand the current usage of Konso People's Indigenous Knowledge in soil conservation mechanisms, the researchers collected data from primary and secondary sources through data collection tools like survey questionnaires, structured interviews, and technical observation from the community leaders, local elders, local community, environmental protection office, communication office, agricultural extension experts, and the culture and tourism bureau in the Konso Zone. Accordingly, 40 key respondents participated in the data collection from the different offices mentioned above. Generally, the discussion

(P): 2959-393X

Volume 1, Issue 2, 2023

DOI: https://doi.org/10.59122/144CFC17



Copyright and License Grant: CC By 4.0



results indicated in the following Table I and Fig. 4 to Fig. 5 illustrate the outcomes of the data being analyzed and discussed.

Therefore, to design and develop the proposed IK framework for soil conservation Nonaka model was selected, because this model is used to codify knowledge and is easy to convey, share, transfer, and categorize the KM model into four stages (SECI) that are used to convert from one type of knowledge to others. Also, for the functional prototype SWI-Prolog programming tool was used for implementation, and the proposed framework was evaluated.

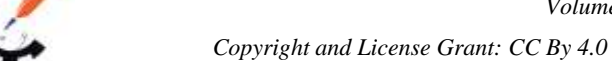
A. Exploring the Current Status of IK of Soil Conservation in Konso People

As depicted in Table I and Fig. 4 to Fig. 5, the findings of this research study reveal that the majority of the respondents, 21(51.2%), agreed with a high to very high response on the Konso community's IK soil conservation, which has been used as a conservation mechanism. 18(46.3%) of the respondents agreed that from low to very low about the key information about soil conservation of Konso community IK. Also, 21(53.7%) of respondents agreed on the futuristic plan for IK soil conservation with low to very low, whereas 16 (42.5) respondents responded that they agreed on the plan for the soil conservation of Konso people's soil conservation mechanisms. 26(65.8%) of respondents agreed with low to very low responses regarding the use of new technology for soil conservation whereas 13(31.3%) agreed that they are using the new technology for soil conservation.

ISSN (E): 2959-3921

Volume 1, Issue 2, 2023

DOI: https://doi.org/10.59122/144CFC17





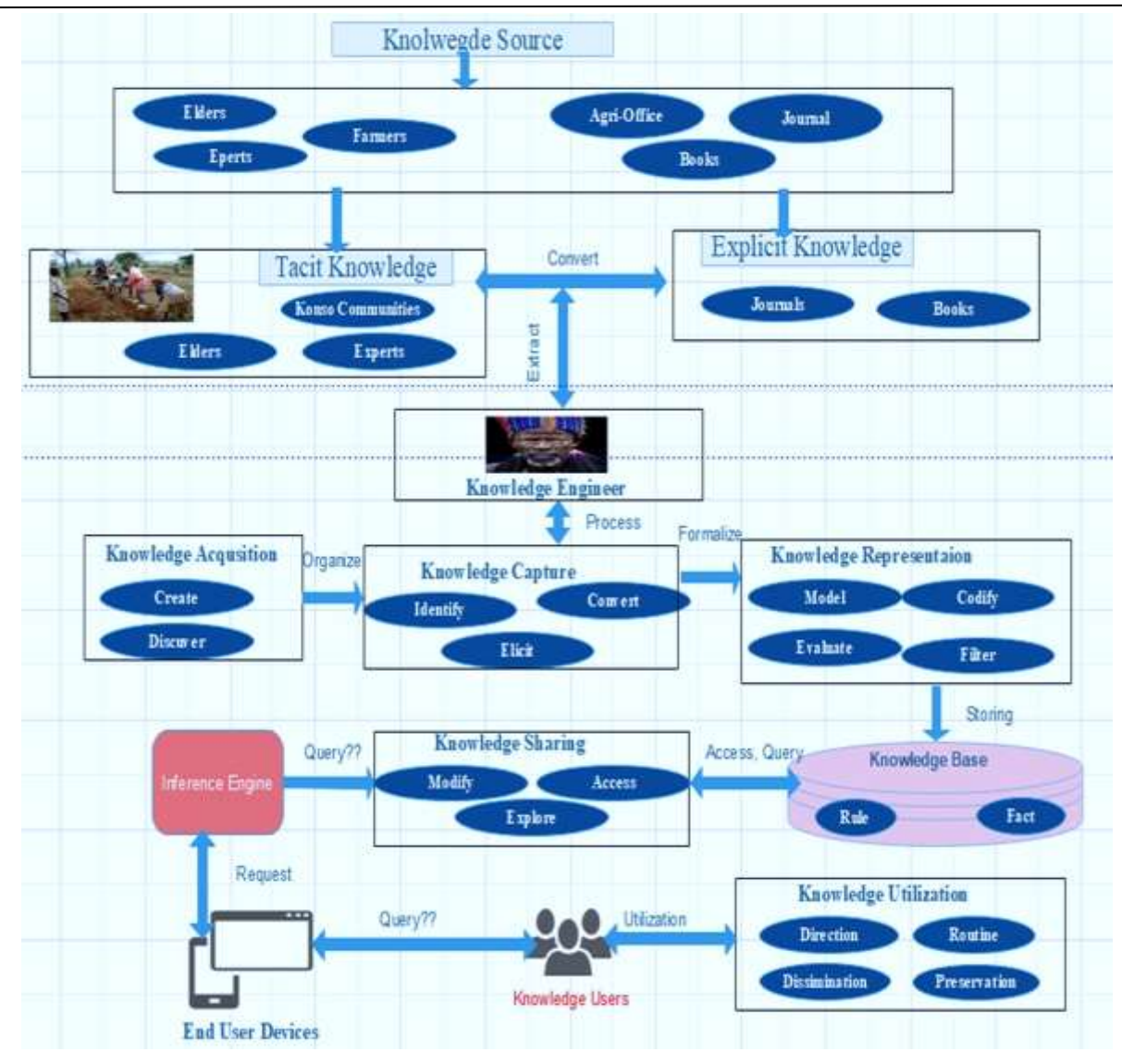


Fig. 3. Proposed indigenous knowledge management framework for soil conservation

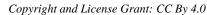
Table I: Evaluation Standard for Current IK Framework for Soil Conservation

Cu	rrent use of IK for	Not at all	Very low	Low	High	Very high
1	Information about key soil conservation	1(2%)	8(19.5%)	10(26.8%)	16(39%)	5(12.2%)
2	Plans for soil conservation	2(4.8%)	9(22%)	12(31.7%)	12(31.7%)	4(9.8%)
3	The use of technology to preserve	1(2.9%)	6(14.6%)	20(51.2%)	11(26.8%)	2(4.5%)
4	processes sharing and dissemination	2(4.9%)	6(14.6%)	17(41.5%)	12(31.7%)	3(7.3%)
5	Information about new initiatives	1(2.5%)	9(22.5%)	21(52.5%)	5(12.5%)	4(10%)

Received: June, 2023; Revised: 10 October 2023; Accepted: 05 Nov 2023; Published: 31 December 2023.

ISSN (E): 2959-3921

DOI: https://doi.org/10.59122/144CFC17





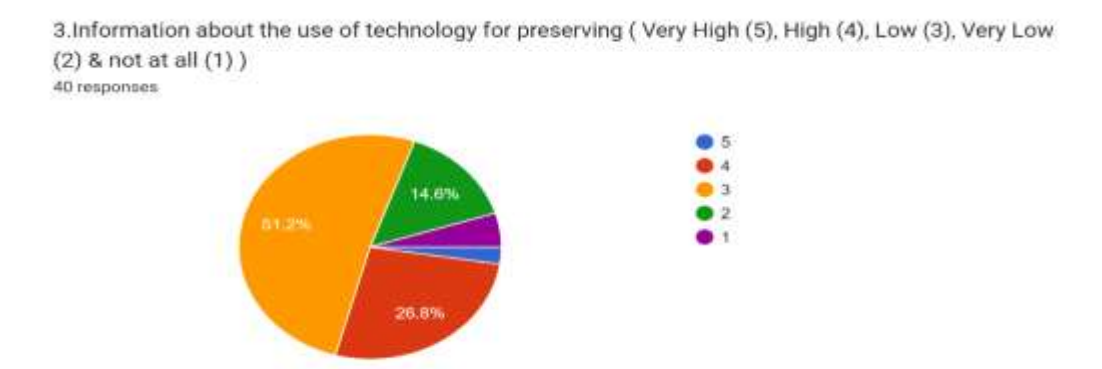


Fig. 4. The use of technology for IK preservation

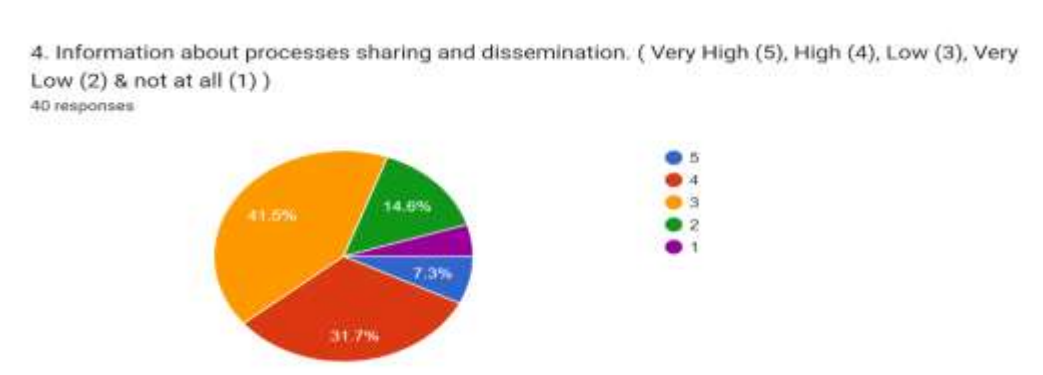


Fig. 5. The process of sharing and dissemination of IK

As shown in Fig. 4 and 5, 26(65.8%) of respondents agreed with low to very low rates regarding the use of new technology for soil conservation whereas 13(31.3%) agreed that they are using the new technology for soil conservation. In addition to this, regarding the IK sharing and dissemination of Konso people's soil conservation and new initiative of knowledge sharing and preservation of Konso people soil's conservation mechanisms, the majority of the respondents responded with low to very low 23(56.1%) and 30(75%) respectively.

B. Evaluation of the Proposed IK Framework for Soil Conservation in Konso Community

The proposed IK framework for soil conservation mechanism was validated using standard validation that ISO-9126 parameters like a) Attractiveness in IK acquisitions, b) Simplicity in IK capturing, c) Efficiency in sharing and utilization, d) Deliverability in knowledge and decision-making, e) Portability in the desired user requirement, f) Usability improvement of IK in resolving a social problem, g) Functionality appropriateness, and h) maintainability for additional requirements.

(P): 2959-393X

Copyright and License Grant: CC By 4.0



As shown in Table II, 80% of respondents strongly agreed and 15% agreed on the suitability of the proposed framework for Soil conservation and 70% and 27.5% of respondents strongly agreed and agreed on the knowledge deliverability of the proposed framework respectively. In addition, 60% and 50% of respondents strongly agreed and agreed on the accessibility and the attractivity of the proposed IK framework for Soil conservation mechanisms respectively which is represented in Fig. 6.

1) End User Validation: In this research study, the validation of the proposed IK framework involved two aspects: evaluating it against established standards and conducting expert acceptance testing with end users. Previous research by scholars has identified various parameters including reliability, usability, maintainability, accessibility, efficiency, and functionality [24] [25], which were considered in this study. For the evaluation process, a diverse group of participants was selected, including computer science professionals, software engineers, IT professionals, and local elders. Their expertise and perspectives were invaluable in assessing the proposed IK framework for the Konso people's soil conservation. As illustrated in Table II and Fig. 6, the results revealed that 87.5% of respondents strongly agreed that the proposed IK framework is both attractive and usable. Additionally, 75% of respondents strongly agreed that the framework is simple, accessible, and functional.

Based on the user acceptance testing and the ISO 9126 criteria, it can be concluded that the proposed framework successfully meets the standards set by ISO 9126. The evaluation results indicate that the IK framework for soil conservation among the Konso people has achieved high acceptance and meets the necessary criteria for reliability, usability, maintainability, accessibility, efficiency, and functionality.

Table II: Evaluation Output for Proposed Framework

Parameters	Strongly Agree	Agree	Neutral	Disagree	Strongly disagree	Total %
Attractive	7(87.5%)	1(12.5%)	0(0%)	0(0%)	0(0%)	100%
Simplified	6(75%)	2(25%)	0(0%)	0(0%)	0(0%)	100%
Efficiency	4(50%)	4(50%)	0(0%)	0(0%)	0(0%)	100%
Accessibility	6(75%)	2(25%)	0(0%)	0(0%)	0(0%)	100%
Portable	4(50%)	4(50%)	0(0%)	0(0%)	0(0%)	100%
Usability	7(87.5%)	1(12.5%)	0(0%)	0(0%)	0(0%)	100%
Functionality	6(75%)	2(25%)	0(0%)	0(0%)	0(0%)	100%
Maintainable	5(62.5%)	3(37.5%)	0(0%)	0(0%)	0(0%)	100%

Received: June, 2023; Revised: 10 October 2023; Accepted: 05 Nov 2023; Published: 31 December 2023.



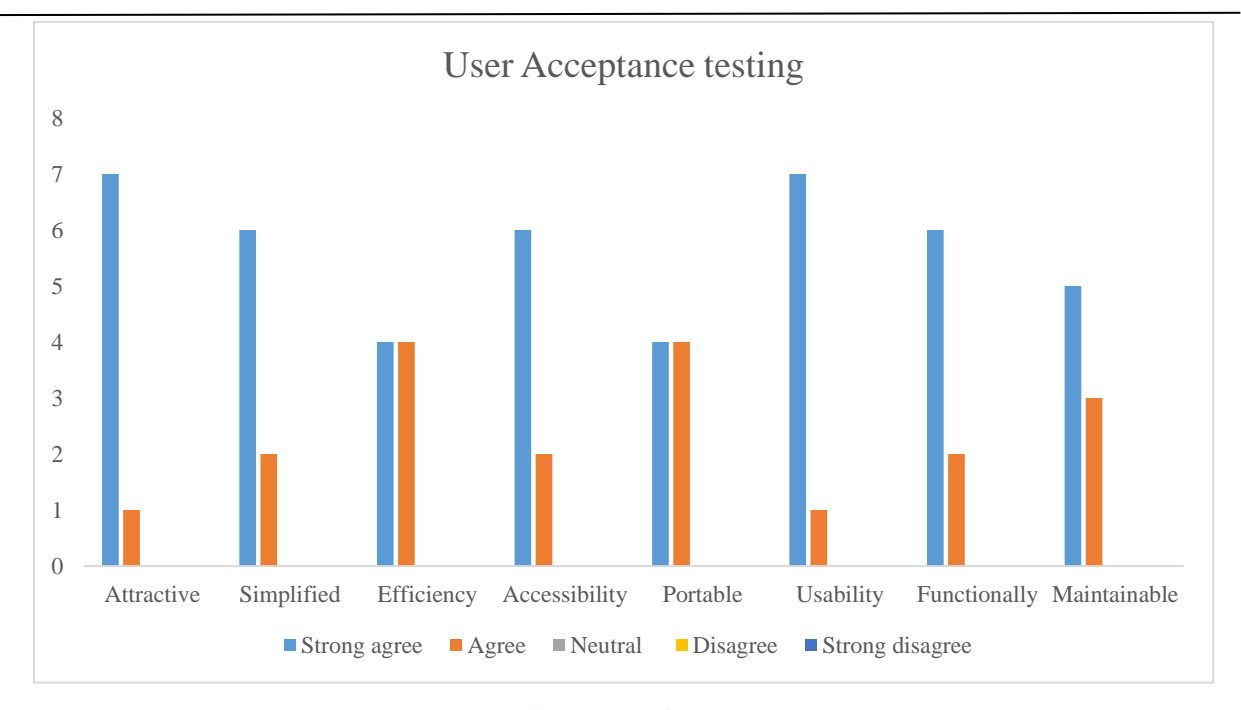


Fig. 6. Representation of proposed framework evaluation output

V. Conclusion

The developed IK management framework for soil conservation is expected to greatly enhance the sharing and preservation of Indigenous Knowledge (IK) within the Konso Community. Numerous research findings have highlighted the diverse applications of IK, such as traditional medicine, conflict resolution, weather forecasting, and soil conservation mechanisms. These types of indigenous knowledge hold significant importance in addressing socio-political issues among the Konso people and in Ethiopia as a whole.

To design the proposed IK framework, this research study utilized the Nonaka Model (SECI), which is well-suited for capturing and managing tacit and explicit knowledge. The results of the study indicated that 26 (65.8%) of the respondents expressed a low-to-very-low level of utilization of new technology for soil conservation, while 13 (31.3%) reported that they are currently utilizing new technology for this purpose. Furthermore, the proposed IK framework for soil conservation mechanisms was subjected to validation using ISO-9126 parameters, including sustainability, knowledge deliverability, attractiveness, and accessibility. The framework was also assessed through end-user acceptance evaluation. The results of these validation processes confirmed the effectiveness and suitability of the proposed framework.

Overall, this research study concludes that the developed IK management framework has the potential to significantly contribute to the utilization and preservation of indigenous knowledge in the context of soil conservation. By incorporating new technology and addressing the identified challenges, the framework can facilitate improved practices and sustainable soil conservation efforts within the Konso community.

Copyright and License Grant: CC By 4.0



Volume 1, Issue 2, 2023

Lastly, the validation of the proposed IK framework was tested by developing the functional prototype. It was implemented using SWI prolog programming language.

Recommendations

Based on the findings of this research study, the following recommendations were forwarded. As the findings of this research are revealed, the government should give attention to further study on soil conservation for the protection of soil degradation mechanisms in other parts of Ethiopia. In addition, the proposed IKMF for soil conservation is limited to the scope of the conservation only without identifying the soil properties, low land, high land, and soil types; henceforth, it is vital to extend this research to develop an integrated IKMF for the whole of Konso people's soil conservation mechanisms.

References

- 1. M. H. Sedato and I. Ahmad, "Oromo indigenous conflict resolution institutions: An example of African indigenous institutions," *Review of Research*, vol. 8, no. 3, p.1.Dec. 2018.
- 2. C. Morrill and D.S. Rudes, "Conflict resolution in organizations," The *Annu. Rev. Law Soc. Sci*, vol. 6, pp. 627–51, Aug. 2010.
- 3. M. H. Sedato and . I. Ahmad, "Oromo indigenous conflict resolution institutions: An example of African indigenous institutions," vol. 8, no. 3, pp. 1-2, 2018.
- 4. J. Adem, "Women and Indigenous conflict resolution institutions in Oromia: Experience from Siinqee of the Wayyu Shanan Arsi Oromo in Adami Tullu Jiddu Kombolcha district of the Oromia National Regional State," M.A. Thesis, Dept. of Social Anthropology, *Addis Ababa University*, Addis Ababa, Ethiopia, 2017.
- 5. T. Ta'a, "Gadaa: The indigenous knowledge system of Oromoo," in Proc. of the 2nd International Conf. on Oromoo Studies, Jimma, Ethiopia, June 2017.
- 6. N. W. Sheehan, "Indigenous knowledge and respectful design: An evidence-based approach," *Design Issues*, vol. 27, no. 4, pp. 68-80, 2011.
- 7. Y. Aredo, "Dress as a form of nonverbal communication in the context of Arsii Oromoo," *Gadaa Journal*, vol. 1, no. 1, p. 111, 2018.
- 8. L. P. Yulianti and K. Surendro, "Ontology model for indigenous knowledge," in *Information Technology Systems and Innovation (ICITSI)*, Indonesia, 2018.
- 9. M. E. Jennex, "What is knowledge management," doi:10.4018/9781599042619. ch001, p. 1, 2007.
- 10. J. F. Sowa, "Knowledge Representation: Logical, Philosophical, and Computational Foundations", New York: Brooks / Cole 2000.



- 11. H. Mitiku, W. Jimma, and C. Diriba, "Managing indigenous knowledge for corrective and preventive cares: The case of Horro Guduru Wollega Zone, Oromia, Ethiopia," *Universal Journal of Public Health*, vol. 4. no.4., pp. 212 217, 2016.
- 12. G. Boru, "Gondooroo as an Indigenous method of conflict resolution and justice administration," *Journal of Culture, Society, and Development*, vol. 23, pp. 18 26, 2016.
- 13. K. J. Sileyew, Research design, and methodology, in *Text Mining Analysis, Programming and Application*, Addis Ababa, Ethiopia: IntechOpen, 2019, pp.1-12.
- 14. V. K. Grover, "Research Approach: An Overview", *Golden Research Thoughts*, vol. 4, no. 8, p. 1, 2015.
- E. Tefere, "A Framework for Indigenous Knowledge Management in Oromo Gada System," p. 28, 24
 September 2018.
- 16. A. R. Hevner, S.T. March, J. Park, and S. Ram, "Design science in information systems research," *MIS Quarterly*, vol. 8, no. 1, p. 76, Mar., 2004.
- 17. G. Bhawna and N. A. Gobind, "Research methodology and approaches," IOSR Journal of Research & Method in Education, vol. 5, no. 3, p. 48, 2015.
- 18. V. K. Grover, "Research approach: An overview," *Golden Research Thoughts*, vol. 4, no. 8, p. 1, 2015.
- 19. S. M. S. Kabir, "Method of data collection," in *Basic Guidelines for Research:* An Introductory Approach for All Disciplines, Chittagong, Bangladesh: Book Zone Publication, 2016, pp. 202-274.
- 20. E. Tefere, "Framework for indigenous knowledge for Gada system," p. 34, 24 September 2018.
- 21. J.C. Mostert and M.M.M. Snyman, "Knowledge management framework for the development of an effective knowledge management strategy," *South African Journal of Information Management*, vol. 9, no 2. 2007.
- 22. K. Kyoratungye, J. R. Aduwo, E. Mugejjera, and J. Lubega, "Knowledge management Frameworks: A review of conceptual foundations and a KMF for IT-based organizations," in *Information Technology*, p. 41, 2009.
- 23. L. Bounegru and E. Karstens, "User evaluation report," Synergetic Content Creation and Communication, Rep. D7.4.1: User Evaluation Report 1.0, European Commission: CORDISEU research results, 2011
- 24. A. Abran (Ed.), "Analysis of Quality Model and Measures," in *Software Metrics and Software Metrology*, New York, USA: Wiley-IEEE Computer Society, 2010, p.208.



ETHIOPIAN INTERNATIONAL JOURNAL OF ENGINEERING AND TECHNOLOGY

About the EIJET

The Ethiopian International Journal of Engineering and Technology (EIJET) is a non-profit peer-reviewed open-access research Journal of Arba Minch Institute of Technology under Arba Minch University, Ethiopia. The scope of the Journal covers multidisciplinary and cross-disciplinary areas of research in engineering and technology. The Journal is indexed in Google Scholar. The Journal publishes all types of quality research papers, case studies, review papers, experimental and empirical papers, shortened thesis/disertations in the broad area of engineering, technology and the other converging areas.

The Journal is specifically dedicated to publish novel research outcomes, contributions and inovative research ideas in the following fields of enginering and technology:-

- Intelligent Computing and Information Technology
- · Mechanical and Metallurgy Engineering
- · Architectural Design and Town Planning
- · Civil and Transport Engineering Systems
- Electrical Engineering and Power Electronics
- · Emerging areas of Renewable Energy

Papers related to allied disciplines, emerging technologies, and future-generation engineering paradigms will be given priority for publication.

The Journal publishes papers from worldwide sources, especially for covering the emerging issues of engineering and technology from developing and developed countries. The Papers from African continent countries having localized problem-solving research will be given priority.

Arba Minch University Arba Minch Institute of Technology Arba Minch, Ethiopia Phone: +251 46 881 4970

Fax: +251 46 881 4971